2010

A COMPUTATIONAL BIOLOGY APPROACH TO THE ANALYSIS OF COMPLEX PHYSIOLOGY: COAGULATION, FIBRINOLYSIS, AND WOUND HEALING

Nathan Menke
Virginia Commonwealth University

© A COMPUTATIONAL BIOLOGY APPROACH TO THE ANALYSIS OF COMPLEX PHYSIOLOGY: COAGULATION, FIBRINOLYSIS, AND WOUND HEALING

A COMPUTATIONAL BIOLOGY APPROACH TO THE ANALYSIS OF COMPLEX PHYSIOLOGY: COAGULATION, FIBRINOLYSIS, AND WOUND HEALING

A dissertation submitted in partial fulfillment of the requirements for the degree of Doctor of Philosophy at Virginia Commonwealth University.

By

Nathan Menke, M.D.
Doctor of Medicine, The Ohio State University, 2002
Bachelor of Science, The Ohio State University Biochemistry, 1997
Bachelor of Science, The Ohio State University Computer and Information Science,1997

Director: Robert F. Diegelmann, Ph.D.
Professor
Department of Biochemistry and Molecular Biology

Virginia Commonwealth University
Richmond, Virginia
May 2010

Acknowledgment

The author wishes to express his heartfelt appreciation to several people instrumental in the completion of this endeavor. I would like to thank my wife, Marie, for her love, support and patience during the past five years it has taken me to graduate. I would like to thank my parents for their unending love and support. I would also like to thank Dr. Diegelmann for his mentorship and patience during this long journey. I would like to thank Dr. Ward for the inspiration, guidance, and constant encouragement in the pursuit of a research career. Finally, I thank my Ph.D. committee (Drs. Barton, Fang, and Witten) for their insight and valuable time committed to this process.

TABLE OF CONTENTS

LIST OF TABLES

LIST OF FIGURES

LIST OF ABBREVIATIONS

a1-PI	a1-protease inhibitor
ABM	agent based modeling
ABMS	agent based modeling and simulation
AP	anti-plasmin
aPC	activated protein C
aTAFI	activated thrombin activatable fibrinolysis inhibitor
AT-H	antithrombin III-heparin
bFGF	basic fibroblast growth factor
CA	cellular automata
CAD	coronary artery disease
CAM	cell adhesion molecule
cAMP	cyclic adenosine monophosphate
CF	coagulation/fibrinolytic
CVA	cerebrovascular accident
DIC	disseminated intravascular coagulation
DVT	deep venous thrombosis
ECM	extracellular matrix
Fg	fibrinogen
FGF	fibroblast growth factor
Fm	fibrin monomer
FSP	fibrin split products
GPU	graphics processing unit
H	heparin
HMWK	high molecular weight kininogen
HUS	hemolytic uremic syndrome
ICAM	intercellular adhesion molecule
IGF-1	insulin-like growth factor-1
IL-1	interleukin 1
IL-6	interleukin 6
IL-8	interleukin 8
ITP	idiopathic thrombocytopenic purpura
K	kallikrein
Ka	kaolin
KGF	keratinocyte growth factor
MMP-8	matrix metalloproteinase-8
ODE	ordinary differential equation
PAI	plasminogen activation inhibitor

PDGF	platelet derived growth factor
PG	plasminogen
PK	prekallikrein
Plt	platelet
Pn	plasmin
TAFI	thrombin activatable fibrinolysis inhibitor
TF	tissue factor
TFPI	tissue factor pathway inhibitor
TGF-a	transforming growth factor alpha
TGF-b	transforming growth factor beta
TIC	trauma induced coagulopathy
TIMP	tissue inhibitor of metalloproteinase
TNF-a	tumor necrosis factor alpha
tPA	tissue plasminogen activator
TTP	thrombotic thrombocytopenic purpura
VCAM	vascular cell adhesion molecule
VEGF	vascular endothelial growth factor

Abstract

A COMPUTATIONAL BIOLOGY APPROACH TO
THE ANALYSIS OF COMPLEX PHYSIOLOGY

By Nathan Menke, M.D.

An abstract submitted in partial fulfillment of the requirements for the degree
of Doctor of Philosophy at Virginia Commonwealth University.

Virginia Commonwealth University, 2010.

Major Director: Robert F. Diegelmann, Ph.D.
Professor
Department of Biochemistry and Molecular Biology

The birth of complexity research derives from the logical progression of advancement in the scientific field afforded by reductionist theory. We present *in silico* models of two complex physiological processes, wound healing and coagulation/fibrinolysis based on two common tools in the study of complex physiology: ordinary differential equations (ODE) and Agent Based Modeling (ABM). The strengths of these two approaches are well-suited in the analysis of clinical paradigms such as wound healing and coagulation.

The complex interactions that characterize acute wound healing have stymied the development of effective therapeutic modalities. The use of computational models holds the promise to improve our basic approach to understanding the process. We have modified an existing ordinary differential equation model by 1) evolving from a systemic model to a local model, 2) the incorporation of fibroblast activity, and3) including the effects of tissue oxygenation. Possible therapeutic targets, such as fibroblast death rate and rate of fibroblast recruitment have been identified by computational analysis. This model is a step toward constructing an integrative systems biology model of human wound healing.

The coagulation and fibrinolytic systems are complex, inter-connected biological systems with major physiological roles. We present an Agent Based Modeling and Simulation (ABMS) approach to these complex interactions. This ABMS method successfully reproduces the initiation, propagation, and termination of blood clot formation and its lysis *in vitro* due to the activation of either the intrinsic or extrinsic pathways. Furthermore, the ABMS was able to simulate the pharmacological effects of two

clinically used anticoagulants, warfarin and heparin, as well as the physiological effects of enzyme deficiency/dysfunction, i.e., hemophilia and antithrombin III-heparin binding impairment, on the coagulation system. The results of the model compare favorably with *in vitro* experimental data under both physiologic and pathophysiologic conditions.

Our computational systems biology approach integrates reductionist experimental data into a cohesive model that allows rapid evaluation of the effects of multiple variables. Our ODE and AMBS models offer the ability to generate non-linear responses based on known relationships among variables and *in silico* modeling of mechanistic biological rules on computer software, respectively. Simulations of normal and disease states as well as effects of therapeutic intervention demonstrate the potential uses of computer simulation. Specifically, models may be applied to hypothesis generation and biological advances, discovery of new diagnostic and therapeutic options, platforms to test novel therapies, and opportunities to predict adverse events during drug development. The ultimate aim of such models is creation of bedside simulators that allow personalized, individual medicine; however, a myriad of opportunities for scientific advancement are opened through *in silico* experimentation.

Introduction

Complexity Theory

Classic scientific approach suggests that the universe may be understood through the study of its individual components, *i.e.* reductionism[1,2]. Through deconstruction of complex problems into their integral parts, the reductionist approach successfully predicts those outcomes perfectly explained through simple mechanistic behaviors. This approach predefines the system as one composed of simple relationships between individual components, unaffected by the properties of the system itself; single causes result in single effects with small perturbations of the system as a whole. Particle physics and molecular biology are examples of fields that have made enormous gains through reductionist analysis. In contrast, complex systems resist characterization in this manner.

A system is a delineated part of the universe which is distinguished from the rest by a real or imagined boundary. Systems may be characterized as open/closed and simple/complex. Closed systems are maintained by internal forces and are not influenced by external forces. Open systems, which are commonly found in biology, are in permanent interaction with their environment. Therefore, in order to understand an open system you must describe the system, its environment, and the interactions between them. Simple systems have single cause and effect, small change in cause results in small change in effect, thereby predictable. Complex systems have circular causality, feedback loops, logical paradoxes and/or strange loops; small changes in cause have the potential to cause large effects, thereby displaying *emergence* phenomena and making them unpredictable[3]. In order to account for these multifactorial characteristics, the system approach attempts to combine both the reductionist and holistic approaches. Complex

systems analysis endeavors to explain how simple entities without any central controller and limited communication can combine to form complicated and sophisticated systems. By definition, complex systems exhibit *emergent* and *self-organized* behavior. Adaptive, non-linear behavior may arise from seemingly small changes in initial conditions. Unlike systems defined by linear relationships, initial conditions cannot predict the magnitude or direction of the outcome. Thus, newer methods such as chaos theory, evolutional economics and network theory have evolved to explain complex systems such as weather/climate, societal behavior, and disease states of living organisms[4].

Analysis of complex systems requires an all-inclusive approach that acknowledges its heterogeneous components and processes. Temporal and spatial variability are integrated as multiple cause/effect mechanisms may occur simultaneously. The following critical properties are addressed first and foremost: 1) *self-organization, i.e.* no overriding controller, 2) *non-linear relationships,* and 3) *emergence*. This analysis is further complicated by potential emergence of component parts. A complex system may, in and of itself, be formed from a series of complex systems. For example, individual organs (heart, brain, liver, *etc…*) are complex systems that contribute to the behavior of the organism as a whole. In fact, each individual cell is also a complex system.

The collective action of a complex system integrates the internal and external environment in a unique manner delineated through the properties within the system. Interactions such as feedback loops, feedforward loops, circular causality, and self-organization result in emergence, whereby simple components produce complex behavior[5]. Through circular causality, the

sequence of cause and effects lead back to the initiating event in a manner that confirms or changes the initial circumstance (A→B→ C→A). Feedback implies a loop whereby the product returns and affects the input. Negative feedback reduces the deviation from a goal state (stabilization effects). Positive feedback increases the deviation from an initial state (destabilizing). Prediction of this behavior does not follow from the reductionist model of characterization of the individual components. Dissection of these systems into its components mislays the complex behavior under investigation. As a result, reductionist theory is unable to predict the behaviors of a system with emergent properties. A hurricane results from a series of conditions involving pressure, condensation, and temperature gradients. A living organism produces complex physiology/behavior from the local actions of cells.

Unique properties emerge as a result of heterogeneous components interacting in a non-linear manner. Nonlinear systems may show sensitivity to initial conditions where a small change in a variable may cause a large effect in the outcome of the system. Conversely, vastly different initial conditions may generate non-unique solutions. The systems show both time and state dependence in that they depend on not only the current state of the system, but also historical events. The most important property of such systems is that they display emergent behaviors that cannot be predicted from analysis of the individual components. In biological systems, emergent behaviors often result in highly ordered and stable systems. Complexity science suggests that life is in accordance with the laws of physics, but physics first principles alone cannot predict life[6]. A more complete understanding of a system requires holism. The holistic approach focuses on organizational principles where the emergent properties of a system arise from the interactions of its parts.

In short, a complex nonlinear system may be viewed as a system consisting of an extremely large and variable number of components. These components are capable of displaying significant temporal and spatial variability but, at the same time, can retain a high degree of interdependence between each other. What we learn from this is that topology and dynamics interact to produce system behaviors. Thus, it is the combination of the dynamics of the various components themselves and the relationship or connections (nature and degree) between the components, which emerge as being of utmost importance. A complex system renders distinction between cause and effect relatively meaningless as the dynamic relationship among components results in effects modifying causes to create new, independent outcomes.

By definition, a complex system is one that satisfies certain critical properties. First, it is composed of many parts that are coupled in a nonlinear fashion with no overlying controller that determines the behavior of the system (the system must be self-organizing). Second, the system must show emergence. That is, the whole system must contain properties that are unpredictable from the parts/component pieces of the network or system. Typically, in such systems, as the number of components and their relationships increase, the complexity also increases. As a result of the spatio-temporal relationships of the system, the system may exhibit a variety of dynamical behaviors from stable flows to seemingly random oscillations. Complex systems may demonstrate many other dynamical behaviors. Possible behaviors include sensitivity to initial conditions where a small change in a variable may oftentimes cause a large effect in the dynamical outcome of the system (butterfly effect)[7]. Other properties include hysteresis, a property in which model parameter sets may generate non-unique solutions with the same initial

parameter conditions, and bifurcation dynamics where radically different behaviors such as going from stable to unstable or stable to oscillatory may occur over very small parametric ranges[8,9]. Spatial and temporal patterns can exhibit properties of self-similarity (fractality) in which changes in scale visualization of the pattern show no alteration in the basic structure of the pattern itself[10,11]. Systems can exhibit self-organization and coalescence, evolution and adaptation[12]. Finally, system dynamics may contain n historical component in which the temporal dynamics of the system, at a particular time point, is partially or fully dependent upon the prior history (dynamical behaviors) of the system or its components.

Reductionist approaches dissect systems in order to better understand its' nature. However, one of the fundamental properties of synergistic complex systems is that subfractionation can and does cause a loss of information (structural, relational, temporal and hierarchical). Subsequently, destruction of emergent properties that are not contained within the subfraction pieces occurs. Despite the fact that upper level hierarchical structures may contain a super emergent dynamics set, sub-levels may contain their own emergent dynamics that are not necessarily seen until the sub-level is separated from the whole system. One must be clear that sublevel emergence is potentially artifactual due to the breaking of links to the whole system. These emergent properties are always present in the whole system but are invisible and cannot be appreciated from a reductionist approach. Thus, we cannot dissect a complex system in the parts, study them and expect to fully understand the system. Dissection of the overall system destroys the important ingredient of semantics-syntax, context dependence, and self-reference; properties that are vital in the production of emergent behaviors. To summarize, complex systems are composed of many components connected in a non-linear manner, must be self organizing, no

overlying controller, must show emergence, and contains properties that are unpredictable from the individual components of the system. As a result of these properties, a complex system cannot be dissected and studied as individual components.

Examples of complex systems are found throughout the natural world[13]. As described above, climate, human behavior, and disease processes all exhibit complex function[14,15]. These examples may be further subdivided or expanded into additional complex systems. Climates are complex systems that affect the emergent behavior of ecosystems. Within ecosystems, complex behavior is exerted through herd mentality, the eruption of a volcano, the gathering patterns of ants and bees[16].

Humans behave in a complex manner, from flight patterns to societal organization of economies and politics to the functioning of the internet[17,18,19]. The integration of numerous individual and societal relationships in the United States results in the election of a president[3]. Combinations of supply and demand produce economic outcomes that differ from predicted linear relationships.

Medical and biological processes are a field of acute interest for complex systems analysis[20]. Individual organs and their inherent functions produce complex behavior, as does their interaction as a whole. Heart rate variability, immune system response, and phenotypic variation result from disparate inputs[21,22]. In this manner, biologic complexity defies reductionist patterns of recognition[23]. As most disease states result from dysfunction of complex systems, newer methods of analysis offer an innovated, personalized approach currently lacking in the

biomedical sciences. Herein, emergent properties of pathophysiological states of wound healing and coagulation/fibrinolysis are characterized. A series of *in silico* experiments using ordinary differential equations (ODEs) and agent based modeling (ABM) demonstrates the potential application of a systems biology approach in these disease states.

Biologic Complexity

Wound Healing - The normal response to tissue injury is a timely and orderly reparative process that results in sustained restoration of anatomic and functional integrity[24]. In contrast, in chronic dermal ulcers the healing process is prolonged, incomplete, and proceeds in an uncoordinated manner resulting in poor anatomical and functional outcome. On the opposite end of the spectrum are the numerous clinical problems associated with excessive healing and fibrosis. Clinically, wounds can be categorized as acute or chronic based on the timeliness of healing[25].

Wound repair is a complex process involving a highly regulated cascade of events requiring interactions among many cell types, soluble factors, and matrix components[26]. There are four distinct phases of acute wound healing consisting of hemostasis, inflammation, proliferation, and remodeling. Following injury, exposure of platelets to the extracellular matrix (ECM) induces them to adhere and aggregate, thus, releasing the contents of their secretory granules. This hemostasis response occurs immediately following tissue disruption and is needed to control bleeding and seal the site of injury. The wide variety of platelet factors liberated by degranulation include those which facilitate hemostasis and also act as chemoattractants [platelet

derived growth factor (PDGF) and transforming growth factor beta (TGF-B)] for cells involved in the next stage of repair, the inflammatory phase.

The process of hemostasis begins immediately upon injury. The immediate goal is to stabilize the wound and thereby prevent exsanguination. Exposed blood vessels vasoconstrict and platelets that are exposed to collagen are activated and begin the process of aggregation at the wound site. These activated platelets release growth factors, cyclic adenosine monophosphate (cAMP), and adhesive glycoproteins, which in turn activate receptors that cause platelets to become sticky and aggregate. The glycoproteins released from activated platelet alpha granules, include fibrinogen, fibronectin, thrombospondin, and von Willebrand factor. The next step in hemostasis involves the coagulation cascade as coagulation factors from the blood combine with coagulation factors released by platelets. The result is a fibrin clot that not only prevents further blood loss, but also serves as a provisional wound healing matrix[27]. Platelets become entrapped in the fibrin clot providing further bulk as well as a membrane on which inactive clotting enzymes are bound and activated further promoting the clotting cascade.

Growth factors released by the platelet alpha granules provide the impetus for the next stage in wound healing. Neutrophils and monocytes are recruited and activated by PDGF and TGF-B. Endothelial cells are activated by vascular endothelial growth factor (VEGF), transforming growth factor alpha (TGF-a), and basic fibroblast growth factor (bFGF). Fibroblasts are activated by PDGF to begin migration to the wound site and produce collagen and glycosaminoglycans, which facilitates cellular migration and interactions with the cell matrix-supporting framework. In addition to factors released from platelets, breakdown fragments from

complement, such as C5a and f-Met-Leu-Phe, a bacterial waste product, also signal and recruit neutrophils to the wound site. In sum, hemostasis initiates the wound healing response through platelet activation at the site of the injury, and the interactions of soluble mediators and growth factors with the ECM to provide the provisional wound healing matrix that sets the stage for subsequent events.

The inflammatory phase begins as early as 2 h after injury. Activated neutrophils leave the circulation to begin the debridement of devitalized tissue and phagocytosis of any infectious agents or foreign bodies. Neutrophils also secrete cytokines and other specific chemical ‘‘signals’’ needed to attract specialized cells that are important in repairing the injured tissue. In addition, neutrophils release a battery of proteolytic enzymes, such as elastase and matrix metalloproteinase-8 (MMP-8), to assist in their movement through the tissue and remove damaged ECM[28,29,30]. Mast cell granules are filled with enzymes, such as chymase and tryptase, histamine, and other active amines; when released these enzymes cause the classic signs of inflammation: rubor (redness), calor (heat), tumor (swelling), and dolor (pain). The crucial inflammatory cells during the inflammatory phase are neutrophils and activated monocytes (macrophages). Neutrophils and macrophages are responsible for bound wound bed preparation and the initial milieu of the healing wound. In order to expedite healing, cellular debris and bacteria are cleared. The inflammatory cells also release cytokines [including interleukins 1 (IL-1), IL-6, IL-8, and tumor necrosis factor alpha (TNF-a)] and growth factors [PDGF, TGF-B, TGF-a, insulin-like growth factor-1(IGF-1), and FGF] that not only serve to continue the inflammatory phase but also initiate the proliferative phase by recruiting fibroblasts and epithelial cells.

In the first 24 h, neutrophils are the predominant inflammatory cell type. The neutrophils are recruited and activated by the soluble mediators released by platelets and the coagulation cascade during the hemostatic phase. The initial goal of the neutrophils is to prepare the wound bed by killing bacteria and removing devitalized tissue. Not only does this begin the process of wound healing but also helps fight infection. Neutrophils are chemoattracted to the wound site by the initial inflammatory cytokines released at the time of injury and subsequent hemostasis process. Normally, the weak adherence of leukocytes results in a rolling type motion along the surface of the endothelial cells. The slower velocity allows more time for binding between the adhesion molecules [selectins, cell adhesion molecules (CAMs), and cadherins] and receptors (integrins) of circulating leukocytes and vascular endothelial cells. Once activated, leukocytes firmly adhere to epithelial cells as a result of the binding between integrin receptors and ligands, such as vascular CAM (VCAM) and intercellular adhesion molecule (ICAM), which are expressed on activated endothelial cells. The activated leukocytes are induced to migrate between the endothelial cells and move into the injured tissue using their integrin receptors to bind to ECM components. At that point, inflammatory cells secrete elastase and collagenase in order to migrate through the basement membrane of the endothelial cell and into the ECM. Once the neutrophils have entered the wound, they begin to phagocytose bacteria and subsequently produce oxygen free radical to kill the entrapped bacteria. In addition, they degrade damaged components of the ECM by releasing large amounts of proteases (neutrophil elastase and neutrophil collagenase). Neutrophils also produce and release inflammatory mediators, such as TNF-a and IL-1, which further recruit and activate more neutrophils as well as fibroblasts and

epithelial cells. After 2–3 days, neutrophils are no longer the dominant cell type as they are depleted by apoptosis allowing tissue monocytes to predominate.

After the first 24 h, activated monocytes (macrophages) are the most numerous inflammatory cell types present in the wound bed. Macrophages are not only active in healing the wound but also in the regulation and progression of the healing process. Macrophages are mandatory components of the normal healing process[31]. Circulating monocytes are attracted to the wound site and extravasate in the same manner as described for neutrophils. Once the monocyte has entered the wound site, they are activated into tissue macrophages by chemokines, cytokines, growth factors, and soluble fragments of ECM components produced by proteolytic degradation of collagen and fibronectin. Macrophages play a similar role as neutrophils in the healing process. They are responsible for killing bacteria and wound debridement through the actions of secreted MMPs and elastase. In addition to the functions shared with neutrophils, the macrophages also play a crucial role in modulating the inflammatory response by regulating the proteolytic destruction of wound tissue and initiating the transition from the inflammatory phase to the proliferative phase. Macrophages downregulate tissue destruction by secretion of inhibitors of the proteases. They also release a wide variety of growth factors and cytokines including PDGF, TGF-B, TGF-a, FGF, IGF-1, TNF-a, IL-1, and IL-6 that serve to recruit and activate fibroblasts and promote angiogenesis. The addition of fibroblasts that synthesize, deposit, and organize the provisional ECM, combined with the ability to decrease proteolytic destruction leads to the initiation of the proliferative phase. As the number of macrophages decrease and the number of fibroblasts increase the wound begins to enter the proliferative phase and exit the inflammatory phase.

During the ‘‘proliferation’’ phase, keratinocytes proliferate, migrate, and differentiate, thus, restoring surface integrity. Endothelial cells from damaged blood vessels begin to send out new capillary buds, while fibroblasts from nearby connective tissue enter the wound site and deposit ECM[32]. In the normal dermis, fibroblasts are quiescent and have a low concentration, but in granulation tissue and the provisional matrix of the wound they are active and exist in high concentrations. Fibroblasts are recruited to the wound site by the soluble products of activated platelets and macrophages. The migration of fibroblasts is far more complicated than that of neutrophils and macrophages as they have to change their morphology and clear a path for their movement from the ECM to the wound site.

Fibroblasts begin their migration by first binding to matrix components (fibronectin, vitronectin, and fibrin) via their integrin receptors. The receptors bind to specific amino acid sequences (R-G-D or arginine–glycine–aspartic acid) or binding sites on the matrix components. The fibroblasts move in a step-wise pattern by extending a cytoplasmic projection from the unbound side of its membrane to find the next binding site. Once a new site is successfully bound, the original site is then released (by local protease activity), and the cell pulls itself forward using its cytoskeleton network of actin fibers.

The concentration gradient provided by chemotactic growth factors, cytokines, and chemokines in conjunction with the alignment of the fibrils in the ECM and provisional matrix determine the direction of fibroblast migration. The fibroblast moves along the fibrils as opposed to across them. The proteolytic enzymes used to facilitate their forward motion include collagenase

(MMP-1), gelatinases (MMP-2 and MMP-9) that degrade gelatin substrates, and stromelysin (MMP-3) that has multiple protein substrates in the ECM.

Collagen is the major ECM component providing strength, integrity, and structure to normal tissues. It is also required to repair defects created by injuries, thereby restoring tissue structure and function[32,33]. During repair, collagen is initially laid down in irregular bundles possessing modest mechanical strength, but as the wound matures, the collagen is cross-linked and then the scar undergoes remodeling indicating the ‘‘maturation’’ phase of healing. The collagen is then organized into a dense structure with increasing tensile strength as the matrix begins the process of contraction. However, the regained tensile strength will never reach normal; the maximum a wound can ever achieve is approximately 80% of normal tensile strength[32,33]. Other components of the ECM that exhibit significant structural and functional roles include fibronectin, laminin, proteoglycans, and glycosaminoglycans[34]. Fibronectin and laminin contain important binding sites for cells, collagen, as well as glycosaminoglycans[35].

Wounds with significant tissue loss heal by the mechanism of contraction, a process whereby the edges of a wound are drawn toward the center, due to forces generated within the wound. Contraction facilitates spontaneous wound closure by reducing the volume required to be filled by granulation tissue as well as the area required to be re-epithelized[33,36].

In order to protect the underlying wound it is necessary to create an epithelial barrier. Epithelization is a complex process that involves epithelial cell detachment phenotypic alterations, migration, proliferation, and then differentiation[37]. An undamaged mature

epidermis consists of five layers of differentiated epithelial cells ranging from the cuboidal basal keratinocytes nearest to the dermis up to the flattened, hexagonal, and tough keratinocytes in the uppermost layer. Only one layer is capable of replication (the basal epithelial cells). These basal cells are normally attached to their neighboring cells by intercellular connectors called desmosomes and to the basement membrane by hemidesmosomes. In order to begin replicating basal cells must become activated by growth factors such as EGF, keratinocyte growth factor (KGF), and TGF-a. The growth factors bind to receptors on the epithelial cells and stimulate migration and proliferation. In addition to the activation of basal cells, growth factors trigger the desmosomes and hemidesmosomes to dissolve. Subsequently, cells may detach in preparation for migration. Integrin receptors are then expressed and the normally cuboidal basal epithelial cells flatten in shape and begin to migrate as a monolayer over the newly deposited granulation tissue, following along collagen fibers. The monolayer is provided with new cells from the proliferating basal cells near the wound margin (cells that are actively migrating are incapable of proliferation). In order for the epithelial cells to penetrate the newly formed scab, necrotic tissue, or escar, the leading edge of the monolayer produces and secretes proteolytic enzymes (MMPs). The migration ceases after the epithelial cells contact each other. Once this contact has been made, the entire epithelial monolayer forms a confluent sheet and enters a proliferative mode and the stratified layers of the epidermis are reestablished and begin to mature to restore barrier function. The intercellular desmosomes and the hemidesmosome attachments to the newly formed basement membrane are also reestablished. TGF-B is one growth factor that can speed up the maturation (differentiation and keratinization) of the epidermal layers. Clinically, epithelialization is the hallmark of healing, but it is not the final event, as the granulation tissue must be remodeled to form the permanent scar.

During late phases of wound healing, scar remodeling involves a variety of matrix degrading enzymes including MMPs, serine proteinases, cathepsins, and glycosidases[36,38]. The goal of the remodeling phase is the conversion of the preliminary wound matrix to the production of a final scar that maximizes wound tensile strength. Fibroblasts are the cells responsible for remodeling. An equilibrium between collagen formation and degradation results in a constant amount of collagen. There are several different classes of proteolytic enzymes in the wound bed that are responsible for the degradation of collagen: MMPs, serine proteinases, cathepsins, and glycosidases[36,38]. Specific MMP proteases required for remodeling include collagenases (which degrade intact fibrillar collagen molecules), the gelatinases (which degrade damaged fibrillar collagen molecules), and the stromelysins (which very effectively degrade proteoglycans). The most important serine protease is neutrophil elastase, which can degrade almost all types of protein molecules. In order to balance the destructive capabilities of the matrix degrading enzymes, inhibitors are also needed. The specific inhibitors of the MMPs are the tissue inhibitors of metalloproteinases (TIMPs) and specific inhibitors of serine protease are a1-protease inhibitor (a1-PI) and a2-macroglobulin. The process of remodeling is dependent on the relative activities of the proteases and their inhibitors.

Tightly controlled regulatory systems maintain a delicate balance between these complex synthetic and degradative processes; normal tissue repair ultimately results from a fine-tuning of this equilibrium. There is now a growing recognition that abnormal wound healing often results from a disruption of degradative/synthesis equilibrium[29,30,39,40,41]. When the balance tips in

favor of matrix degradation, the end result may be a chronic ulcer, where as reduced degradation and/or increased matrix synthesis results in fibrosis.

Research scientists and clinicians have focused historically on the effects of cytokines and growth factors on individual cells *in vitro*, out of context of both the injury and the organism[42]. The relationships among the various cell types and the dynamics of the wound healing process has remained uncharacterized. As a result, therapies to improve wound healing have either failed or shown minimal improvements in outcomes. One possible reason for such failures is that the complex, multi-scale, multi-temporal, hierarchical nature of wounds has thus far been underappreciated. In order to account for these relationships, an overarching systems biological approach would allow one to draw upon the nuanced methodologies of complexity theory[43,44]. Fueled by the ongoing identification of numerous inflammatory and immune mediators produced in the normal response to acute soft tissue injury, ample evidence of this oversimplification can be found in the failure of single mediator-targeted therapies. Many features of the wound healing process are consistent with complexity theory: 1) Multiple cell types interact using paracrine and autocrine signaling (signals may be amplified/dampened based on the state and history of the individual cell in a non-linear manner) 2) There is no overlying control mechanism 3) The process of wound healing progresses through hemostasis, inflammation, proliferation and remodeling 4) A mature scar is produced that restores anatomical and function to the wound.

These concepts apply to the problem of understanding and modeling the dynamics of a healing wound detailed below. The wound healing system is composed of multiple levels of

organizational scale including: multiple cell types (fibroblasts, neutrophils, macrophages, *etc…*), intercellular messengers (cytokines, chemokines, hormones, growth factors, *etc…*), synthetic products (collagen, proteoglycans, *etc…*), and enzymes (MMPs and TIMPs). The different cell types produce and respond to the same cytokines in an autocrine and paracrine manner (multiple pathways of interaction). As a result, a signal may be quickly amplified in the system or dampened. The feedback loops that control the release and effects of the cell signals produce nonlinear behavior. The behavior of the cells is determined not only by the current state of the wound, but also the individual receptors that have been activated at earlier time points (state-dependent and history-dependant behaviors). The normal process of wound healing contains many separate but interacting events and host responses including microcirculatory oxygen transport, immune and inflammatory responses, metabolic changes, and the neuroendocrine system modulation. An unknown degree of these and secondary responses will occur due to complex changes in genome expression. Instead of viewing each of these responses as separate and independent mechanisms involved in the development of a healed wound it must be argued that events leading to healing should be viewed through the complexity theoretic lens and that wound healing is most effectively studied as a complex nonlinear system. Additionally, the intracellular signaling pathways also consist of a complex system in itself (sub-system hierarchies). Within each cell, there are multiple pathways that when activated by a receptor, amplify a signal. Many times there are pathways that directly oppose each other that lead to measured responses (multi-scale interaction). Cross talk and divergent pathways lead to many complex relationships among the various signaling pathways. Therefore, a wound must be considered a complex system composed of components that are themselves complex systems (modular hierarchies of complex systems).

Based on the previous discussion, it is clear that the study of the dynamics of wound healing cannot be approached solely through traditional reductionist methodologies. We have established that the experimental understanding currently demonstrates that wound healing is a highly complex process that involves multiple cell types all of which are interacting in a nonlinear fashion. These interactions take place over different time scales, across different organismal hierarchies, and generate relationships through which unpredictable emergent properties can occur[45,46]. For example, there are many feedback loops and redundancies in the wound healing network (Figure 1) that make wound healing difficult to study. Feedback loops give rise to the potential for oscillatory behavior, chaotic dynamics, and other nonlinear phenomena. Topological structure of the network can give rise to unpredicted properties that are defined, not by dynamical relations, but rather by spatio-structural ones[47,48]. Thus, it is not sufficient to understand healing dynamics in terms of classical chemical reaction mechanisms; rather, we must examine the integration of topological (spatio-structural and hierarchical) and temporal (multi-scale) perspectives in order to truly understand the underlying mechanisms of wound healing.

The previous description of complex nonlinear systems, as applied to wound healing, is highly attractive in attempting to explain our failure in creating successful mono-target therapies. New understandings tell us that the cells involved in wound healing and the cytokines and growth factors used to transmit signals could be better categorized as highly complex, layered, modular networks with stochastic dynamics at risk for dysfunction. The extent to which acute and chronic soft tissue wounds can be modeled in terms of complex nonlinear systems, based on the

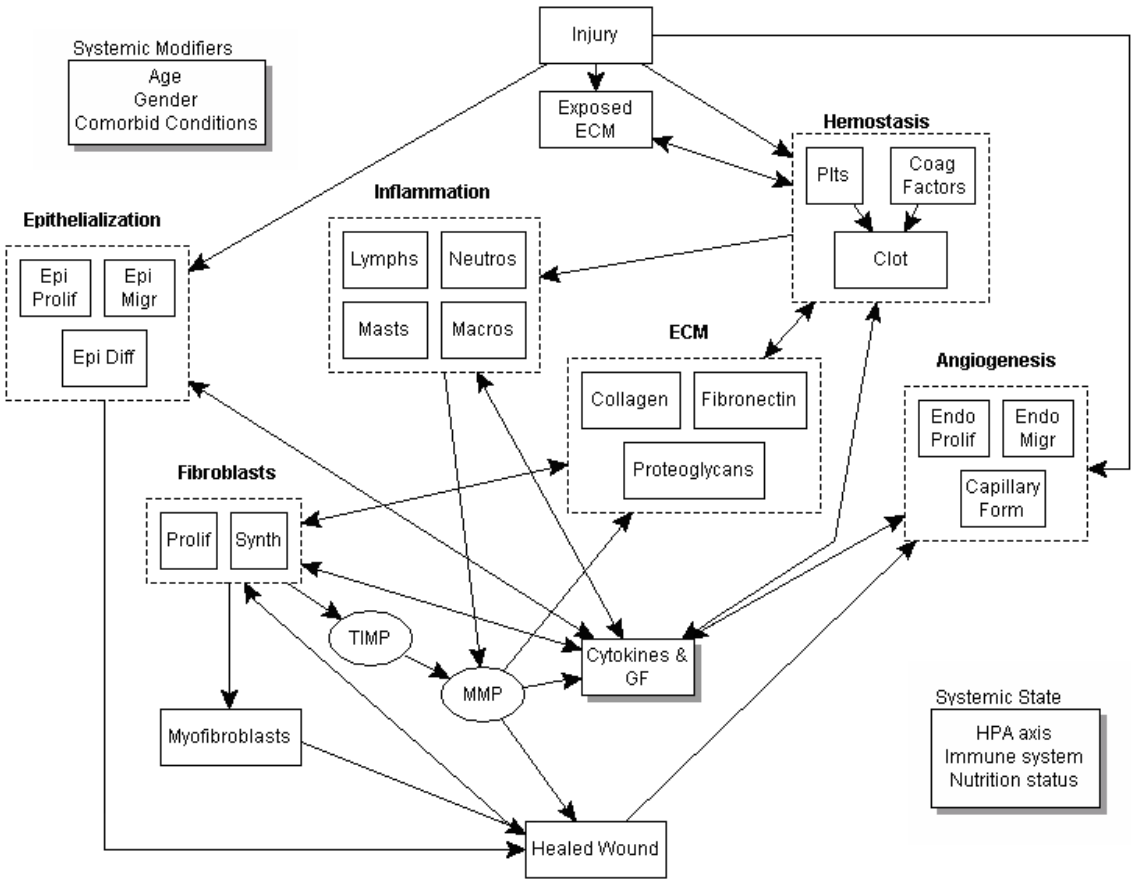

Figure 1: Wound Healing Schema. The schema demonstrates the multiple feedback loops and interactions among the components of the wound healing process.

preceding discussions and assumptions, is not at all clear. Examining the wound healing process as a complex system may allow for discovery and for analysis of possible important emergent properties of the system. These emergent properties, which again, can only be appreciated from the whole of the interactions within the system, are what hold the potential promise of breakthroughs in treatments and diagnostics.

Understanding that wound healing is most realistically represented through complexity theoretic viewpoints now allows the traditional reductionist philosophy to be potentially complemented by

the increasingly powerful new concepts of complexity theory. Effective studies of complex systems must be made by analysis of the parts followed by a sophisticated reconstitution or synthesis in order to model as much of the system as is known at the given time. The resulting model must allow for almost an infinite number of input variables and provide a means to interact with it. In essence, the resulting model is itself desired to exhibit its own emergent properties allowing science to catch the necessary glimpses that provide for the creation of new hypotheses. Manipulation of such a model will provide direction as to the subsequent approach needed to take the next generation of steps in discovery.

An important concept while discussing normal wound healing is the concept of feedback and feedforward loops. In order for wound healing to progress in a coordinated manner, each stage in the healing process must not only self-perpetuate but also initiate the next stage. Furthermore, each progressive stage must have the ability to turn off the previous stage once it has reached the critical point at which it is no longer dependant on the previous stage for positive feedback to continue. The interlocking feedback/feedforward loops allow for an orderly progression of wound healing and prevents any one stage from inhibiting and/or preventing progress into the next stage. The mechanism by which the different phases inhibit and promote each other is through the expression of soluble mediators such as growth factors and cytokines. Each cell type involved is capable of responding to and releasing a multitude of factors that allows the formation of feedback/forward loops to control cell concentrations as well as activity.

In chronic wounds, failure of the normal wound healing process prevents normal wound closure. There are multiple etiologies for the formation of chronic wounds that include diabetic ulcers,

venous stasis ulcers, and pressure ulcers. Although ischemia is an underlying cause, each of these wounds results from different pathological mechanisms; however all non-healing wounds have remarkably similar wound healing trajectories as well as similar inflammatory profiles. In the chronic wound, neutrophils are the predominant cell type with large amounts of proteases and inflammatory cytokines. Because of the excessive amount of inflammation, it is likely that these wounds have failed to progress from the predominantly inflammatory phase to a predominantly proliferative phase. The wound is not able to mature, and the disorganized ECM degrades liberating breakdown products, thus, causing further inflammation. As a result, the chronic pressure ulcer becomes enmeshed in an inflammatory phase that self-perpetuates without providing enough forward momentum to propel the process to the next stage of wound healing. The effect of chronic inflammation is further tissue destruction and worsening of the chronic wound thereby causing more inflammation and preventing any progress towards a healed wound.

Coagulation & Fibrinolysis- The coagulation and fibrinolytic (CF) systems comprise a series of zymogen to enzyme conversions which ultimately terminate in the active proteolytic enzymes thrombin and plasmin, respectively[49]. These enzymes catalyze the deposition and removal of fibrin. When the system is functioning properly, blood is maintained in a fluid state yet rapidly clots to seal endothelial injuries. A proper balance between the activities of the two cascades is required both to protect the organism from excessive blood loss upon injury and to maintain blood fluidity within the vascular system. Imbalance of the two cascades range from the full spectrum of bleeding disorders (*e.g.* hemophilias) to thrombotic events (*e.g.* heart attacks and strokes).

In the event of injury to the endothelium, the CF system balances the need for localized clot formation against the need to prevent system wide activation[50]. This finely tuned system is composed of an assortment of molecular and cellular "agents" (e.g. substrates, enzymes, cofactors, inhibitors, platelets, white blood cells and endothelial cells) which interact to generate a stable clot in order to rapidly obtain hemostasis. The new cellular model of hemostasis proposes that the classical pathways of coagulation, *i.e.*, the intrinsic and extrinsic pathways, mediate on specific cell surfaces in a tightly regulated manner. In this model, activation of factor VII (extrinsic, Figure 2) and factor XII (intrinsic, Figure 2) result in the formation of multi-molecular complexes, the tenase and prothrombinase complexes, which eventually generate thrombin. Thrombin then cleaves fibrinogen to form fibrin monomers, which polymerize to form a three-dimensional clot[51].

Clot formation is regulated *in vivo* primarily through the antithrombin III-heparin (AT-H), activated protein C (aPC), and tissue factor pathway inhibitor (TFPI) pathways (Figure 2)[52,53,54]. These regulating systems limit the excessive formation of cross-linked fibrin under hemostatic conditions thereby preventing thrombotic diseases.

The blood coagulation system is always active and primed for explosive generation of thrombin. The positive feedback of the coagulation cascade in association with the negative feedback loops of the three inhibitory systems (AT-H, aPC, and TFPI) imparts threshold properties to the coagulation pathways[55,56,57]. As a result, there is a non-linear response to stimuli. Furthermore, the presence of multiple coagulation inhibitors that act at different locations in the cascade leads to a synergistic inhibition of explosive thrombin generation. Thus, there must be a

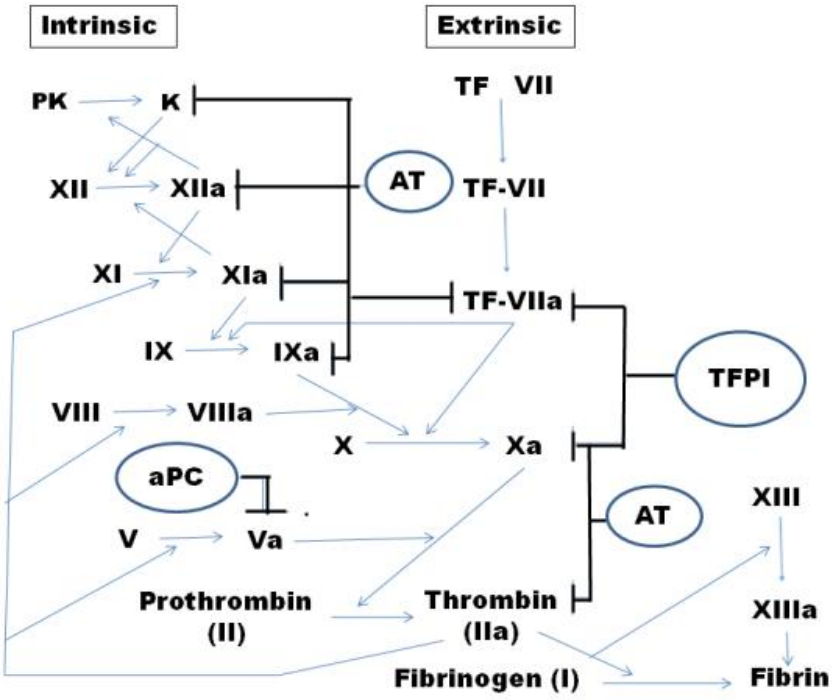

Figure 2: Coagulation Cascade and Inhibitors- Inhibitors denoted by circles. The intrinsic pathway is initiated by Prekallikrein or XII. The extrinsic pathway is initiated by TF. The intrinsic and extrinsic pathway joins at the common pathway that begins after Factor X activation. AT, TFPI, and aPC are the three inhibitory pathways.

significant pro-coagulant stimulus to overcome the inhibitory systems of coagulation. The threshold effect and non-linear response of the coagulation system prevents activation when it is not needed and localizes the response when it is needed.

The specificity of interactions, both molecular and cellular, involved in these complex processes implies that systemic effects displayed by the CF system occurs through emergence of localized events. The CF system may be viewed as a multi-component molecular machine, in which

individual components are linked through multiple feedback and feedforward loops. This introduces non-linear relationships among the components. A static diagram such as the classically portrayed coagulation pathway (Figure 2) cannot adequately describe this dynamic evolutionary network. Not surprisingly, the effects of several disease states on the imbalances in the CF system are difficult to characterize utilizing the classic coagulation pathway. For example, the influence of diseases that favor coagulation (*e.g.* coronary artery disease (CAD), disseminated intravascular coagulation (DIC), cerebrovascular accidents (CVA), and deep venous thrombosis (DVT)), or those that impair coagulation (*e.g*. hemophilias, thrombocytopenias, and von Willebrand disease) remain poorly characterized in terms of the interactions of all components in the system over time.

Coagulation is the first step in the repair of the damaged vessel[58]. *Primary hemostasis* is defined by the formation of the hemostatic plug composed of platelets at the site of injury. *Secondary hemostasis* is defined as the formation of fibrin strands by proteins in the blood plasma, called coagulation factors that respond in a complex cascade which strengthen the platelet plug. Secondary hemostasis occurs simultaneously with primary hemostasis. The coagulation cascade is a network of biochemical pathways that perform the critical function of preventing blood loss and repairing damage to the vasculature. The overall network is divided into two major pathways: the intrinsic system and the extrinsic system. The intrinsic and extrinsic systems converge to form a final common pathway . The common pathway leads to the formation of α-thrombin. Thrombin serves to cleave fibrinogen to fibrin monomers. The fibrin monomers then spontaneously polymerize to form a three-dimensional polymer = clot.

The coagulation cascade is tightly regulated to limit the excessive formation of cross-linked fibrin under hemostatic conditions and prevent spontaneous clot formation. The three systems are the AT–heparin pathway, the tissue factor pathway inhibitor pathway , and the activated protein C pathway (aPC).

Once the endothelial damage is repaired, the clot must be dissolved to allow wound healing to progress normally. The fibrinolytic system operates to dissolve the pre-formed clot once the underlying damage has been repaired (Figure 3)[59,60]. Fibrinolysis is achieved primarily through the proteolytic action of plasmin on the fibrin polymers that reinforce and maintain the integrity of a thrombus. Plasmin hydrolyzes the fibrin mesh at various places thereby making it soluble. The dissolution of the fibrin clot produces circulating fragments that are cleared by other proteases or by the kidney and liver. Similar to coagulation, the fibrinolytic system is composed of interlocking positive and negative feedback loops.

Clot lysis is regulated *in vivo* primarily through the anti-plasmin (AP), plasminogen activation inhibitor (PAI), and thrombin activatible fibrinolysis inhibitor (TAFI) pathways (Figure 3)[59,61,62,63,64,65,66]. Under normal conditions, these regulating systems delay the onset of clot fibrinolysis until coagulation is complete.

The CF system has characteristics that make it difficult to study. The system is either at rest or activated, *i.e.* nonstationarity. The system is not a homogenous chemical system (spatial heterogeneity) in that clotting is localized at the site of endothelial injury. Lastly, the effects of blood flow lead to continuous changes in coagulation factor concentrations and mechanical

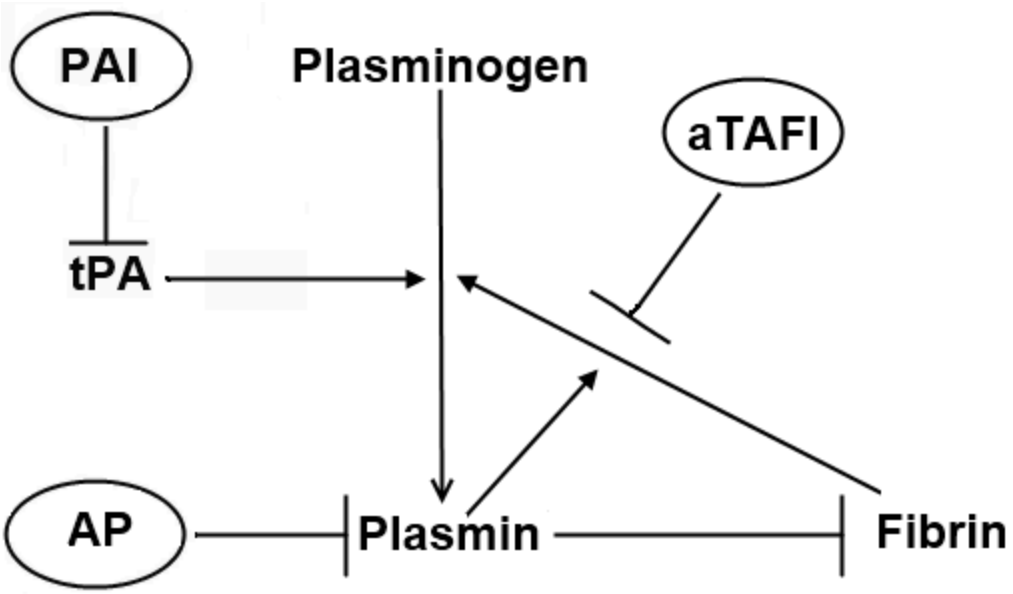

Figure 3: Fibrinolytic Cascade and Inhibitors- Inhibitors are denoted by circles. The fibrinolytic pathway is initiated by tPA activation of Plasminogen. Plasmin hydrolyzes fibrin. Plasmin and fibrin catalyze the conversion of Plasminogen to Plasmin

stresses on the clot. The complexity of the coagulation system has lead to difficulty in creating therapeutic modalities. New pharmaceutical agents that modulate hemostasis have been introduced into clinical practice such as recombinant factor VIIa and activated protein C. The utility of these agents has been limited by the lack of measurement tools to characterize coagulopathy . There is limited ability to determine: 1) indications 2) timing 3) dose of administration. This has led to large scale, expensive but ultimately equivocal clinical trials.

In addition to the inherent characteristics of the CF systems that make it difficult to study, the fact that the CF system is a complex system adds further difficulties. The CF system is composed of a heterogenous collection of components including zymogens, enzymes, co-factors, inhibitors, membrane surfaces and multiple cell types (endothelial cells, platelets, and white blood cells). The CF system has no overlying controller and is composed of a series of local

biochemical reaction. The biochemical reactions that govern the system by their very nature are non-linear. Lastly, threshold effects, localized clot formation, and time delayed fibrinolysis emerge from the simple reactions of the heterogenous components.

One approach to approaching the study of the CF system is to integrate computational models with the experimental data. The ideal computational model would allow the study of complex diseases that involve coagulation such as DIC, trauma induced coagulopathy (TIC), cardiac arrest, sepsis, DVT, MI, arterial thrombosis, genetic coagulopathy (hemophilia A/B, von Willibrands disease, AT deficiency, factor V leiden, etc...), acquired coagulopathy (thrombotic thrombocytopenic purpura (TTP), hemolytic uremic syndrome (HUS), idiopathic thrombocytopenic purpura (ITP), thrombocytopenia, etc...). The model would find novel mediators effecting coagulation, discover new therapeutic targets and treatment strategies. Utilizing such as model would allow for testing over millions of iterations using the *in silico* model. The outcomes associated with the model would include creation of bedside tools for real-time outcome determinations and dosing adjustments, enhance the probability for success once the therapy is translated into the clinical setting, discover new mediators effecting coagulation and interactions between systems including their proximal and distal effects, discover new diagnostic and therapeutic targets that modulate the coagulation cascade to enhance outcomes, create predictive tools for real-time outcome determinations of a patient's clinical state, create real-time bedside tools to perform on-the-fly dosing adjustments for patients with simple or complex coagulopathies or thrombotic disorders, and develop new software and algorithms for simulation.

Computational Biology

Due to the complex nature of biological systems, attempts to model them have concentrated on simple, idealized versions. More recently, the traditional division of science into theory and experiment has been complemented by computer simulation. A model is defined as a simplified representation of a real system. Models are designed to: 1) describe phenomenon in such a manner as to be comprehensible 2) make predictions. Models are used to explore general mechanisms underlying complicated phenomena through: 1) examining (im)plausibility of a proposed mechanism, 2) examining the effects of variations on simple models, and 3) acting as virtual experiments to gain intuitive understanding of complex phenomena[3,67].

Fields such as mechanical engineering have successfully used computer models in the design of tangible products such as automobiles and airplanes. When using computers to model complex systems, they are used to model ideas. Simulations may be the only means available for exploring complex systems when experiments are not feasible or they may be used to reduce the time and cost performing “real” experiments. Such synthetic frameworks allow investigation of systemic behaviors in biologic systems that are difficult if not impossible to study *in vivo*.

The idea that “All models are wrong, but some are useful" is critical for understanding the role of computer simulations in the examination of complex systems. Models may lack universal application, yet may still lead to new insights, new ways of examining phenomena, improved models, and tools to build better models. A crucial component in the utilization of models is understanding the limitation of the model, so that false conclusions are not derived from any

results. The art of model building is the exclusion of irrelevant parts of the problem and correct interpretation of the results.

Model building of complex systems poses unique challenges. As discussed earlier, a system is defined as a collection of interacting elements that together produce, by virtue of their interactions, some system wide behavior. In complex systems, the loss of emergent properties that define the system prohibits an understanding of the system by studying the individual parts. It is analogous to understanding the operation and construction of the space shuttle by reading its parts inventory. Therefore, the system must be studied in a dynamic manner over time and characterizing not just the components but also their relationships. For example, studying the characteristics of isolated structures of a cell in isolation inadequately characterize the behavior of the cell as a whole. Models based on computational systems biology attempt to integrate experimental and computational research[68,69,70,71]. Ideally, computational systems biology will provide tools to bridge the gap between traditional reductionist experiments, genomics/proteomic data, and clinical care (translational medicine).

In this manner, technological and theoretical advances in computer science and mathematics have offered new options to complement experimental study design. As opposed to *in vivo* studies that are performed in living organisms and *in vitro* studies that are undertaken using cell cultures, *in silico* studies utilize computational techniques[72,73,74]. The patterns discovered by such techniques and the synthesis of experimental data and theoretical concepts allow creation of models to explain complex phenomena. Effective studies of complex systems must be made by analysis of the parts (the “omic” tree) followed by a non-linear recombination to model as much

of the system as is known at the time[75,76]. In essence, the resulting model must exhibit its own emergent properties, allowing science to catch necessary glimpses that provide for the creation of new hypotheses. Manipulation of the model will then provide direction to the subsequent methodologies necessary to take the next steps in discovery. The computational challenge is creating models that contain sufficient elements and power to successfully predict how the process will respond to interventions. To develop useful integrative systems biology approaches, complexity theory and its computational tools must be utilized. This complexity approach is consistent with the overall NIH Roadmap initiative and specifically with the computational biology approach discussed in the initiative (http://nihroadmap.nih.gov/bioinformatics).

Ideally, a well-constructed computational model will offer a virtual laboratory to test biological hypotheses and therapeutic options prior to testing these theories *in vitro* or *in vivo[77]*. The ability of any model, from cell cultures to *in vivo* animal models to mathematical models, to make accurate predictions is dependent on the accuracy of the relation between the model and the real-world process that is being modeled[78]. This is especially true of mathematical models as all the observations are done *in silico*. Therefore, such a model will require extensive validation in order to prove it is an accurate reflection of the biological process being modeled.

Validation of a mathematical model is focused at two points: the underlying assumptions and the behavior of the model. The validation of the assumptions of the model can be addressed through comparing the architecture and rules of the model with what is known about the components of the modeled system. The difficulty lies in verifying the assumptions in the context of the *in*

silico model as all models represent some degree of abstraction. Validation of the behavior of the model consists of comparing the behavior of the model with some real-world data set of expected behavior. When the behavior of the model matches the real-world process, then the model is deemed valid for that particular test. *I.E.* the plausible validity of the model is based on similarity to real world findings. Conversely, if the model behavior does not match, then the model is invalid and must be reevaluated. Once the model is altered, the model must undergo the validation process anew (Figure 4). One problem involves determining the next step when a model behavior does not reflect real world behavior. The lack of fit may be due to calibration or to an error in the basic structure of the model; this validation will require extensive literature searches to obtain additional mechanistic insight as well as trial and error attempts at reconstruction.

The advantages of developing a successful mathematical/computational model cannot be overstated. Scientist will be able to test hypothesis nearly instantaneously. A successful model will target promising novel therapeutic approaches, thereby improving the success rates of clinical studies. It will also promote the discovery of new therapeutic approaches that come directly out of the modeling process. The time from bench to bedside will be decreased as millions of experiments may be run on a model in a very short period of time allowing the investigator to choose the best possible intervention strategy prior to any clinical trial[79]. Intervention strategies may be streamlined and personalized prior to clinical application.

Ordinary differential equations- ODEs provide a valuable tool for analysis and prediction of biological systems over time. The ODE paradigm is based on a series of equations that describe

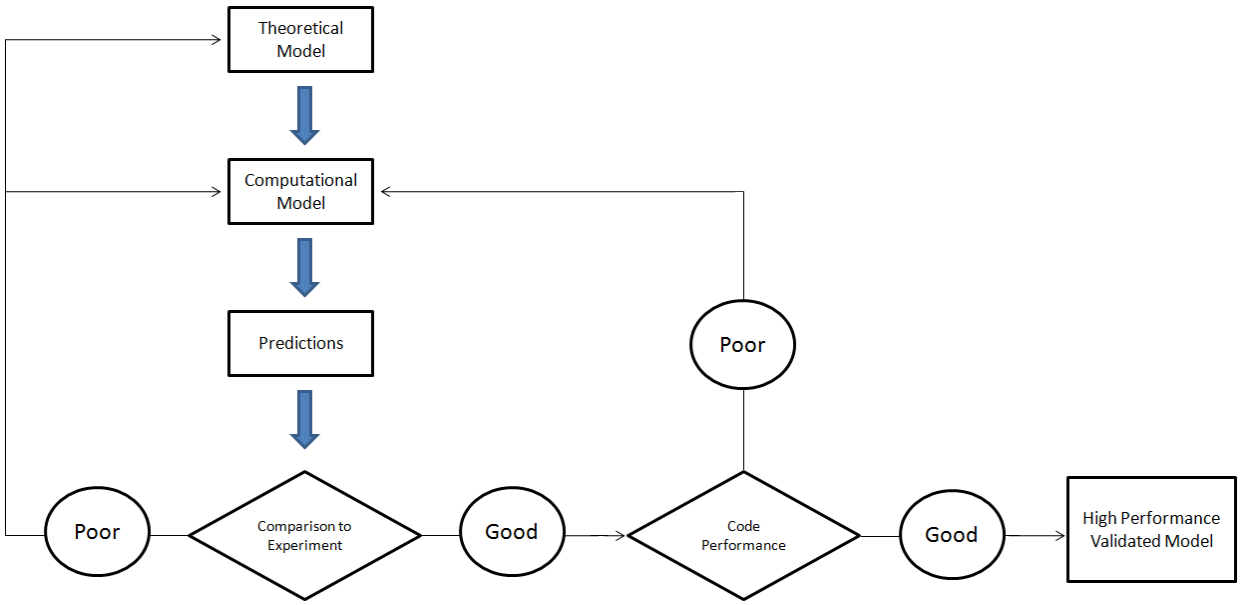

Figure 4: Computational Modeling Flow Diagram. The flow diagram demonstrates the iterative process required for creation of a high performance, validated model.

the change in the states of the variables of the system over time[80]. The differential equations are derived from a combination of known and hypothesized kinetics of the components of the biologic system[81,82]. In general, the equation variables represent average concentrations of the various components. Furthermore, parameters are embedded in the equations that represent the state of the system being modeled. If they are not too complex, a system of ODEs can be solved analytically. Otherwise, they can be solved computationally and analyzed using methods from nonlinear analysis to explore the properties of the system. Because these equations are based on biologic interactions, ODE can predict outcomes beyond the range of available data. The most valuable aspect of an ODE is the ability to manipulate the variables allowing the manipulation of a biologic mechanism and providing an outcome that may be analyzed; thereby, allowing *in silico* experiments and subsequent *in vivo* experimental validation.

Such a dynamic systems can used to capture the gross behavior of the system. The advantages of using ODE include: 1) the ability to explore properties of the system using non-linear analysis techniques 2) prediction of outcomes beyond the range of available data, and 3) manipulation of variables to determine the effects on the system. Unfortunately, there are also disadvantages of ODE including: 1) multiple feedback loops lead to equations that are difficult to solve, 2) *a priori* necessity of a complete description of the system, and 3) spatial dynamics are difficult to simulate.

Agent Based Modeling - In order to address the shortcomings associated with ODE models, we present the application of a computational systems biology approach using agent based modeling and simulation (ABMS)[83,84]. ABMS provides a powerful alternative to differential equations. ABMS is a relatively new modeling paradigm derived from cellular automata (CA). CA was originally developed by Stanislaw Ulam and John von Neumann and more recently popularized by Stephan Wolfram[85,86,87]. CA is an abstract mathematical representation of a machine, which can be made to operate on a set of rules. A CA is a 2-D grid consisting of spaces called "cells". Each cell is allowed to assume a finite number of states, each of which is determined by a pre-defined set of update rules. A CA update rule is defined as the rule that every CA follows that determines its state at the next time step as a function of its current state and the state of its neighbors. Thus, CA are complex systems in that you have large numbers of components with no central controller and only local communication. Such CA may exhibit emergent behaviors that cannot be predicted from the CA rule. ABMS is an extension of CA in that it has mobile components that can move through the grid.

ABMs analyze biological systems based on the interactions among its components. ABMs are dynamic systems that are discretized: time, space, and internal state[3,88,89,90]. ABM behavior is defined by rules that are a function of their local environment and their state. ABM models are built on a grid of usually square spaces that are capable of entering a finite number of states. Each agent is assigned a state with a discrete probability of interacting with agents around it. Every agent has the same set of rules for updating its internal state. Based on the values of its neighboring agents and its current state. At each time step, the rules are applied to the whole grid and a new generation of agents is created

ABMs are based on creating rules and defining mechanisms of behavior for the individual components of system. The components of a system are classified into types of agents by virtue of shared behavior. The behavior mechanisms are expressed as a series of conditional rules that allow easy conversion into computer programs. Again the rules are created based on known and hypothesized mechanisms. A simple example would be the creation of an agent that represents fibroblasts that when exposed to TGF-B synthesizes collagen. The model defines a world based on defined characteristics and generates populations of the various types of agents. The agents are able to interact based on programmed behaviors that are defined by their rule systems initiated by inputs from their environment. For example, fibroblasts would respond to growth factors and cytokines that are secreted by other fibroblasts that they encounter in their immediate neighborhood. In order to mimic real systems, the agents run in a parallel. The resulting dynamics of the system then emerge from the multiple interactions between the agents over time rather than dictated by an overlying controller. This type of modeling is “bottom up,” as all

measured output parameters and the resultant outcomes from the model are generated by the actions of the individual agents. One of the advantages of ABM is the intuitive rule based definitions that are easily understood by non-mathematicians. Furthermore the mechanistic rule based nature of ABMs allows the simulation of any intervention that deals with a defined mechanism.

Agent based modeling is an approach to simulating the behavior of a complex system in which agents interact with each other and with their environment through simple local rules. Again the rules will be derived from experimental data as well as literature-mining. The advantage of such a technique include: 1) non linear relationships are easily modeled 2) the model is intuitive and does not require higher level mathematics for use and understanding, and 3) flexibility. The disadvantages of agent based modeling include: 1) difficulty with validation 2) large amounts of computational power needed for large simulations.

ABMS provide significant advantages over other modeling paradigms when modeling biologic systems[79,83,84]. The models are flexible in that changes in agent behavior may be done without having to reprogram the whole model. This flexibility allows a wide range of behaviors to be captured. The coding of such models may be mechanistic based. Every aspect of how agents behave and interact must be explicitly coded. Additionally, the variables that determine the agents' behavior must also be defined. This behavior is usually coded at mechanistic levels allowing hypothesis to be easily tested. The agents are able to adapt and change their behavior based on their environment. As all biological processes are inherently dynamic, the ability of such agents to capture the dynamic behavior of systems is critical. The models are easily

scalable. Once the behavior of a given agent is defined, inhabiting a system with multiple instances is easy. Therefore, examining the behavior of a system of arbitrary size is more a function of computational speed and systems resources rather than ability to generate larger models. One of the greatest strengths of such models is to create virtual experiments. The experiments can be repeated an arbitrary number of times and the data can be analyzed using traditional statistics. This allows direct comparisons between the *in silico* models and *in vivo/vitro* experimental data. ABMS allow constructive proofs of systems. *I.E.* you create a model that generates a behavior. Regardless of in vitro/vivo observation of this behavior, the in silico model results imply that there is at least one set of conditions that may create such behaviors. This allows us to grow generative models that capture systems as they are expanded. Another important aspect of such models is their ability to run many experiments at a very low cost. Once the model is created, the cost of running such models is usually minimal.

An *In Silico* Approach to the Analysis of Acute Wound Healing

Nathan B. Menke MD[1,2], John W. Cain PhD[3,4] , Angela Reynolds PhD[4], David M. Chan[3,4], Rebecca A. Segal PhD[3,4,*], Tarynn M. Witten PhD [1,3], Danail G. Bonchev PhD[3,4], Robert F. Diegelmann PhD[1,2], and Kevin R. Ward MD[1,2,3]

[1]Virginia Commonwealth University, Department of Emergency Medicine, PO Box 980401 Richmond, VA 23298
[2] Virginia Commonwealth University, Department of Biochemistry, PO Box 980614, Richmond, VA 23298
[3] Virginia Commonwealth University, Center for the Study of Biological Complexity, 1000 West Cary Street, Suite 111, Richmond, Virginia 23284
[4] Virginia Commonwealth University, Department of Mathematics, PO Box 842030, Richmond, VA 23284

*Corresponding Author: Virginia Commonwealth University, Harris Hall 4177, 1015 Floyd Ave Richmond, VA 23284-2014, (804) 828-4756 (Office), (804) 828-8785 (Fax), rasegal@vcu.edu

Abstract

The complex interactions that characterize acute wound healing have stymied the development of effective therapeutic modalities. The use of computational models holds the promise to improve our basic approach to understanding the process. By modifying an existing ordinary differential equation model of systemic inflammation to simulate local wound healing, we expect to improve the understanding of the underlying complexities of wound healing and thus allow for the development of novel, targeted therapeutic strategies. The modifications in this local acute wound healing model include: evolution from a systemic model to a local model, the incorporation of fibroblast activity, and the effects of tissue oxygenation. Using these modifications we are able to simulate impaired wound healing in hypoxic wounds with varying levels of contamination. Possible therapeutic targets, such as fibroblast death rate and rate of fibroblast recruitment, have been identified by computational analysis. This model is a step towards constructing an integrative systems biology model of human wound healing.

Introduction

A soft tissue injury elicits a well-prescribed wound healing response[1, 2]. The process of wound healing is designed to restore anatomic and functional characteristics of the tissue; however, little progress has been made in improving the wound healing response time or in preventing complications such as fibrosis, infections, and formation of non-healing wounds[3]. In this paper, we describe a computational model of acute wound healing designed to allow a system-level analysis of the wound healing response using ordinary differential equations (ODEs). As a first step to a more comprehensive model, we have explored the combined effects of bacterial infections, inflammation, and tissue hypoxia on the rate and success of wound healing since these processes are well-known as affecters of healing. As this model matures, it will provide the opportunity to test new mechanisms and novel therapeutic of wound healing strategies *in silico*.

Despite burgeoning interest in the field of computational biology, work of limited scope has been published on modeling the acute wound. Most of these studies demonstrate the difficulties of adequately accounting for the myriad of potential interactions[9]. For example, in their respective works on epidermal wound healing, Stekel et al.[10], Walker et al.[11] and Morel et al.[12] do not attempt to simulate healing by fibroblasts and do not implement inflammatory changes in their models. Dallon et al.[13] constructed an ODE model of collagen deposition focusing on the fibroblasts and their relationship to the underlying extracellular matrix, but do not account for inflammation or repair of underlying tissue damage. Schugart et al.[14] recently published a model of wound angiogenesis as a function of tissue oxygen tension but the model does not specifically address the wound healing process.

Reynolds et al.[15-16] created an ODE model designed to simulate inflammation and repair on a systemic level in the setting of a systemic insult such as sepsis. We have modified and extended their work to apply it to a local wound. ODEs provide a valuable tool for analysis and prediction of biological systems over time[17]. ODEs model the changes in important physiological variables over time. The equations are derived from a combination of known and hypothesized kinetics of the components of the biological system. In our model, the state variables represent average concentrations of the various dynamic components. Furthermore, parameters are used in the equations to account for static components of the system being modeled. The system is solved numerically and the properties of the system can be explored mathematically. Because these equations are based on biological interactions, ODEs can predict outcomes beyond the range of available data. The most valuable aspect of a mathematical model is the ability to manipulate the variables and parameters, perform experiments *in silico,* and examine their results. The biological mechanisms of a wide range of potential situations may then be analyzed together with their outcomes. *In vivo* validation would then follow from *in silico* experimentation.

Materials and Methods

As a first attempt to capture the dynamics of local wound healing over time, a four-variable system of ordinary differential equations was developed. The variables in this model represent total local tissue (D)amage, (P)athogen level, overall i(N)flammation, and the concentration of (F)ibroblasts. For each of these variables we used known biological interactions to develop a differential equation that describes the rate of change for the variable. The interactions included in this model are depicted in the model schematic, Figure 1.

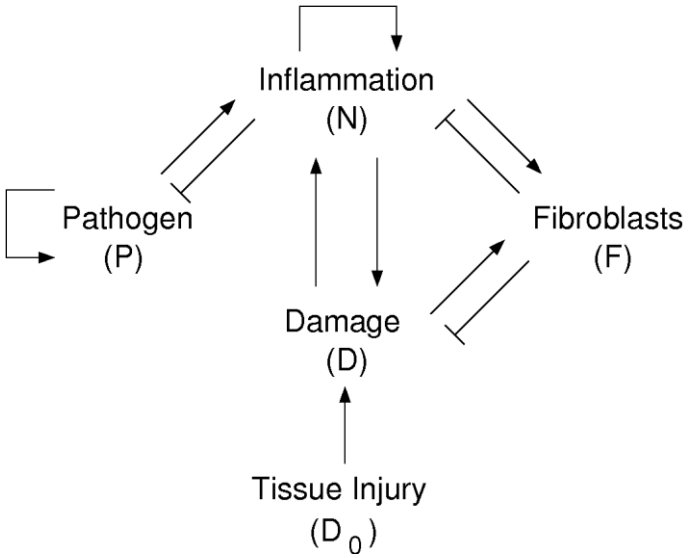

Figure 1: Model schema that illustrates the interactions between the four variables. Arrows indicate positive feedback and bars indicate negative feedback.

The fundamentals of the model are based on the observations that tissue damage is increased by inflammation and hypoxia, while wounds are repaired by fibroblasts[18-21]. Interpreting the interactions in Figure 1, we developed the four variable model, given below in Equations (1)-(4). This model was adapted from the four variable model created by Reynolds et al., which is included in Appendix A.

$$\frac{dP}{dt} = p_{growth} P\left(1 - \frac{P}{P_\infty}\right) - \frac{k_{pm} s_m P}{\mu_m + k_{mp} P} - k_{pn} f(N;F) P \tag{1}$$

$$\frac{dN}{dt} = \frac{s_{nr} R(P,N,D;F)}{\mu_{nr} + R(P,N,D;F)} - \mu_{fn} FN - \mu_n N \tag{2}$$

$$\frac{dD}{dt} = k_{dn} f_s(f(N;F)) - \mu_d D - \mu_{df} DF + \beta_d g(O_2)\left(\frac{D^2}{D^2 + x_d^2}\right) \tag{3}$$

$$\frac{dF}{dt} = s_f + \frac{k_{fn} f(N + k_{fnd} D; F)}{1 + f(N + k_{fnd} D; F)} - \mu_f F \tag{4}$$

where $f_s(V) = \frac{V^6}{x_{dn}^6 + V^6}$,

$f(V;F) = \frac{V}{1 + (F / F_\infty)^2}$,

$R(P,N,D;F) = f(k_{np}P + k_{nn}N + k_{nd}D;F)$,

$g(V) = \frac{-\alpha\left[1 - \exp((1+\alpha)(O_{crit} - V))\right]}{1 + \alpha\exp((1+\alpha)(O_{crit} - V))}$,

and, $p_{growth} = \begin{cases} k_{pg}, & if \quad O_2 \geq O_{crit} \\ k_{pg} + \beta_p\left(1 - \frac{O_2}{O_{crit}}\right), & if \quad O_2 < O_{crit} \end{cases}$.

The difficulties in modeling complex physiologic processes are defining the system variables and representing their interactions mathematically. To address this, we have combined related cell types and signaling process together. As a result, it is not possible to have units on many of the biological quantities. Specifically, because tissue damage is complex and involves many biological markers, it is a difficult quantity to measure. Thus in this model D has no units. Instead, we track the relative changes over time and evaluate healing based on percentage change of damage (D), with a return to under 10% damage considered healed.

Pathogen Equation

In developing Equation (1), the pathogen equation, we made similar assumptions to those used to develop the pathogen equation in Reynolds et al. We assumed that the pathogen population has

a growth rate of p_{growth} and a carrying capacity of $P\infty$ giving rise to the first term of Equation. Unlike the Reynolds et al. model we take into account that the pathogen population is increased in low oxygen environments[19]. Therefore, p_{growth} is a function of the oxygen level in the local environment and determined by the function:

$$p_{\text{growth}} = \begin{cases} k_{pg} & \text{if } O_2 \geq O_{\text{crit}} \\ k_{pg} + \beta_p \left(1 - \frac{O_2}{O_{\text{crit}}}\right) & \text{if } O_2 < O_{\text{crit}} \end{cases}$$

This relationship between tissue oxygenation levels and bacterial growth is illustrated in Figure 2a. with O_{crit} set to 5, which is equivalent to a transcutaneous oxygen level of 30mm Hg[22, 23]. If the tissue oxygen level is above the critical value, p_{growth} is fixed at 0.3, since the effects of hyperbaric oxygen on wound healing are not included in this model. However, this function does capture the increase in anaerobic pathogen reproduction that occurs in hypoxic environments. The second term in Equation (1) is directly from the Reynolds et al. model and accounts for local immune mediators that immediately interact with the pathogen, such as defensins and non-specific antibodies.

Inflammation recruited to the wound is generally thought to assist in the destruction of pathogens and thereby is assumed to decrease pathogen levels, while causing some degree of tissue damage[2, 4, 24-26]. The effect of this process on pathogen level is modeled with the third term of Equation (1). We model the depletion of pathogen from an encounter with an inflammatory cell with a term of the form $-k_{pn} N\ P$. However, since fibroblasts modulate the inflammatory response by initiating wound repair, N in this term is replaced with $f(N;F)$.

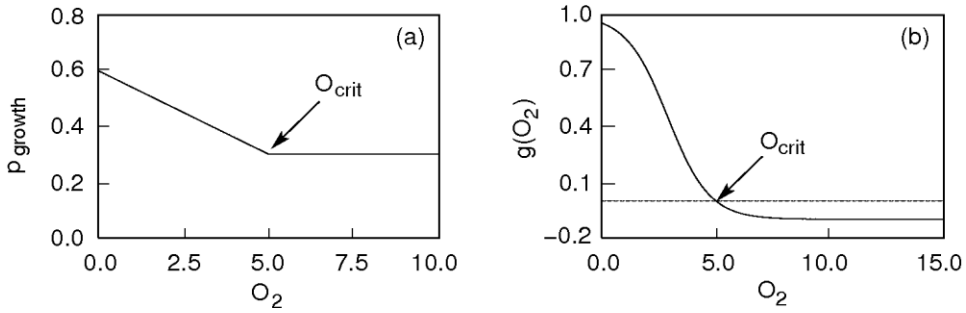

Figure 2: (a) Dependence of the pathogen growth rate on tissue oxygenation. Anaerobic pathogen growth rate increases at lower oxygen levels. (b) Graph of the function $g(O_2)$, illustrating the impact of tissue oxygenation on rate of damage increase. Oxygen levels below the critical level O_{crit} promote additional damage, whereas higher oxygen levels decrease the rate of damage.

The function $f(N;F)$ represents the inhibition of inflammatory cells by fibroblasts. We use the same definition of the function $f(N;F)$ as in Reynolds et al., since we are modeling the down-regulation of the same cell population. Including this inhibition produces the third term of Equation (1): $-k_{pn}f(N;F)P$.

Inflammation Equation

Inflammatory cells are recruited by pathogens, damaged tissue, and other inflammatory cells and mediators[21, 25]. Incorporating this activation of the inflammatory cells into the model we get the first term of inflammation equation, Equation (2). First we assume that inflammatory cell activation is triggered by the three variables N, D, and P giving a rate of activation of $R = k_{np}P + k_{nn}N + k_{nd}D$. As in the pathogen equation, Equation (1), we account for the inhibition of inflammation due to the presences of fibroblasts and we replace the basic activation rate with one that includes inhibition $R(P,N,D;F) = f(k_{np}P + k_{nn}N + k_{nd}D;F)$. The process of activation occurs on a faster time scale than the other interactions included in this model, this allows us to

not explicitly track the resting population of inflammatory cells, and to model activation with the sigmoid function $\frac{s_{nr} R(P,N,D;F)}{\mu_{nr} + R(P,N,D;F)}$. Further details on the derivation of this term are in Reynolds et al.

Fibroblasts are recruited to the wound by tissue damage and inflammation and are able to repair tissue damage and modulate the inflammatory response [2, 4, 27-29]. This modulation of the inflammatory response is represented with the term $-\mu_{fn} FN$ in Equation (2). The inflammation population will decrease at greater rate when fibroblasts are at a higher level.

The majority of cell types, such as inflammatory cells and fibroblasts, are not immortal; their half-life determines the duration of their efficacy[30, 31]. Therefore, as traditionally found in most ODE models, the half-lives of inflammatory cells and fibroblasts were used to represent the average decay rate of a cell[17]. Incorporating the intrinsic decay of the inflammatory cells we get the final term of Equation (2), $-\mu_n N$.

Damage Equation

Tissue is damaged not only by the initial wound, but also by the influx of inflammatory cells to the wound site during the inflammatory stage of wound healing. To model this dependence of the damage level on the inflammation we use $k_{dn} f_s(N)$. The function f_s is a nonlinear function of N, because low levels of inflammation are not as effective at inducing tissue damage. We also include inhibition of inflammatory cells in this term. Therefore, in Equation (3), we have the term $k_{dn} f_s(f(N;F))$.

The amount of damage that is repaired is proportional to both the current amount of damage and the amount of fibroblasts present. This leads to the term $-\mu_{df} DF$ in the damage equation, Equation (3). Damage is decreased at a faster rate when fibroblast levels are higher. Also we include the term $-\mu_d D$ in Equation (3) to model intrinsic tissue repair.

The final term in Equation (3) models the impact of tissue oxygenation O_2 level on the rate of change of damage. This impact is described by the function $g(O_2)$ (Figure 2b), which is designed to capture the increase in damage in hypoxic environments and to represent a small healing effect if O_2 is larger than the critical value, O_{crit}[22. 23].

Fibroblast Equation

The final equation, Equation (4), models the fibroblast population. We assume in normal skin there is a background source of fibroblasts, s_f. This gives rise to a baseline level of circulating fibroblasts, which exist in both pre-wounded tissue and healed tissue.

In response to tissue damage and inflammation, the fibroblast population will increase. The second term in Equation (4) models this growth when inflammation and/or damage are nonzero. The term has the form $\frac{k_{fn}(N + k_{fnd} D)}{1 + (N + k_{fnd} D)}$ because we assume the dependence of the fibroblast population on levels of damage and inflammation is nonlinear. That is, at low levels of inflammation and damage the recruitment of fibroblast is slow, while at high levels the process

of fibroblast recruitment saturates. As with other terms involving inflammation the process is inhibited using the same function, *f*, so the final form of the term is $\frac{k_{fn} f(N + k_{fnd} D; F)}{1 + f(N + k_{fnd} D; F)}$.

As described above, fibroblast have an intrinsic death rate, μ_f, and this is modeled by the final term of Equation (4), $-\mu_f F$.

Simulations

Our model equations were solved numerically using both the software package XPPAUT[32] (XPPAUT is a freely available software package for solving differential equations available for download at http://www.math.pitt.edu/~bard/xpp/xpp.html) and several of our own independently developed C++ computer programs. A list of baseline parameters is included in Table 1 for reference. The parameters were derived from experimental values found in the literature or estimated such that the system behaved in a biologically appropriate manner[15, 22, 23]. We performed several *in silico* experiments to investigate the effects of (i) varying the amount of initial damage, D(0), and the initial pathogen levels, P(0), and (ii) varying certain parameters such as the tissue oxygenation level O_2 and the rate of fibroblast recruitment s_f.

In each experiment, we simulated two weeks of the wound healing process (336 hours) after the initial wound insult in order to observe more of the transient effects en route to steady state[33]. Two weeks provides an adequate amount of time for normal wounds to heal. The resulting end state of the wound was categorized as one of three types:

- *Healed* if the damage is decreased by 90% within 2 weeks (i.e. for D(0)=10, damage is less than 1 after 2 weeks);

- *Non-healing wound* if damage remains higher than 10% of initial damage and pathogen levels decrease to zero (i.e. for D(0)=10, P(0)>0, damage is greater than 1 but pathogens are nonexistent after 2 weeks); and
- *Chronic infection* if both damage and pathogen levels remain at above 10% of their initial levels after 2 weeks (i.e. for D(0) =10, P(0) = 1, damage is greater than 1 and pathogen is greater than 0.1 after 2 weeks).

The non-healing wounds as defined above correlate clinically to wounds in which there is impaired wound healing, but are not infected[2-4, 24, 34, 35]. Chronic infections as defined above correlate clinically to wounds that are infected and are thereby unable to heal normally[2-4, 34, 35].

Results

All simulations started immediately after the wound formation. In the model, this translated to no initial inflammation (N(0)=0) and to the initial level of fibroblasts at a normal background level (F(0)=0.1). Initial damage and initial pathogen levels were set to represent different injury scenarios. Unless otherwise specified, all parameter values were set to their baseline values (Table 1).

Figure 3 is the baseline simulation and shows normal healing behavior in a small, uncontaminated wound with normal perfusion (D(0) =0.2 and P(0) = 0). As expected, this type of wound elicits a brief period of a slightly elevated inflammatory response and an increase in fibroblast level. This scenario results in normal healing of the wound, which is represented by the damage variable decreases to zero within two weeks.

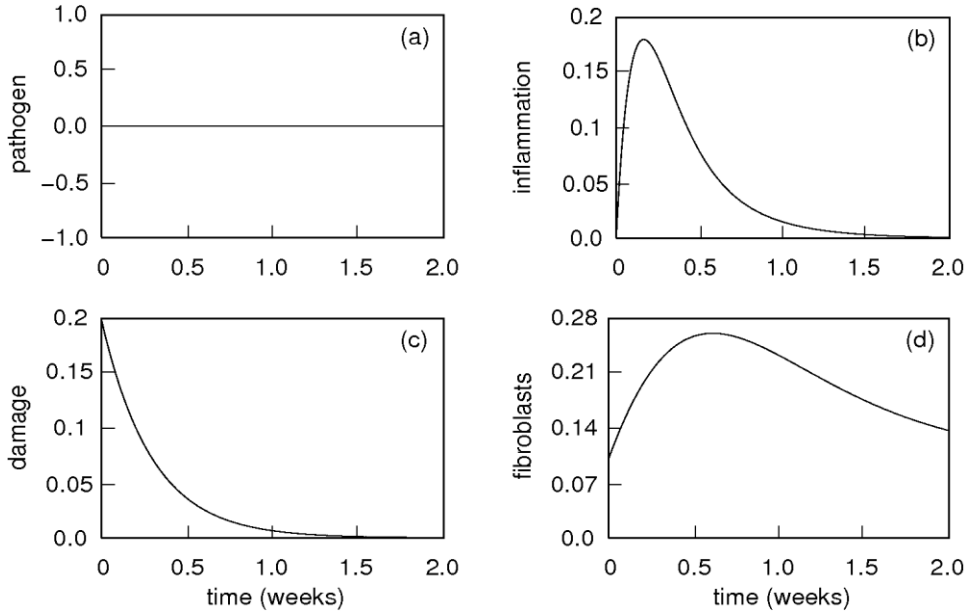

Figure 3: Healing behavior of a small, "clean" wound (D(0) = 0.2, N(0) = 0, F(0) = 0.1, and P(0) = 0). (b) Inflammation peaks within two days after initial insult, and decays to 0 within two weeks. (c) Damage steadily decreases, and after two days the amount of wound damage is approximately half its initial amount. (d) Fibroblasts peak three to four days after initial insult, and then return to their baseline value within two weeks.

The first experiment focused on increasing the initial wound size (D(0) = 2; 10-fold increase from Figure 3) while leaving pathogen levels at zero (P(0) = 0). Figure 4 illustrates the effect of this change on the behavior of the wound. The significantly increased initial wound size, leads to a non-healed wound at two weeks where damage, fibroblasts, and inflammation all plateau at an elevated level. This correlates clinically to large acute wounds that require prolonged healing times and are at increased risk for developing infections[4, 36].

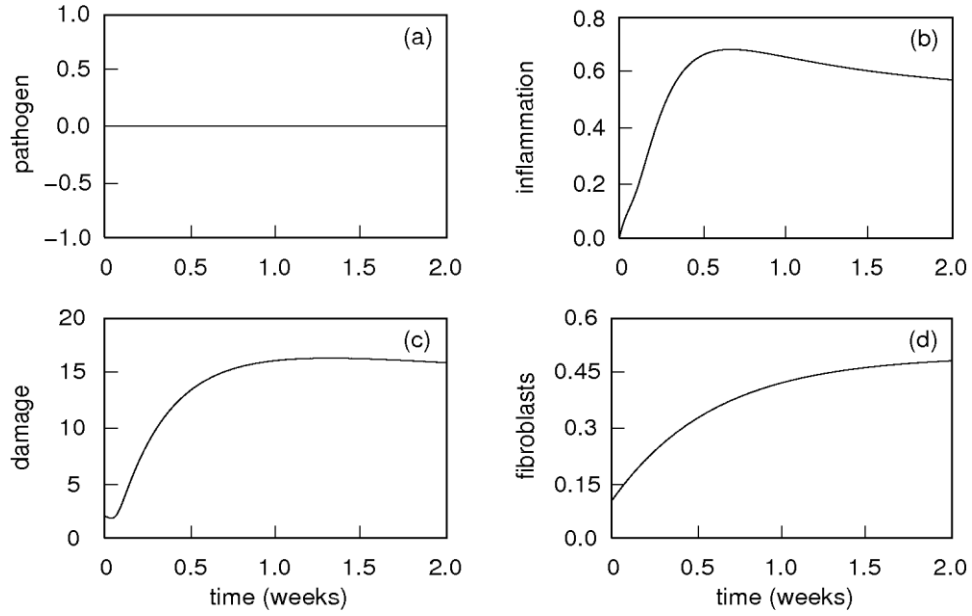

Figure 4: Non-healing wound of large initial size and no initial pathogens (D(0) = 2, N(0) = 0, F(0) = 0.1, and P(0) = 0). (a) The pathogen level remains at 0 for the duration of the simulation. (b-d) Inflammation, damage, and fibroblast levels plateau at elevated levels, and the wound persists even after two weeks.

Figure 5 shows the impact of tissue oxygenation levels on wound healing behavior by plotting the pathogen and damage levels for three different levels of O_2. For each level of oxygenation the wound has a moderate initial size and pathogen level (D(0) = 0.5 and P(0) = 0.3). All parameters except O_2 were held at their baseline values. If the tissue oxygenation is at the borderline level ($O_2 = O_{2crit}$=5.0; equivalent to a transcutaneous oxygen level of 30mm Hg[22, 23]), the wound begins to heal after a two-day transient period during which the amount of tissue damage increases in size as a result of the inflammatory response (Figure 5 a,b).

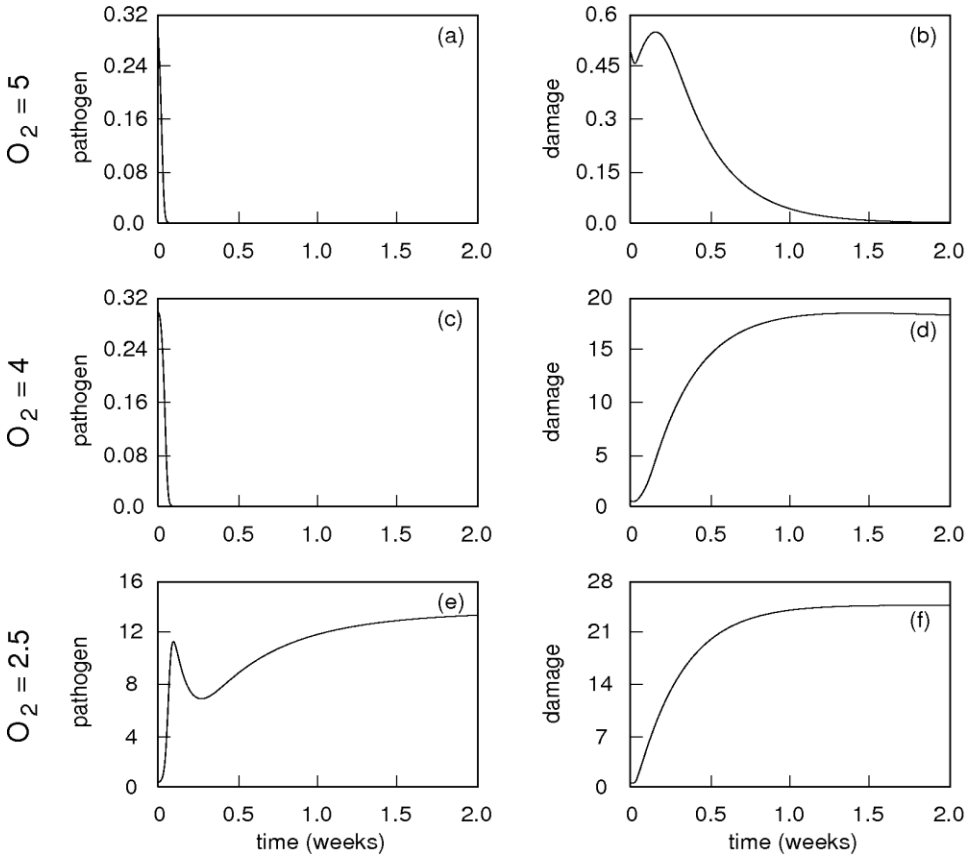

Figure 5: Transients for pathogen and damage with various O_2 values**.** For all three O_2 values the initial conditions used were D(0) = 0.5, N(0) = 0, F(0) = 0.1, and P(0) = 0.3. (a) and (b): are the pathogen and damage transients, respectively, for a O_2 value of 5, which is the value of O_{2crit}. (c) and (d): the pathogen and damage transients, respectively, for a O_2 value of 4.0, which results in a non-healing wound. (e) and (f) : the pathogen and damage transients, respectively, for a O_2 value of 2.5, which results in a chronic infection.

Both the damage and inflammation return to zero and the fibroblasts are decreasing toward their background level by the end of two weeks. We also simulated the same wound in a reduced oxygen environment, where O_2 is below the critical level (O_2 = 4.0), which leads to significant impairment in wound healing (Figure 5 c,d). The pathogens are successfully removed, but damage persists beyond two weeks. Finally, if the tissue oxygenation is further lowered (O_2 = 2.5), both pathogens and damage plateau at an elevated level, corresponding to chronic infection (Figure 5 e,f). These represent the types of non-healing wounds, both infected and non-infected, seen in patients with vascular insufficiency[2, 37].

In a third experiment, we investigated the combined effect of tissue oxygenation (O_2) and fibroblast mortality rate (μ_f) on the wound healing behavior, leaving all other parameters at their baseline values. By increasing the fibroblast mortality rate, we simulated the premature senescence of fibroblasts observed in older patients and diseases such as diabetes mellitus[4, 36, 38]. Figure 6 illustrates the wound healing behavior for different choices of initial conditions. In Figure 6a, the initial damage and pathogen levels are low (D(0) = 0.2 and P(0) = 0.2), and the wound always heals within two weeks if $O_2 > O_{crit}$ and fibroblast half life is at baseline (μ_f = 0.01). If the mortality rate is increased beyond a critical value ($\mu_f > 0.14$), the high mortality of fibroblasts invariably results in a non-healing wound. In hypoxic environments, we observe non-healing wounds even when fibroblast mortality is low as a direct result from tissue necrosis. Figure 6b shows the impact of doubling the initial pathogen level (P(0) =0.4). In this case, both the regions of non-healing wound and chronic infection become substantially larger.

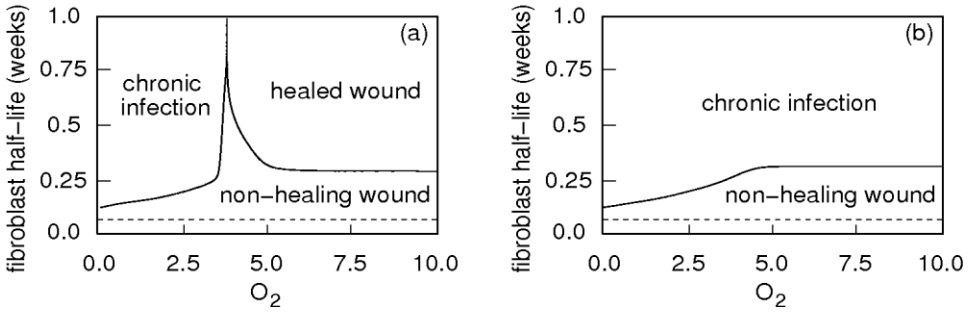

Figure 6: Long-term wound behavior for various choices of tissue oxygenation O_2 and fibroblast mortality (μ_f) (N(0) = 0 and F(0) = 0.1). (a) A wound with initial damage D(0) = 0.2 and pathogen level P(0) = 0.2. Large fibroblast mortality always leads to non-healing wound. If the fibroblast mortality is lower, then we observe chronic infection in hypoxic environments and healing if tissue oxygenation is appropriately large. (b) If the initial pathogen level is doubled to P(0) = 0.4, the regions of chronic infection and non-healing wound are substantially larger, and the wound is unable to heal within 2 weeks time. Simulations were not run for fibroblast half-life values less than 12 hours (marked by the dashed lines in each plot), since values below this level are typically unseen.

To understand if an advanced therapy might impact wound outcome, we designed an *in silico* experiment to investigate the possible impact by varying the rate of fibroblast recruitment (s_f), and analyzed the long-term healing behavior. We simulated the first two weeks after initial

insult for a wound with baseline initial conditions D(0) = 0.5, N(0) = 0, F(0) = 0.1, and P(0) = 0, for all parameters except fibroblast recruitment (s_f). For larger recruitment rates ($s_f > 0.012$), the wound heals within two weeks, whereas a non-healing wound results if recruitment is impaired ($s_f < 0.011$). Increasing s_f, i.e. recruiting more fibroblasts, has a strong impact on the overall healing time. For example, if $s_f = 0.001$, the wound requires 158.2 hours to shrink to 10% of its original size, as compared to 139.0 hours if s_f is doubled to 0.002 (Figure 7).

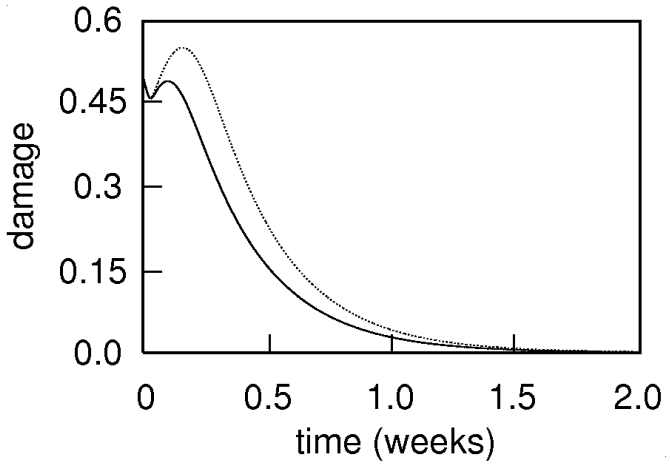

Figure 7: Comparison of damage vs. time for different fibroblast recruitment rates (D(0) = 0.5, N(0) = 0, F(0) = 0.1, and P(0) = 0). The dashed curve is damage transient for the baseline fibroblast recruitment rate, $s_f = 0.001$. The solid curve is the damage transient with the same initial conditions and a fibroblast recruitment rate twice baseline, $s_f = 0.002$.

By doubling s_f, the healing time decreases by about 12%. The maximum amount of damage, which accumulated as the wound healed, decreased by 11%. Furthermore, when s_f=0.002 the influx of inflammation to the wound site did not elicit more damage than the initial level of D=0.5. These experiments correlate to the use of agents such as recombinant PDGF[39] and basic fibroblast growth factor, bFGF[40]. The Akita et al.[40] study reported a 20% decrease in healing

time with the use of bFGF, which is on the same order of magnitude as the decrease seen our model experiment.

Discussion:

Mathematical models offer a non-invasive intermediary step between animal models and human subject studies that allows hypotheses and therapies to be tested prior to clinical studies. An *in silico* model would potentially increase the success rate of clinical trials or aid in designing more appropriate animal studies. These animal or clinical studies would then in turn, validate the model.

As an initial step to creating such a model, we have modified an ODE model of the acute wound healing response to a soft tissue injury. The model includes factors such as bacterial contamination and wound oxygenation. Assuming normal conditions, our model predicts the typical progression of healing behavior for a wound. The ODE model was also able to successfully simulate the impairment in wound healing found in a hypoxic wound environment and a contaminated wound. With extremely low levels of oxygen, our model predicts a chronic infection where the wound does not heal and pathogens persist in the wound. Both of these states are well documented clinically[35, 38].

We also examined the situation of elevated and depressed fibroblasts mortality rates. Clinically, instances of elevated fibroblast mortality are seen in diabetic and elderly patients. Here we saw that with high rates of fibroblast mortality the wound cannot heal. Additionally, a scenario of moderately low fibroblast mortality and high initial pathogen levels predicts the state of chronic

infection. Finally, we examined the case where fibroblast production is either impaired or enhanced. Impaired fibroblast production results in a non-healing state, but under conditions where the production is increased we have wounds that heal at notably faster rates. This provides a framework from which to test a new hypothesis in a living model.

The present study represents only a first step toward developing a detailed mathematical model of acute wound healing. Consequently, there are many opportunities for improving upon our existing model; these include,

- With the exception of time *t*, all quantities are measured in arbitrary units. By expanding the model to include variables that represent specific cell types and mediators one may estimate parameter values and assign physiologically meaningful units.
- In its present form, our model does not incorporate time delays. This prevents the simulation of the time lags inherent in signaling pathways as well as in fibroblast recruitment after the onset of inflammation.
- We did not attempt an exhaustive study of the impact of individual parameters on long-term healing behavior. Although we chose to focus on parameters such as the production and death rates of fibroblasts, it is likely that other parameters have a profound impact on healing.
- We focused on strongly interlinked local factors (inflammation, fibroblast function and recruitment, bacterial contamination, and tissue oxygenation) with resultant dynamic non-linear behaviors. Factors such as depth and shape of the wound, wound contraction, epithelization, and angiogenesis have not been addressed.

- We have not included systemic effects on wound healing, e.g., nutritional status, age, sex, and underlying comorbidities.

Despite the limitations inherent in our model, it does demonstrate the to use a systems biology approach to human wound healing. Mathematical models show great potential as a platform for hypothesis generation and experimentation prior to further refinement *in vitro* and *in vivo*. A refined method of computational analysis would decrease overall cost, time, and need for invasive testing. In the future, we hope to further elucidate the process of inflammation, epithelization, contraction, angiogenesis, and systemic effects, in order to create a model that more closely corresponds to the actual wound environment. Because our simplified model produces qualitatively reasonable results, we are optimistic that including systemic effects will enhance our understanding of the acute wound-healing process, ultimately leading to improved clinical therapies.

References

1. Singer AJ, Clark RA. Cutaneous wound healing. N Engl J Med 1999;341(10):738-46.
2. Diegelmann RF, Evans MC. Wound healing: an overview of acute, fibrotic and delayed healing. Front Biosci 2004;9:283-9.
3. Menke NB, Diegelmann RF. Biochemical Pathways of Wound Healing: Implications for Development of Disease-Specific Diagnostics. In: Makowski G, ed. Advances in Clinical Chemistry. Boston: Elsevier; 2006:168-88.
4. Menke NB, Ward KR, Witten TM, Bonchev DG, Diegelmann RF. Impaired wound healing. Clin Dermatol 2007;25(1):19-25.
5. Buchman TG. Nonlinear dynamics, complex systems, and the pathobiology of critical illness. Curr Opin Crit Care 2004;10(5):378-82.
6. Marshall JC. Complexity, chaos, and incomprehensibility: parsing the biology of critical illness. Crit Care Med 2000;28(7):2646-8.
7. An G. Mathematical modeling in medicine: a means, not an end. Crit Care Med 2005;33(1):253-4.
8. Buchman TG. In vivo, in vitro, in silico. Crit Care Med 2004;32(10):2159-60.
9. Sherratt JA, Dallon JC. Theoretical models of wound healing: past successes and future challenges. C R Biol 2002;325(5):557-64.
10. Stekel D, Rashbass J, Williams ED. A computer graphic simulation of squamous epithelium. J Theor Biol 1995;175(3):283-93.
11. Walker DC, Southgate J, Hill G, et al. The epitheliome: agent-based modelling of the social behaviour of cells. Biosystems 2004;76(1-3):89-100.
12. Morel D, Marcelpoil R, Brugal G. A proliferation control network model: the simulation of two-dimensional epithelial homeostasis. Acta Biotheor 2001;49(4):219-34.
13. Dallon J, Sherratt J, Maini P, Ferguson M. Biological implications of a discrete mathematical model for collagen deposition and alignment in dermal wound repair. IMA J Math Appl Med Biol 2000;17(4):379-93.
14. Schugart RC, Friedman A, Zhao R, Sen CK. Wound angiogenesis as a function of tissue oxygen tension: A mathematical model. PNAS 2008;105(7):2628-33.
15. Reynolds A, Rubin J, Clermont G, Day J, Vodovotz Y, Bard Ermentrout G. A reduced mathematical model of the acute inflammatory response: I. Derivation of model and analysis of anti-inflammation. J Theor Biol 2006; 242(1):220-36.
16. Day J, Rubin J, Vodovotz Y, Chow CC, Reynolds A, Clermont G. A reduced mathematical model of the acute inflammatory response II. Capturing scenarios of repeated endotoxin administration. J Theor Biol 2006;242(1):237-56.
17. Borrelli RL, Coleman CS. Differential Equations: A Modeling Perspective. 2nd ed. Hoboken, NJ: John Wiley & Sons, Inc; 2006.
18. Sen CK, Roy S. Redox signals in wound healing. Biochim Biophys Acta 2008;1780(11):1348-61.
29. Kuhne HH, Ullmann U, Kuhne FW. New aspects on the pathophysiology of wound infection and wound healing--the problem of lowered oxygen pressure in the tissue. Infection 1985;13(2):52-6.
20. Murdoch C, Muthana M, Lewis CE. Hypoxia regulates macrophage functions in inflammation. J Immunol 2005;175(10):6257-63.
21. Eming SA, Krieg T, Davidson JM. Inflammation in wound repair: molecular and cellular mechanisms. J Invest Dermatol 2007;127(3):514-25.
22. Ballard JL, Eke CC, Bunt TJ, Killeen JD. A prospective evaluation of transcutaneous oxygen measurements in the management of diabetic foot problems. J Vasc Surg 1995;22(4):485-90; discussion 90-2.
23. Caselli A, Latini V, Lapenna A, et al.. Transcutaneous oxygen tension monitoring after successful revascularization in diabetic patients with ischaemic foot ulcers. Diabet Med 2005;22(4):460-5.
24. Braiman-Wiksman L, Solomonik I, Spira R, Tennenbaum T. Novel insights into wound healing sequence of events. Toxicol Pathol 2007;35(6):767-79.
25. Martin P, Leibovich SJ. Inflammatory cells during wound repair: the good, the bad and the ugly. Trends Cell Biol 2005;15(11):599-607.
26. Weiss SJ. Tissue destruction by neutrophils. N Engl J Med 1989;320(6):365-76.
27. Grinnell F. Fibroblasts, myofibroblasts, and wound contraction. J Cell Biol 1994;124(4):401-4.

28. Buckley CD, Pilling D, Lord JM, Akbar AN, Scheel-Toellner D, Salmon M. Fibroblasts regulate the switch from acute resolving to chronic persistent inflammation. Trends Immunol 2001;22(4):199-204.
29. Smith RS, Smith TJ, Blieden TM, Phipps RP. Fibroblasts as sentinel cells. Synthesis of chemokines and regulation of inflammation. Am J Pathol 1997;151(2):317-22.
30. Harley CB, Futcher AB, Greider CW. Telomeres shorten during ageing of human fibroblasts. Nature 1990;345(6274):458-60.
31. Greenhalgh DG. The role of apoptosis in wound healing. Int J Biochem Cell Biol 1998;30(9):1019-30.
32. Ermentrout B. Simulating, Analyzing, and Animating Dynamical Systems: A Guide to XPPAUT for Researchers and Students. Philadelphia: SIAM; 2002.
33. Mast B. The Skin. In: Cohen I, Diegelmann R, Lindblad W, eds. Wound Healing; Biochemical and Clinical Aspects. Philadelphia: W.B. Saunders Company, ; 1992:344-55.
34. Bergan JJ, Schmid-Schonbein GW, Smith PDC, Nicolaides AN, Boisseau MR, Eklof B. Chronic Venous Disease. N Engl J Med 2006;355(5):488-98.
35. Watkins PJ. ABC of diabetes: The diabetic foot. BMJ 2003;326(7396):977-9.
36. Mustoe TA, O'Shaughnessy K, Kloeters O. Chronic wound pathogenesis and current treatment strategies: a unifying hypothesis. Plast Reconstr Surg 2006;117(7 Suppl):35S-41S.
37. London NJM, Donnelly R. ABC of arterial and venous disease: Ulcerated lower limb. BMJ 2000;320(7249):1589-91.
38. Harding KG, Moore K, Phillips TJ. Wound chronicity and fibroblast senescence--implications for treatment. Int Wound J 2005;2(4):364-8.
39. Lobmann R, Schultz G, Lehnert H. Proteases and the Diabetic Foot Syndrome: Mechanisms and Therapeutic Implications. Diabetes Care 2005;28(2):461-71.
40. Akita S, Akino K, Imaizumi T, Hirano A. Basic fibroblast growth factor accelerates and improves second-degree burn wound healing. Wound Repair Regen 2008;16:635–41.

Table 1. Baseline parameter values. * denotes estimated parameter

Parameter	Value	Comments
k_{pm}	0.6	Rate at which inflammatory cells kill pathogen nonspecifically*.
k_{pn}	0.6	Rate at which inflammatory cells kill pathogen by phagocytosis[15].
μ_n	0.05	Half-life of activated inflammatory cells[15].
F_∞	0.30	Maximum fibroblast density*.
k_{mp}	0.01	Rate at which non-specific inflammatory response is exhausted by pathogens*.
k_{np}	0.1	Rate of activation of inflammatory cells by pathogens*.
k_{nd}	0.015	Rate of activation of inflammatory cells by damaged tissue*.
s_f	0.001	Rate of fibroblast recruitment*.
s_m	0.005	Rate of inflammatory cell recruitment*.
k_{nn}	0.01	Rate of activation of inflammatory cells by activated inflammatory cells*.
k_{dn}	0.35	Maximum rate of damage by activated inflammatory cells*.
k_{fn}	0.004	Rate of fibroblast recruitment by inflammatory cells*.
k_{pg}	0.55	Rate of pathogen growth[15].
s_{nr}	0.08	Rate of inflammatory cell recruitment*.
x_{dn}	0.1	Level of inflammatory cells needed to bring damage to half its maximum*.
k_{fnd}	48	Effectiveness of tissue damage and inflammatory cells to

		recruit fibroblasts[15].
P_∞	20	Maximum pathogen density[15].
μ_{nr}	0.12	Half-life of inactivated inflammatory cells[15].
μ_d	0.02	Baseline damage repair rate[15].
μ_f	0.01	Half-life of the fibroblasts*.
μ_m	0.002	Half-life of non specific inflammation[15].
μ_{df}	0.002	Determines the amount of damage healed per unit damage per fibroblast*.
μ_{fn}	0.002	Determines that anti-inflammatory effects of fibroblasts*.
α	0.1	Along with μ_d, determines the amount of damage inflicted by hypoxia*.
x_d	2	Along with β_d determines the rate of tissue damage caused by hypoxia*.
β_p	0.3	Along with O_2/ O_{crit} ratio, determines the increase in anaerobic reproduction rate induced by hypoxic conditions*.
β_d	0.3	Determines the rate of tissue damage caused by hypoxia*.
O_{crit}	5	Critical oxygen level below which wound healing is impaired. Equivalent to a transcutaneous oxygen level of 30mm Hg[22, 23].
O_2	User Defined	Level of tissue oxygenation.

*Estimated parameter

Appendix A

The original equations from Reynolds et al.[15] are:

$$\frac{dP}{dt} = k_{pg}P\left(1-\frac{P}{P_{\infty}}\right) - \frac{k_{pm}s_m P}{\mu_m + k_{mp}P} - k_{pn}f(N^*)P$$

$$\frac{dN^*}{dt} = \frac{s_{nr}R}{\mu_{nr}+R} - \mu_n N^*$$

$$\frac{dD}{dt} = k_{dn}f_s(f(N^*)) - \mu_d D$$

$$\frac{dC_A}{dt} = s_c - \frac{k_{cn}f(N^* + k_{cnd}D)}{1+f(N^* + k_{cnd}D)} - \mu_c C_A$$

$$R = f(k_{np}P + k_{nn}N + k_{nd}D)$$

$$f(V, C_A) = \frac{V}{1+(C_A / C_{A\infty})^2}$$

C_A represents the amount of system anti-inflammatory mediator. The parameters s_c, k_{cn} and k_{cnd} correspond to S_f, K_{fn}, and K_{fnd}, respectively. N^* represents inflammation and all other variables and parameters are represented by the same notation as used in our model.

A Computational Model of Coagulation and Fibrinolysis

Nathan Menke[1,*] MD, Kevin Ward[1,2] MD, Lemont Kier[3] PhD
Cha-Kun Cheng[4] PhD, and Umesh Desai[5] PhD

[1]Virginia Commonwealth University Reanimation Engineering and Shock Center, PO Box 980401 Richmond, VA 23298
[2]Virginia Commonwealth University, Department of Emergency Medicine, PO Box 980401 Richmond, VA 23298
[3]Virginia Commonwealth University, Center for the Study of Biological Complexity, 1000 West Cary Street, Suite 111, Richmond, Virginia 23284
[4]Virginia Commonwealth University, Department of Computer Science, 401 West Main Street, Room E4225, P.O. Box 843019, Richmond, Virginia 23284
[5]Virginia Commonwealth University, Department of Medicinal Chemistry, 410 North 12th Street Room 155, P.O. Box 980581, Richmond, Virginia 23298

*Corresponding Author: Lincoln Hospital Medical and Mental Health Center, Department of Emergency Medicine, 234 East 149th Street Bronx, New York 10451, (804) 365-8632, (610)672-9405, nbmenke@aol.com

Abstract:

The coagulation and fibrinolytic systems are complex, inter-connected biological systems with major physiological roles. The complex, nonlinear multi-point relationships between the molecular and cellular constituents of two systems render a comprehensive and simultaneous study of the system at the microscopic and macroscopic level a significant challenge. We present an Agent Based Modeling and Simulation (ABMS) approach for simulating these complex interactions. Our ABMS approach utilizes a set of 106 rules to define the interactions among the 59 enzymes and factors of the coagulation/fibrinolysis (CF) system interacting with each other in a dynamic manner. These rules simulate the interaction of each "agent", such as substrates, enzymes, and cofactors, on a two-dimensional grid. This ABMS method successfully reproduces the initiation, propagation, and termination of blood clot formation and its lysis *in vitro* due to the activation of either the intrinsic or extrinsic pathways. Furthermore, the ABMS was able to simulate the pharmacological effects of two clinically used anticoagulants, warfarin and heparin, as well as the physiological effect of an enzyme deficiency/dysfunction, i.e., hemophilia and antithrombin III-heparin binding impairment, on the coagulation system. The results of the model compare favorably with *in vitro* experimental data under both physiologic and pathophysiologic conditions which assist in substantiating the model.

Introduction:

The coagulation and fibrinolytic systems maintain a constant, delicate balance between thrombotic response to acute blood loss versus the requirement of the vascular system to allow constant blood flow. Zymogen to enzyme conversions throughout these two cascades generates the proteolytic enzymes, thrombin and fibrin, that catalyzes the deposition and removal of fibrin respectively. Disruption of this equilibrium results in thrombotic events (e.g. pulmonary embolus) versus hemorrhagic events stemming from underlying coagulopathies (e.g. vonWillebrand's disease)[1]

In the event of an injury to the endothelium, the coagulation system balances the need for localized clot formation against the need to prevent system wide activation. This finely tuned system is composed of an assortment of molecular and cellular “agents” (e.g. substrates, enzymes, cofactors, inhibitors, platelets, and endothelial cells which interact to generate a stable clot in order to rapidly obtain hemostasis. The new cellular model of hemostasis proposes that the classical pathways of coagulation, i.e., the intrinsic and extrinsic pathways, mediate on specific cell surfaces in a tightly regulated manner. In this model, activation of factor VII (extrinsic, Fig. 1) and factor XII (intrinsic, Fig. 1) result in the formation of multi-molecular complexes, the tenase and prothrombinase complexes, which eventually generate thrombin. Thrombin then cleaves fibrinogen to form fibrin monomers, which polymerize to form a three-dimensional clot. Following repair of the underlying damage to the endothelium, the fibrinolytic system acts to dissolve the pre-formed clot. Fibrinolysis is achieved primarily through the proteolytic action of plasmin on fibrin polymers that reinforce and maintain the integrity of a thrombus (Fig 2).

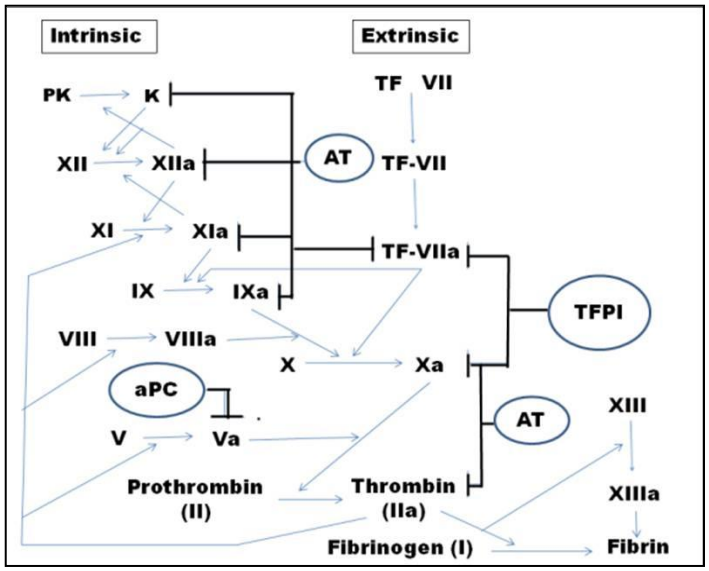

Figure 1: Coagulation Cascade and Inhibitors- Inhibitors denoted by circles. The intrinsic pathway is initiated by Prekallikrein or XII. The extrinsic pathway is initiated by TF. The intrinsic and extrinsic pathways join at the common pathway that begins after Factor X activation. AT, TFPI, and aPC are the three inhibitory pathways.

Clot formation is regulated *in vivo* primarily through the antithrombin III-heparin (AT-H), activated protein C (aPC), and tissue factor inhibitor (TFPI) pathways (Fig. 1)[2]. These regulating systems limit the excessive formation of cross-linked fibrin under hemostatic conditions. Similarly, anti-plasmin (AP), plasminogen activation inhibitor (PAI), and thrombin activatable fibrinolysis inhibition pathways prevent clot lysis until coagulation is complete (Fig 2).

The specificity of interactions, both molecular and cellular, involved in these complex processes supports the concept that the CF system displays global effects through emergence of localized events. The CF system may be viewed as a multi-component molecular machine[6], in which individual components are linked through multiple feedback and feedforward loops. This introduces non-linear relationships among the components. A static diagram such as the classically portrayed coagulation pathway

(Figure 1) cannot adequately describe this dynamic evolutionary network. Moreover, the effects of several disease states on the imbalances in the CF system are difficult to understand. For example, the influence of diseases that favor coagulation (*e.g.* coronary artery disease, disseminated intravascular coagulation, cerebrovascular accidents, and venous thrombosis), or those that impair coagulation (*e.g*. hemophilias, thrombocytopenias, and von Willebrand disease) remain poorly characterized in terms of the interactions of all components in the system over time.

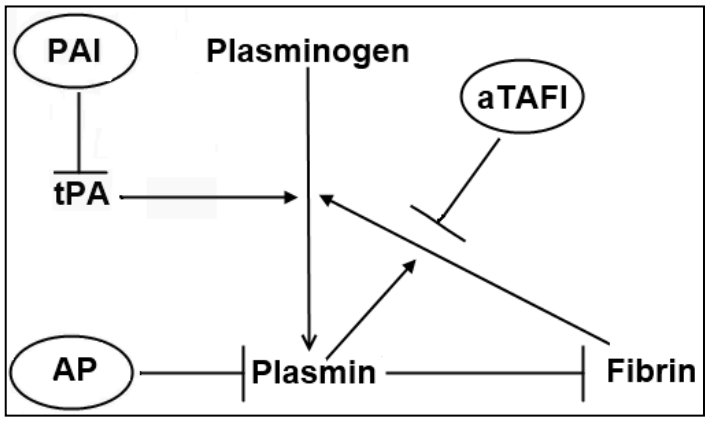

Figure 2: Fibrinolytic Cascade and Inhibitors- Inhibitors are denoted by circles. The fibrinolytic pathway is initiated by tPA activation of Plasminogen. Plasmin hydrolyzes fibrin. Plasmin and fibrin catalyze the conversion of Plasminogen to Plasmin.

To date, most computational models of the coagulation system have focused on using ordinary or partial differential equations (ODEs and PDEs) [15-18]. The differential equations describe the change in the states of the variables of the system over time and are derived from known or hypothesized kinetics. ODE models can readily simulate coagulation in vitro as it is a relatively homogenous system[3-5]; however, such models face significant limitations when modeling *in vivo* hemostasis because of complicating factors such as non-stationarity, spatial heterogeneity and the effects of blood flow[6]. Therefore, derivation of differential equations suitable for *in vivo* modeling becomes

problematic. Additionally, these models are incapable of demonstrating the randomness and variability within the system as it normally operates.

In order to address the shortcomings associated with ODE models, we present the application of a computational systems biology approach using agent-based modeling and simulation (ABMS) to understand the CF system and predict selected outcomes. ABMS provides a powerful alternative to differential equations[7-9]. ABMS is a relatively new modeling paradigm derived from cellular automata (CA)[10, 11]. ABMS has mobile autonomous entities (agents) that can move through a 2-D grid. Each agent is allowed to assume a finite number of states, determined by a pre-defined set of rules. Every agent is individually updated at the end of each operating period according to the pre-set rules. The rules are a function of the current state of the agent and the state of its neighbors.

As a first step, we created a model designed to simulate the *in vitro* environment. The goal of the model is to simulate common lab tests performed on patients.

Materials and Methods:

In this *in vitro* model all substrates, reactions, and products from the intrinsic, extrinsic, common, fibrinolytic, AT-H, TFPI, PC, AP, PAI, and TAFI pathways have been included. In order to create realistic simulations, physiologic concentrations of factors were used in the *in silico* experiments. The rates associated with the reactions were taken from the literature and were assumed to be performed in saturating phospholipid and calcium conditions. The simulations were designed to test experimental conditions that create

interesting thrombin profiles or to demonstrate perturbations associated with pathology or pharmaceutical agents associated with the system.

The ABMS approach utilized in this paper uses a two dimensional particle system. The particle model is one in which particles or 'agents' are able to move about and interact on a discrete spatial grid. In this case, the agents of the system are the reactants, enzymes, and products, as defined in the entity table (Appendix 1). Each agent's location on the spatial grid is defined in a two dimensional grid where the agent's location is determined by its x and y coordinates. Each coordinate pair (x, y) is defined as a unique grid location. Multiple agents may occupy a grid location. A total of 6,241 grid locations (Figure 3) were used in the coagulation simulations and 321 for the fibrinolytic simulations. A unit time step of the simulation represents 0.01 seconds.

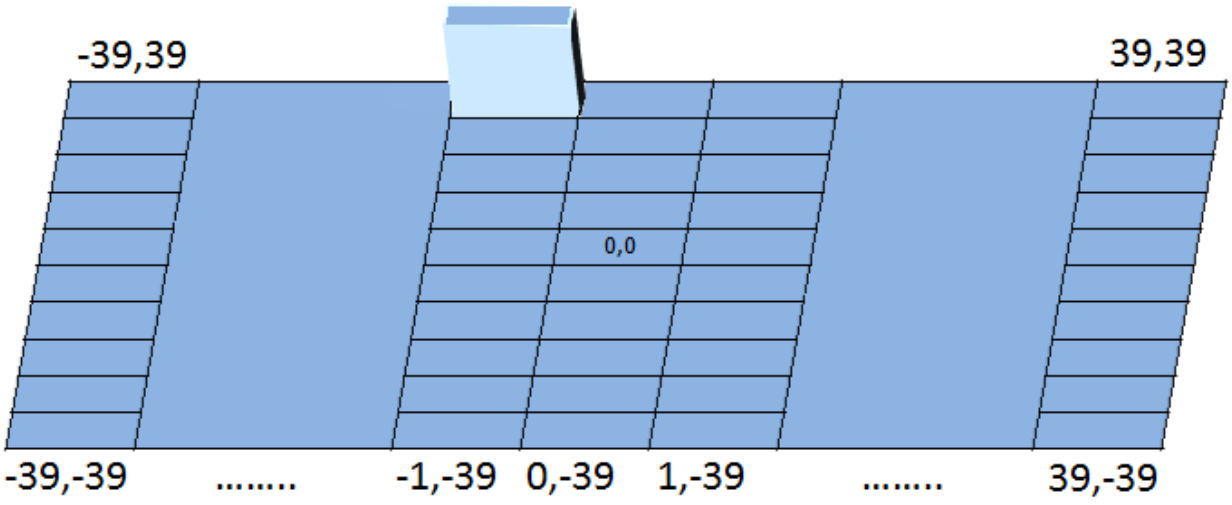

Figure 3: Spatial Grid - The spatial grid is three dimensional in that multiple agents are able to inhabit the same location.

Each grid location of the ABMS can be empty or can be occupied by one or more agents . The neighborhood of each agent was defined as all agents located in the

same grid location. After each time step, an agent was afforded complete freedom to move in a random manner to one of the adjacent cells. The movement of each agent, its joining, association, and dissociation with its neighbors are governed by probability rules. The movement parameter determines the extent of movement (0 implies every cell is stationary). The joining-association parameter determines the extent of a given agent interacting with an adjoining agent. The breaking parameter determines the extent of disruption of con-joined agents . The joining- breaking interactions were defined by the kinetics of the chemical equations that define the agents' behavior (Appendix 2).

ABMS of Coagulation – To simulate the coagulation phenomenon *in vitro* the probability of each interaction event has to be assigned based on biochemical properties. Each coagulation event is an enzymatic reaction with typical affinities in the nanomolar to sub-nanomolar range. These high affinities imply that the probability of conversion is directly correlated to the kinetics of the reactions. The movement parameter is set at one for every agent in the simulations which means they are free to diffuse across the grid. The initial configuration of ABMS contained a pre-defined number of agents for the initial reactants , which is proportional to the known concentration of agent under normal physiologic conditions. For example, 340,000 antithrombin agents were utilized corresponding to its 3.4 μM concentration in normal plasma. Likewise, 30 agents of VIII were present at initial conditions corresponding to its physiologic concentration of 0.3 nM. These agents were randomly distributed on the 2-D grid at time t=0.

Both the prothrombinase and tenase complexes are formed through a combination of three factors *in vivo*. For example, prothrombinase complex is formed by a combination of prothrombin, factor Xa and factor Va, while the intrinsic tenase complex is formed when factors VIIIa and IXa combine with factor X. These three body complexes are not directly simulated in ABMS, as *in vivo*, these complexes must arise through sequential combination of two molecules and thus, we utilized a sequential two-body collision approach to generate each complex.

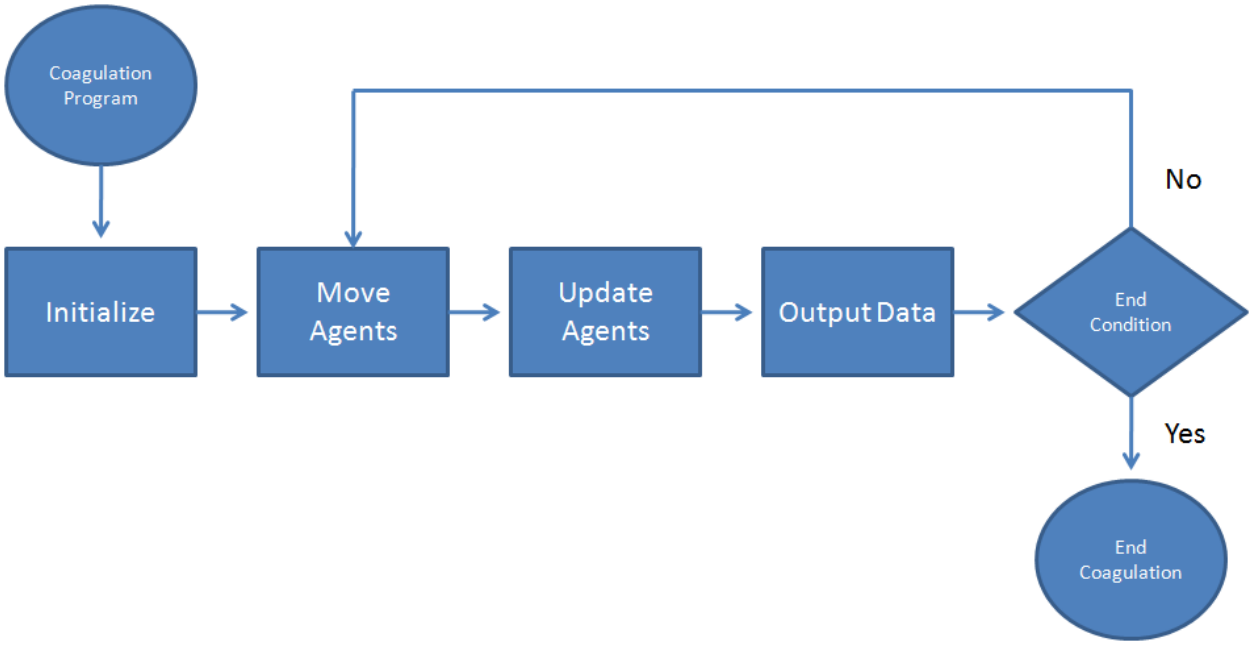

Figure 4: Computational Algorithm- The simple computational algorithm that controls the flow of the simulations.

The spatial grid is in the shape of a square allowing the agents to interact and bounce off the edge of the grid. The system was acellular with complete absence of platelets, RBC, or WBC representing plasma that is used in coagulation/fibrinolysis assays. The reactions and rate constants represented by the rule table are representative of

experimentally observed rates under saturating phospholipid and calcium concentrations. Figure 4 illustrates the algorithm used for running the simulations.

Computational Hardware and Software – A software package designed to run ABMS was utilized to design and perform the simulations (Netlogov4.04[12]). The user determines the subset of, reactions, reactants and coagulation factors, the probabilities of reactions, initial agent concentrations, and termination conditions for each simulation. The concentration of every coagulation factor was stored every 100 time steps (1 virtual second). All simulations were carried out on an Intel based desktop personal computer running Microsoft Windows XP. Because of the nature of the software and the large number of interactions, each simulation took between 1-72 hours depending on the initial and stop conditions.

Coagulation Simulations – Unless otherwise stated, modeling of the system was performed under conditions that simulated the mean physiologic concentrations of each soluble factor involved in the cascade, which were derived from literature reports (Appendix 3). The model was designed to simulate volumes of 2mL using 6241 grid locations. The model was tested under 1) conditions in which the type of agents was limited to a small subset of the coagulation factors or 2) conditions in which all the coagulation factors were represented. The simulations were designed to test experimental conditions that demonstrate pathology associated with the system. Each simulation was run ten times. Comparisons between the ABMS output and experimental data were used to determine the validity of the system.

Both PT and aPTT experiments were terminated when 99% of the initial fibrinogen was converted to fibrin monomers. When running PT experiments, an additional end condition of 135 seconds was defined. This time equates to an INR > 10 which is a commonly reported value in clinical laboratories. Similarly, an end condition of 150 seconds was defined for aPTT experiments.

Fibrinolysis Simulations – Unless otherwise stated, modeling of the system was performed under conditions that simulated the mean physiologic concentrations of each soluble factor involved in fibrinolysis, which were derived from literature reports in human blood under normal physiological conditions (Appendix 3). Fibrinolysis experiments are typically done on volumes of 100μL which corresponds to 321 grid locations. The model was tested under conditions in which the type of agents was limited to a small subset of the CF factors. Given the time scale of hours rather than minutes, each simulation was run five times. Comparisons between the ABMS output and experimental data were used to determine the validity of the system.

Simulations - Simulating the CF system is challenging because not all interactions have been fully defined. Further, whether ABMS technology can reliably predict the functional behavior of the CF system has not been established. Thus, to establish that validity of ABMS in understanding the CF system, three sets of simulations were performed. The first set of experiments tested the applicability of the CF model. The second set of experiments attempted to simulate perturbations of these pathways so as to mimic

clinical disease states by measuring prothrombin time (PT) and activated partial thromboplastin time (aPTT). Finally, the third set of experiments measured the effects of pharmaceutical agents upon these CF pathways

Statistical Analysis –The statistical package R v2.7.0 was used for all statistical calculations. All confidence intervals in the paper are at the 95% level.

Results:

Three sets of simulations were performed to: 1) Validate the model using previously published data and known *in vivo* and *in vitro* conditions associated with the intrinsic, extrinsic, common pathway, and fibrinolysis; 2) Simulate perturbations of pathways mimicking clinical disease states by measuring prothrombin time (PT) and activated partial thromboplastin time (aPTT) as well as; 3) Measure the effects of pharmaceutical agents upon these pathways.

Model Validation Simulations - Model validation was performed through the first set of simulations. Through successful reproductions of the *in vitro* experiments performed by van't Veer et al.[13, 14], Wang et al.[15], Christensen et al.[16], Masson et al.[17], Bajzar et al.[1] and *in silico* experiments performed by Hockin et al.[18] as described below, the behavior of the ABMS was validated.

Simulation of the Extrinsic Pathway Without Regulation - The intrinsic and extrinsic pathways can function independently of each other to generate a clot. *In vivo*, the most

important pathway for the initiation of clot formation is the extrinsic pathway (abnormally low levels of PK, HMWK, or XII have no effects on bleeding times); therefore the initial simulations are focused on validating the behavior of the extrinsic pathway. To validate the use of ABMS in predicting the functional property of the extrinsic pathway, only seven agents were introduced on the rectangular grid including TF-VIIa, V, VIII, IX, X, TFPI, AT, and PC. TF-VIIa complex initiates coagulation resulting in the formation of factor IIa, the level of which is proportional to the level of clot formation under normal conditions. TFPI, AT, and PC were used to assess the ability of ABMS to reflect system regulation.

The first simulation was performed in the context of the procoagulants (TF-VIIa, II, V, VIII, IX, and X). Formation of thrombin was initiated by TF-VIIa at various concentrations (5pM, 30pM, and 130pM). At each concentration of TF-VIIa, the most notable characteristic of the procoagulant simulation (Figure 5a) is its biphasic behavior composed of an initiation phase followed by a propagation phase. This sigmoidal growth profile is characteristic of multi-step reactions. The increasing concentrations of TF-VIIa resulted in shortening initiation times, arbitrarily defined as the time needed to form 20 nM of IIa (Table 1). Additionally, an increased maximum rate of IIa formation during the propagation phase was observed as a function of concentration (Table 2). The sigmoidal factor IIa growth profile coupled with a dependence on initiator concentration suggest that ABMS may be expected to simulate the coagulation cascade*.

*Elimination of rules 33 or 27, which relate to the generation of thrombin from Xa and generation of Xa from TF-VIIa, respectively, suppressed all thrombin formation under all conditions (data not shown).

Table 1: Initiation phase length (s). Initiation time is defined as the time it takes to form 20nM of IIa. The initiation time is a function of the TF-VIIa initiating concentration. The combinations of TFPI and AT have the largest effect on the initiation times.

	5pM	30pM	130pM
NI	38.7+/-7.06	20.7+/-2.31	11.8+/-1.57
TFPI	74.5+/-21.04	39.1+/-10.38	16.2+/-4.11
AT	59.7+/-10.75	27.9+/-4.44	14.6+/-3.20
TFPI + AT	N/A	50.8+/-13.83	34.2+/-13.04

Table 2: Maximum thrombin generation rate (nM IIa /s). The maximal rate is a function of the TF-VIIa initiating concentration. The combinations of TFPI and AT have the largest effect on thrombin generation rates.

	5pM	30pM	130pM
NI	43.8+/-6.22	82.7+/-3.50	110.3+/-6.54
TFPI	30.2+/-5.46	41.0+/-5.24	68.5+/-9.16
AT	19.1+/-5.80	47.0+/-6.03	85.9+/-5.92
TFPI + AT	0.7+/-1.48	13.4+/-3.53	37.4+/-7.55

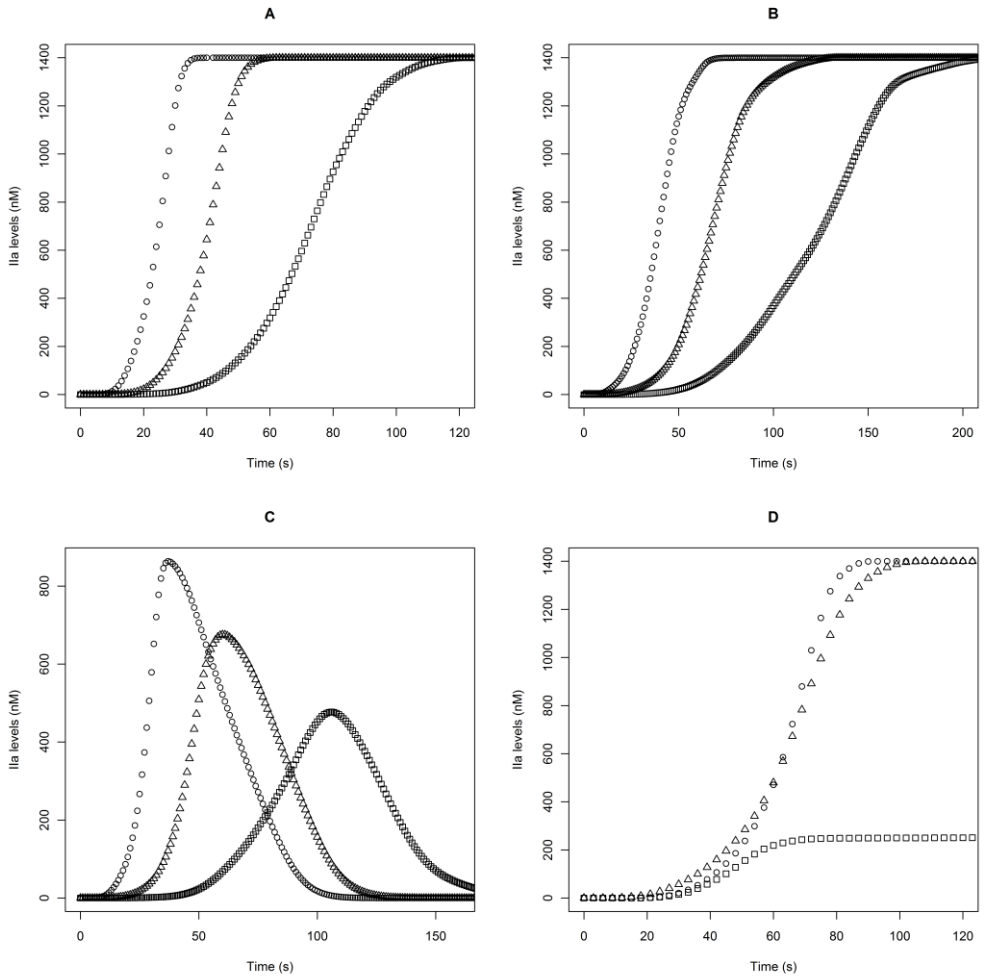

Figure 5: Total thrombin generation with and without inhibitors. A-C: The initiating concentrations of TF-VIIa illustrated: circle = 130 pM, triangle = 30 pM, and square = 5 pM. A) No inhibitors present B) 2.5nM TFPI present C) AT 3.4µM present D) The initiating concentration of TF-VIIa is 5pM in the presence of 65nM PC. TM concentration: circle = 0 pm, triangle = 0.1pm and square = 10pm. N=10.

Simulation of the Extrinsic Pathway With Regulation- To assess whether ABMS simulates the regulatory aspects of coagulation, we examined the behavior of the system in the presence of TFPI, AT, and PC. When TFPI at 2.5 nM (TFPI's normal plasma concentration) is added to the titrations observed in Figure 5a, a significant extension of the initiation phase is observed with only small effect on the maximal rate of propagation. As seen experimentally, adding TFPI to samples with TF-VIIa below 100pM leads to a doubling of the initiation time (Figure 5b, Tables 1&2). It is important to note that addition of TFPI as the only regulator of the extrinsic pathway does not alter the final level of factor IIa, and hence the clot, formed in the process.

To assess the effect of adding an irreversible coagulation inhibitor, AT was introduced at a concentration of 3.4 μM (AT's normal plasma concentration) to the titrations observed in Figure 5a. The addition of AT leads to formation of characteristic bell shaped curves for the formation of IIa at all concentrations (Figure 5c). These profiles are similar to those found in studies of coagulation in plasma. The AT has little effect on either the initiation time rate or the maximal rate of thrombin generation during the propagation phase at 130pM concentrations of TF-VIIa (Tables 1&2) suggesting that AT alone is an effective regulator of coagulation primarily at low levels of TF-VIIa. This is in line with experiments in plasma, which show that AT is not effective in rapidly reducing a bolus of factor IIa stemming from its slow kinetics.

The last important inhibitor for the coagulation system is PC. Figure 5d demonstrates the effects of 65 nm PC and TM on the thrombin generated by the extrinsic system. Starting with an initial concentration of 5pM TF-VIIa, thrombin is plotted against time as TM concentration is varied (0, 0.1, and 10 nm). PC in the absence of TM and at low TM concentration has minimal effects. At high concentrations of TM, the rate of thrombin generation during the propagation phase is decreased. Furthermore, a significant interruption of the propagation phase occurs leading to a biphasic propagation phase; thus, activation following thrombin generation illustrates the dynamic feedback characteristic of the PC pathway.

Simulation of Hyper Anticoagulation - To assess whether a pro-thrombotic state can be reliably controlled by either of the two natural regulators, the concentrations of AT and TFPI were increased to levels dramatically higher than normal at a fixed TF-VIIa concentration (130pM). Figure 6a demonstrates the effects of increased concentrations of TFPI on IIa formation from 1.25 nM (½ baseline) up to 25 nM (20x baseline). There is a progressive elongation of the initiation times with only minimal decrease in reaction rates. The maximal levels of IIa reached for all concentrations of TFPI is the same suggesting that even a 20-fold increase in TFPI is not able to shut down the pro-coagulant signal. On the contrary, increasing AT concentrations from 1.7 μM (½ baseline) up to 20.4 μM (6x baseline) does not alter the initiation time dramatically (Fig. 6b), but essentially shuts off the pro-coagulant signal. As AT concentrations increase, the total amount of IIa generated decreases. Initiation times and maximal IIa rate are decreased as well. At AT levels >7x baseline, IIa formation is totally inhibited (data not shown). These results support the concept that the AT regulatory system is expected to play a major role in anticoagulation therapy.

Fibrinolytic Simulations -The fibrinolytic simulations were limited to the following agents: Pg, mPG, P, tPA, fibrin, PAI, AP, TAFI, II, and TM. Plasminogen activation by tPA is stimulated by fibrin and augmented by plasmin catalyzed feedback modification of fibrin. A modified version of plasminogen designed to simulate the Glu^{1} and Lys^{78} form of plasminogen (mPG) was utilized. mPG does not generate plasmin thereby attenuating the self-activating positive feedback associated with plasmin. In order to investigate the rate of plasminogen activation, the concentration of the mPG is plotted against time

under various conditions (Fig 7). The control group has neither aTAFI nor PG. Therefore, the rate of mPG activation is solely related to tPA concentration. The group associated with P. At early time points, mPG consumption is equivalent among all the groups. Later on, when native P is present, the rate of mPG consumption is

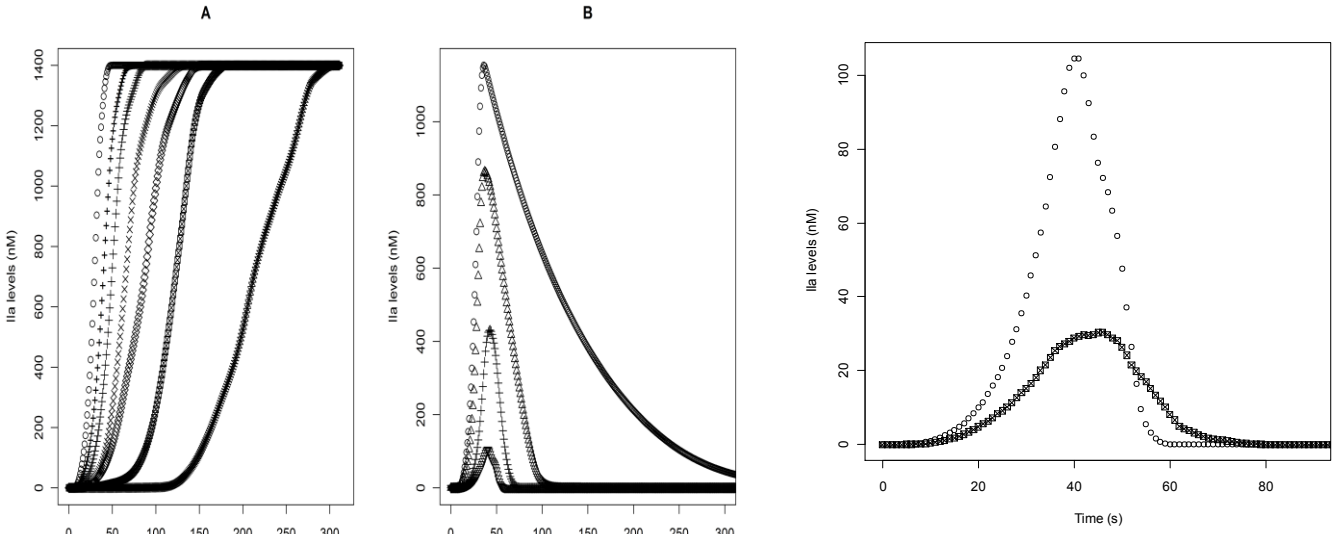

Figure 6: Figure 4: Total thrombin generation profile with 130pM TF-VIIa with AT & TFPI. A) thrombin generation profile with 130pM TF-VIIa at various levels of TFPI. Circle = ½ baseline concentration, + = baseline, large plus = 2x baseline, X = 4x baseline, x = 6x baseline, square = 10x baseline, and x = 20x baseline **B) thrombin generation profile with 130pM TF-VIIa at various levels of AT.** circle = ½ baseline concentration, triangle = baseline, plus = 2x baseline, X = 3x baseline **Insert:** thrombin generation profile with 130pM TF-VIIa at 4x AT (circle) and 6x AT (squares). N=10.

with PG and no ATAFI evaluate the positive feedback associated with P. The ATAFI groups investigate the effects of ATAFI on the suppression of the positive feedback is accelerated. This effect is attenuated by aTAFI and is eliminated at aTAFI concentrations of 5nM resulting in a curve virtually indistinguishable from the control.

Antiplasmin inhibits fibrinolysis by rapidly forming a reversible bond with plasmin. In order to investigate the kinetics associated with AP, the unbound P concentration was

plotted against time with AP and P present in equimolar concentrations. Figure 8 shows the majority of P is bound within 5 seconds.

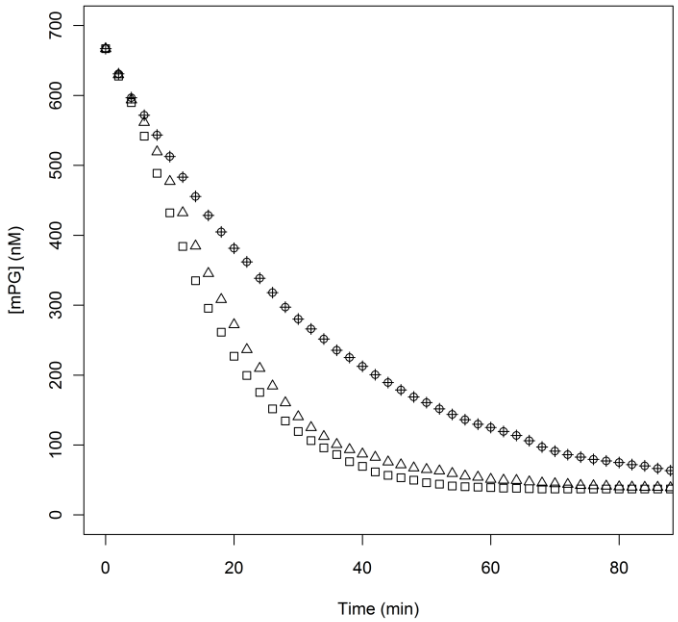

Figure 7: Effect of aTAFI on the activation of plasminogen. The concentration of uncleaved modified plasminogen is plotted against time. Fibrinogen was present in 3µM and 200nM modified plasminogen. The reactions were initiated by 5nM tPA. Controls (circle) lacked P and aTAFI. P 5nM and aTAFI (*square* = 0nM, *triangle* = 1nM and plus = 5nM) were present in the experimental groups. The control and 5nM aTAFI groups overlap and cannot be distinguished. N=5.

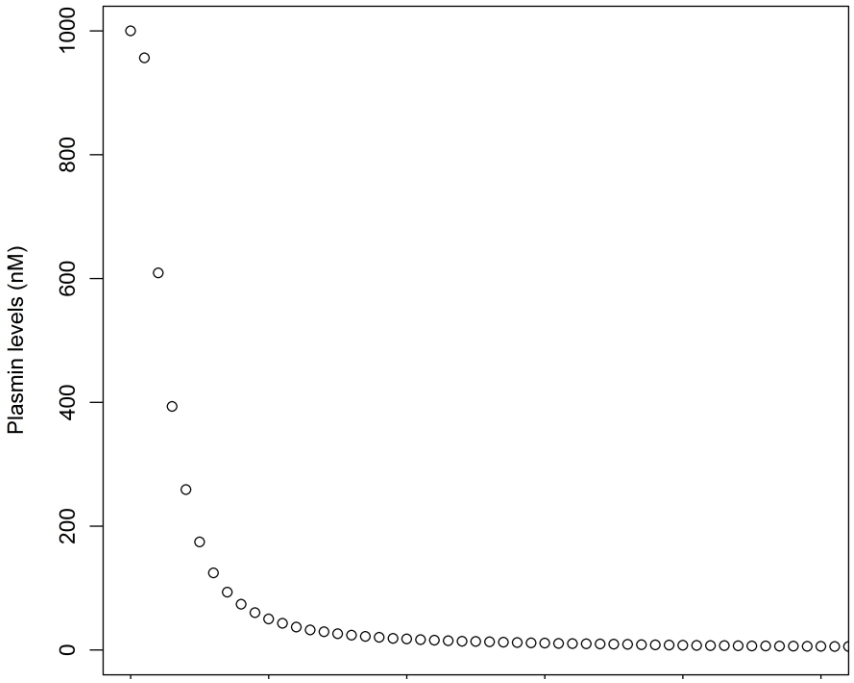

Figure 8: Plasmin-Antiplasmin binding kinetics. Equimolar concentrations (1000nM) of Plasmin and Antiplasmin were combined. Unbound Plasmin concentration is plotted over time. N=5.

PAI inhibits tPA by reversibly binding tPA. The rate of PG activation by tPA was used to determine the effectiveness of PAI. Following two minutes of equilibration of various tPA concentrations +/- PAI with fibrin, PG was added (Figure 9). The rate of initial PG activation was plotted vs. time. The presence of a constant amount of PAI induces the formation of tPA-PAI complexes and a concomitant decrease in the amount of tPA that can bind to fibrin. As a result of this relative decrease in tPA concentration, the rate of plasminogen activation is decreased.

Figure 10 demonstrates the kinetics of TAFI activation by IIa-TM. TM concentration was varied over different concentrations of TAFI in the presence of IIa (1nm) . The initial rate of TAFI activation was plotted vs. time. The rate of TAFI activation is significantly increased in the presence of TM.

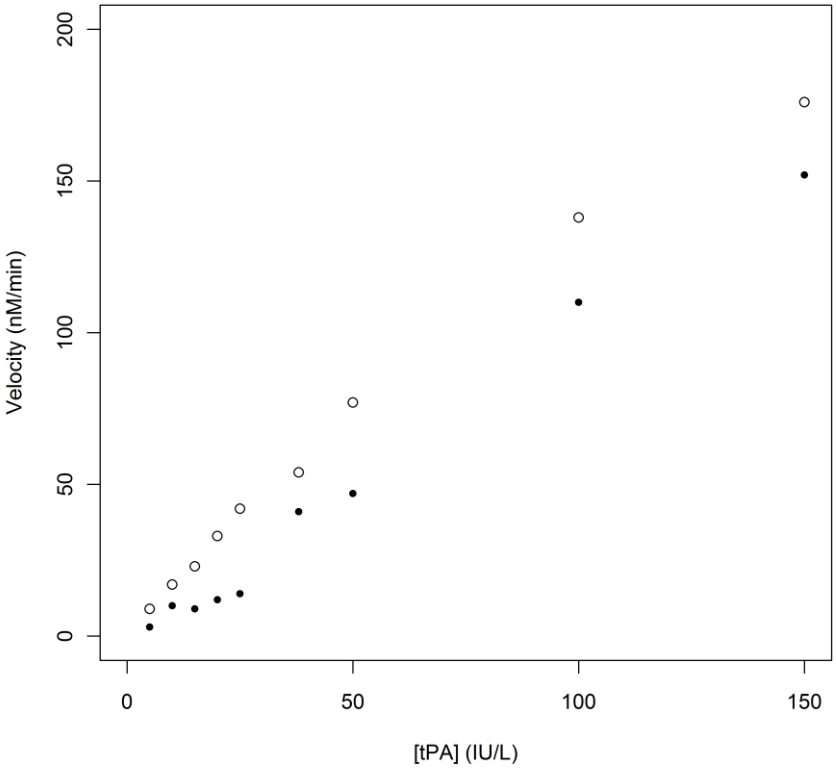

Figure 9: Effect of PAI on the rate of plasminogen activation by tPA. The rate of activation of plasminogen was plotted vs. tPA concentration. Various concentrations of tPA (5, 10, 15, 20, 25, 38, 50, 100, and 150 IU/mL) were combined with 200nM plasminogen and 3µM fibrin in the absence (open circles) and presence of 20 IU/mL PAI (closed circles). In the presence of PAI, the velocity curve is shifted to the right indicating delayed plasminogen activation. N=5.

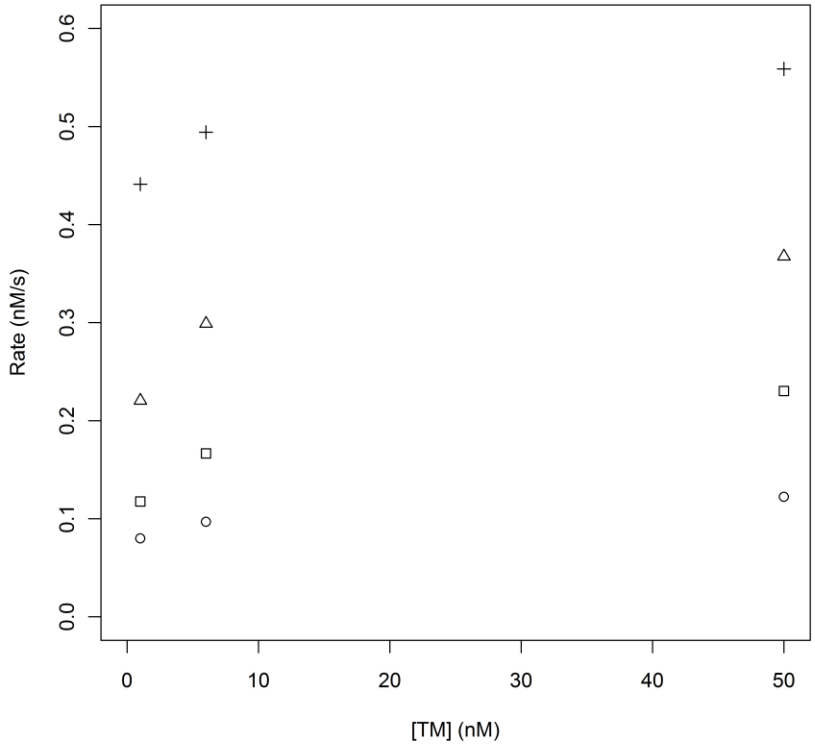

Figure 10: Thrombomodulin concentration dependence of initial rates of TAFI activation. The thrombin concentration is 1 nM. The TM concentration was varied from 1nM, 6 nM to 50nM. The TAFI concentration was varied from 0.26 (circles), 0.52 (square), 1 (triangle), to 2 (plus) µM (from bottom to top). TM increases the catalytic efficiency of TAFI activation by IIa. N=5.

To determine the effects of aTAFI on tPA mediated fibrinolysis, lysis assays were performed on a system of purified fibrinolytic components in the presence and absence of 63 nM aTAFI. The system was composed of: fibrinogen (3 uM), tPA, (5nM) and plasminogen (5nM). Lysis times were defined as the time required to lyse half of the fibrin. The lysis times were 33m +/- in the absence of aTAFI and 70m +/- in the presence of aTAFI.

Simulation of Common Coagulation Tests- The results described above of ABMS in simulating the extrinsic pathway indicated that it might be possible to reliably simulate the entire clotting cascade. Two *in vitro tests*, the prothrombin time (PT) and the activated partial thromboplastin time (aPTT), are commonly utilized in assessing the coagulation status of patients. Depending on the initiator, either TF (PT) or kaolin (aPTT), the test probes the fidelity of the extrinsic or the intrinsic pathway as a part of the whole cascade. As these test are performed on human plasma , except for the bolus of the initiator, all factors of the clotting cascade are typically present at their normal plasma levels (Appendix 3). In order to simulate plasma, the full CF system (utilizing all 106 rules and 57 agent types) was included in the simulations using the normal mean concentration for the factors. In order to initiate coagulation in the PT assay, excess TF (100,000 agents) was introduced. This TF concentration is 100x that of VII; therefore the initial reaction is driven by VII concentrations. Figure 11 shows the formation of clot in the PT assay. In a manner similar to plasma PT, the ABMS displays initiation, propagation and termination of the coagulation signal. A median clotting time

of 13.7s +/- 1.2 (normal *in vitro* PT is between 12-15s). These results suggest that the clinically utilized PT assay can be readily simulated using ABMS.

Similarly, the fidelity of the intrinsic pathway was tested by performing aPTT simulations. In order to initiate coagulation, the intrinsic pathway is activated by using excess kaolin (100,000 agents) to activate factor XII. The results were found to be similar to the PT assay with the exception of a longer initiation phase (Fig 11); the final clot level and the rate of clot formation were identical to the simulated PT assay. A median clotting time of 29.7s +/- 2.0 s was calculated for the simulated aPTT test, which compares favorably with the normal *in vitro* aPTT of 24-40s. Thus, all the parameters characteristic of both the PT and aPTT assays, including the clot time, rate and level of clot formation, support the conclusion that ABMS can reliably model the entire blood coagulation cascade.

Simulation of Clinical Pathologies - The next step in analyzing the behavior of the ABMS is simulating clinical pathologies. In the first scenario, we simulated hemophilia B (Christmas disease). Hemophilia B is a disease in which patients have an increase in their aPTT times, spontaneous hemorrhages, and difficulty clotting after minor injuries due to abnormal levels of Factor IX. In order to simulate Hemophilia B, the system was perturbed by examining the effects of decreased concentration of Factor IX on the aPTT

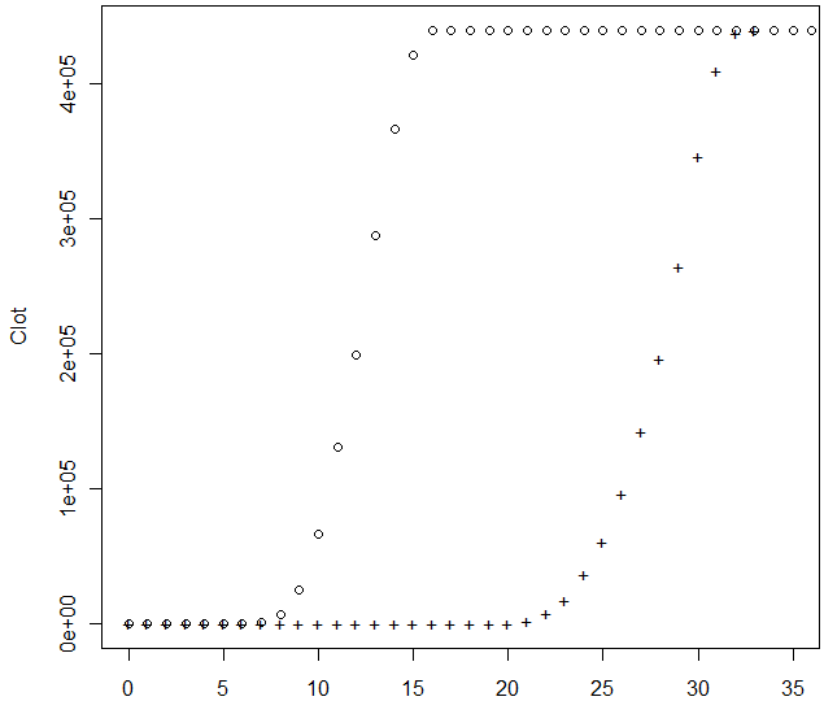

Figure 11: Figure 9: Clot as a function of time when measuring the PT (circles) and aPTT (plus) of normal plasma. The initiation, propagation and termination of clot formation are demonstrated. aPTT times are ~2x longer than PT times due to longer initiation phase. N=10.

assay described in the previous section. In this case, the full CF system was included in the simulations using the normal mean concentration for the factors with the exception of Factor IX. The clinical assay used to monitor Hemophilia B is the aPTT. The aPTT times of Hemophilia B patients was simulated by decreasing the initial Factor IX concentrations otherwise using the full system as described above (Figure 12a). Mild hemophilia is defined as Factor IX activity 10-40% of normal with resultant aPTT times that are normal or only slightly increased. Figure 12a demonstrates the range of aPTT to be between 30-40 s. Moderate hemophilia is defined as factor IX activity between 1 and 10%. Using 2% of normal Factor IX levels gives aPTT times equal to 101.9s +/- 23.88. Severe hemophilia is defined as Factor IX levels < 1%. At this Factor IX concentration, clot formation was totally inhibited and the aPTT times were greater than

160s as the simulations were terminated. These aPTT times are an accurate reflection of those seen clinically in Hemophilia B patients.

Another interesting clinical condition is one in which AT binding to heparin is impaired. Despite normal plasma AT levels, impaired AT-H binding is associated with a hypercoagable state characterized by an increased risk of thromboembolic disease as well as intrauterine fetal demise (IUFD)[19-23]. This condition was simulated by changing the joining parameter that determined whether AT and H react when they collide (increasing it to 10x baseline to decreasing it to 1/1000 baseline). A concentration of heparin (H8000) that leads to impaired clotting was used to demonstrate the effect of the change in AT-H binding. The clinical test used to measure the effects of heparin is the aPTT. Figure 12b demonstrates the effects of changing the AT-H binding probability from 10x baseline to 1/1000 baseline. The aPTT time decreased from > 160s, in the case of 10x baseline, to clotting times that are the equivalent of blood with no heparin, in the cases of 1/100 baseline and 1/1000 baseline binding probability. The results demonstrate that decreasing the AT-H binding probabilities leads to a hypercoagulable state.

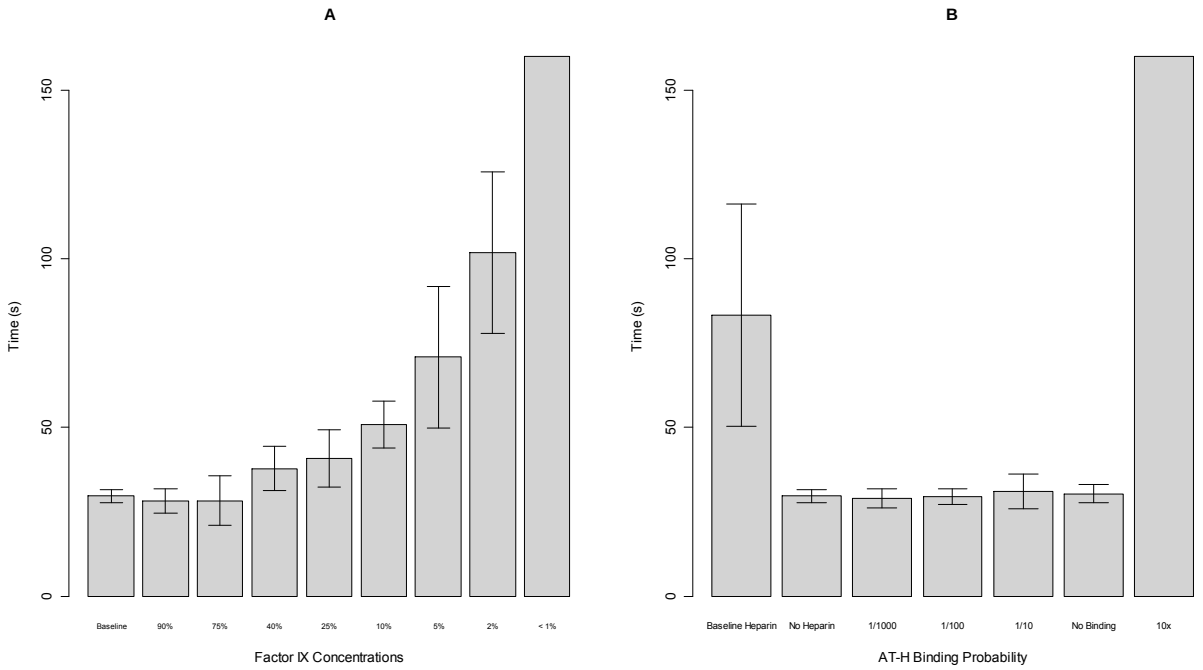

Figure 12: aPTT times under pathophysiologic conditions. A) Hemophilia B- As factor IX concentration decreases aPTT times increase until clotting is totally inhibited in severe hemophilia (<1% baseline IX concentrations) B) AT-H binding deficiency- Impaired binding of heparin to AT returns aPTT times to baseline. Increasing binding probabilities lead to total inhibition of clotting. N=10.

Pharmacologic Simulations - Pharmaceutical agents, e.g., heparin and warfarin, are routinely used to modulate the coagulation state of patients. To test whether the effect of these agents can be incorporated in the coagulation model, simulations were performed in the presence of heparin and warfarin. These results show that drugs such as heparin, warfarin, activated protein C, etc… can easily be simulated using the model. Figure 13a demonstrates the effects of therapeutic and supra-therapeutic heparin on the aPTT times. Heparin is a commonly used inpatient drug given via IV for anti-coagulating patients for DVT, PE, and MI. Heparin serves to activate AT thereby increasing the reaction rate a thousand-fold. As heparin concentration increases from 3000 Units to 11,000 Units so do the aPTT times from ~30s to the maximum of 160s in a non-linear manner. As is well known to clinicians, the simulations demonstrate that the change in concentration from therapeutic levels (8000U) to super-anticoagulated levels (11,000 Units) is very small, and can make heparin titrations problematic.

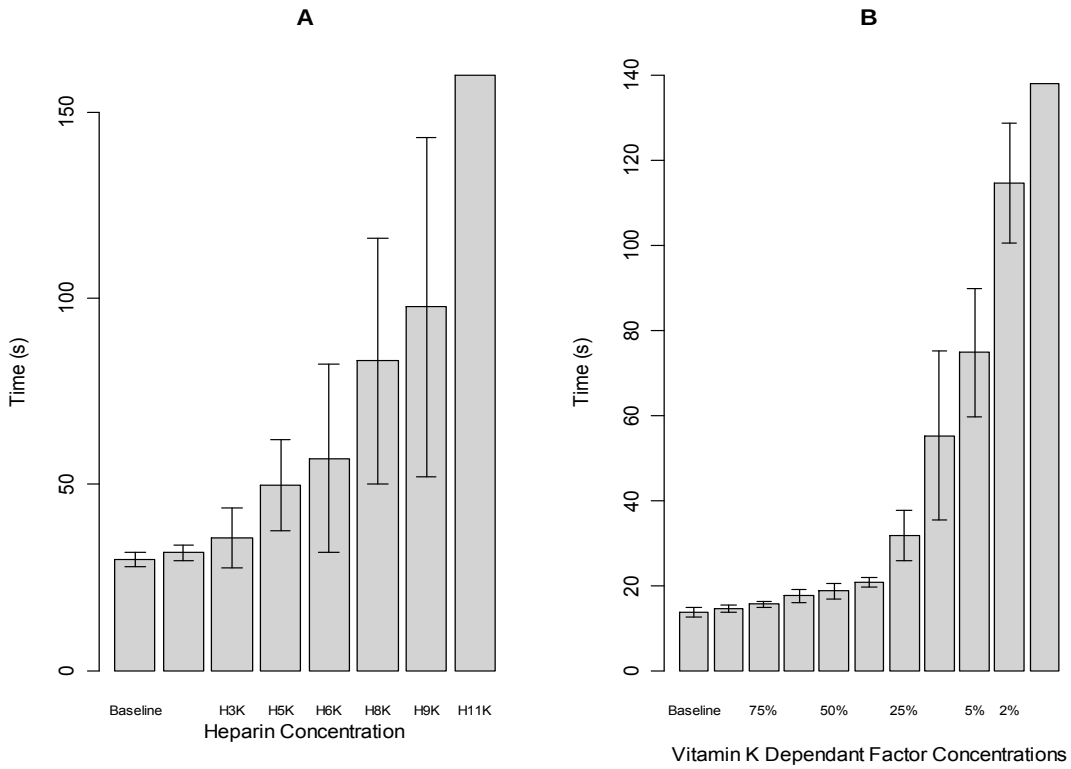

Figure 13: Effects of pharmacologic agents on coagulation assays. A) Heparin – As heparin concentrations increase, so do aPTT times. B) Coumadin – As Vitamin K dependant factors decrease, PT times increase. N=10.

Similarly, Figure 13b demonstrates the effects of therapeutic and supra-therapeutic levels of the medication warfarin. Warfarin is a common medication used in the outpatient setting, given by mouth, to patients that require long term anti-coagulation. . Warfarin inhibits the vitamin K-dependent formation of fully functional coagulation factors. The clinical test used to monitor the effects of warfarin is the PT time. The consequences of warfarin administration were simulated by decreasing concentrations of vitamin K dependant factors (II, VII, IX, and X) from 90% baseline levels to 1% baseline levels. As expected, decreasing levels of the coagulation factors led to increasing PT times in a non-linear manner until the maximum of 150s is reached.

Discussion:

The initial results of this paper indicate that the *in vitro* CF system can be readily simulated using ABMS. The model used in this paper successfully simulated aPTT and PT times at normal physiologic conditions, abnormal physiologic conditions (hemophilia B and AT-H binding defect), and after pharmaceutical interventions (warfarin and heparin). Furthermore, the emergence of a threshold for the generation of thrombin was conclusively demonstrated. The non-linearities of the CF system were captured using this ABMS. The ability of ABMS to simulate results that are found in clinical studies was demonstrated. The ability to predict clinical trials would be an invaluable tool for clinical research. The ability to vary initial concentrations of CF factors that mimics what would be seen in a normal population combined with the error bars associated with the data are unique to ABMS and provide the ability to simulate *in vitro* experiments and clinical trials.

The CF systems interact strongly at the molecular and cellular level; they thereby operating as a coherently linked system, to generate several pathological and physiological responses. The highly complex CF system presents a challenging problem of identifying the root cause of many known coagulation defects. To date the contribution of each system as a part of the network has not been attempted. We have developed an ABMS of the CF cascade that allows systematic evaluation of each of its components – individually and as a complex entity. The model allows a comprehensive analysis of the CF cascade that provides insight into understanding and predicting the pathophysiologic responses arising from variations in molecular and cellular components.

Computational systems biology is a rapidly growing field that provides tools to analyze and understand dynamic evolutionary networks such as the one presented by CF[9-11]. A major advantage of this approach is its rapid, real time analysis of multiple biological systems, each of which can be a highly coordinated independent network interacting with other networks in the group at one or more branch points. These independent networks can be thought of as small molecular machines, which work co-operatively to form a large, multi-component molecular machine producing one or more physiological responses. Understanding the mechanism and co-operativity of these networks as well as predicting the physiological response to appropriate pharmaceutical agents is an extremely difficult and intricate task. Advanced systems biology techniques, e.g., computational technology, hold major promise in achieving this goal and consequently may be extremely useful in understanding patho-physiological conditions and their treatment.

ABMS allows a real time analysis of the coagulation system that is difficult if not impossible to obtain through in *vivo* experiments. Additionally, ABMS provides an opportunity to understand the complex interplay among the various subsystems at any point in time. Reductionist *in vitro* experimental techniques have allowed a detailed understanding of the individual chemical reactions involved in the process of coagulation. ABMS represents a non-reductionist approach of studying the biologic process as a whole, while retaining the information at an individual level. The information obtained by studying the individual reactions is used as the basis for the

rules governing the updating of the ABMS. The advantages of ABMS include the ability to simulate the non-linear aspects of the coagulation system. As the agents are able to change state based on their environment, the model adapts and accounts for changes such as dearth/excess of coagulation inhibitors, absence of factors, or therapeutic interventions. The time required to update the model is one disadvantage of ABMS as it is computationally expensive for large systems with many elements; however a specific advantage of this model is its ability to allow for the addition of newly discovered mediators, which can impact upon both coagulation and inflammation. More importantly, the model has a high probability of exhibiting *emergence* in which its outputs produce unanticipated results, which can then be biologically confirmed. Such properties are particularly useful in the discovery of diagnostic and therapeutic interventions. Comprehensive modeling of the traditional coagulation cascade allows virtual experimentation of the effects of local and systemic injury on coagulation.

Only by creating models, which account for these seemingly diverse but clearly connected processes can one hope to improve our overall understanding of the coagulation process and to create more powerful diagnostic and therapeutic options. We have employed an ABMS in our current approach due to the potential ability to quantitatively analyze individual components of each system at every point of simulation. ABMS is a dynamic modeling and simulation tool that allows the study of dynamic non-linear networked systems. ABMS represents a non-reductionist approach of studying the biologic process as a whole, while retaining the information at an individual level. The complexity of the system has stymied experimental efforts to gain

a system level understanding of the coagulation cascade and its subnetwork components. ABMS may readily provide elucidation of the pathophysiology of diseases related to the coagulation system. The model may also provide insight into individual disease processes such as genetic and acquired disorders of coagulation.

A major advantage with ABMS is the ability to monitor each coagulation factor as 'clotting' proceeds. This implies that the effect of a large number of factors that influence coagulation (*e.g*. natural and pharmaceutical anticoagulants, natural and pharmaceutical fibrinolytic agents, and intrinsic and external inflammation mediators) can be simulated readily. These ABMS are expected to provide information on the overall progress of clotting as well as on individual coagulation factor as a function of time. Thus, ABMS of the coagulation cascade affords the ability to simulate the effect of heparins / low molecular weight heparins, coumadins, and factor Xa / thrombin inhibitors at a systemic level for the first time.

Computational modeling allows the creation of rapid and inexpensive virtual laboratories to generate and test hypotheses[13, 14]. More importantly, simulations provide clinical tools to design and test novel therapeutic strategies, while affording opportunities to predict adverse events during drug development. Additionally, bedside simulations will allow personalized medicine in that replacement factor concentrations can be calculated for individual hemophiliac patients, heparin doses can be titrated, etc… Additional applications of the model include discovery of new mediators, understanding of proximal

and distal effects of interactions between systems, discovery of new diagnostic and therapeutic options, and development of new software and algorithms for simulation.

References

1. Bajzar L, Morser J, Nesheim M. TAFI, or Plasma Procarboxypeptidase B, Couples the Coagulation and Fibrinolytic Cascades through the Thrombin-Thrombomodulin Complex. J Biol Chem 1996;271:16603-8.
2. Monroe DM, Hoffman M. What Does It Take to Make the Perfect Clot? Arterioscler Thromb Vasc Biol 2006;26:41-8.
3. Zhu D. Mathematical modeling of blood coagulation cascade: kinetics of intrinsic and extrinsic pathways in normal and deficient conditions. Blood Coagul Fibrinolysis 2007;18:637-46.
4. Hockin MF, Jones KC, Everse SJ, Mann KG. A Model for the Stoichiometric Regulation of Blood Coagulation. J Biol Chem 2002;277:18322-33.
5. Jones KC, Mann KG. A model for the tissue factor pathway to thrombin. II. A mathematical simulation. J Biol Chem 1994;269:23367-73.
6. Bonabeau E. Agent-based modeling: methods and techniques for simulating human systems. Proc Natl Acad Sci U S A 2002;99 Suppl 3:7280-7.
7. An G. Agent-based computer simulation and sirs: building a bridge between basic science and clinical trials. Shock 2001;16:266-73.
8. Bankes SC. Agent-based modeling: A revolution? PNAS 2002;99:7199-200.
9. Bonabeau E. Agent-based modeling: Methods and techniques for simulating human systems. PNAS 2002;99:7280-7.
10. Rider RE. Aspects of Ulam: From Cardinals to Chaos. Science 1989;246:134-.
11. Wolfram S. Cellular Automata and Complexity: Collected Papers: Westview Press; 1994.
12. Wilensky U. NetLogo. Evanston, IL: Center for Connected Learning and Computer-Based Modeling, Northwestern University; 1999.
13. van `t Veer C, Mann KG. Regulation of Tissue Factor Initiated Thrombin Generation by the Stoichiometric Inhibitors Tissue Factor Pathway Inhibitor, Antithrombin-III, and Heparin Cofactor-II. J Biol Chem 1997;272:4367-77.
14. van `t Veer C, Golden NJ, Kalafatis M, Mann KG. Inhibitory Mechanism of the Protein C Pathway on Tissue Factor-induced Thrombin Generation. SYNERGISTIC EFFECT IN COMBINATION WITH TISSUE FACTOR PATHWAY INHIBITOR. J Biol Chem 1997;272:7983-94.
15. Wang W, Boffa MB, Bajzar L, Walker JB, Nesheim ME. A Study of the Mechanism of Inhibition of Fibrinolysis by Activated Thrombin-activable Fibrinolysis Inhibitor. J Biol Chem 1998;273:27176-81.
16. Christensen U, Bangert K, Thorsen S. Reaction of human alpha2-antiplasmin and plasmin stopped-flow fluorescence kinetics. FEBS Lett 1996;387:58-62.
17. Masson C, Angles-Cano E. Kinetic analysis of the interaction between plasminogen activator inhibitor-1 and tissue-type plasminogen activator. Biochem J 1988;256:237-44.
18. Hockin MF, Jones KC, Everse SJ, Mann KG. A model for the stoichiometric regulation of blood coagulation. J Biol Chem 2002;277:18322-33.
19. O'Ddonnell JS, Hinkson L, McCarthy A, Manning R, Khan A, Laffan MA. Antithrombin Nagasaki (Ser 116 to Pro): a rare antithrombin variant with abnormal heparin binding presenting during pregnancy. Blood Coagul Fibrinolysis 2006;17:217-20.
20. Tsiang M, Jain AK, Gibbs CS. Functional Requirements for Inhibition of Thrombin by Antithrombin III in the Presence and Absence of Heparin. J Biol Chem 1997;272:12024-9.
21. Owen MC, Borg JY, Soria C, Soria J, Caen J, Carrell RW. Heparin binding defect in a new antithrombin III variant: Rouen, 47 Arg to His. Blood 1987;69:1275-9.
22. Bauters A, Zawadzki C, Bura A, et al. Homozygous variant of antithrombin with lack of affinity for heparin: management of severe thrombotic complications associated with intrauterine fetal demise. Blood Coagul Fibrinolysis 1996;7:705-10.

23. Dewerchin M, Herault J-P, Wallays G, et al. Life-Threatening Thrombosis in Mice With Targeted Arg48-to-Cys Mutation of the Heparin-Binding Domain of Antithrombin. Circ Res 2003;93:1120-6.
24. O'Brien DP, Kemball-Cook G, Hutchinson AM, et al. Surface plasmon resonance studies of the interaction between factor VII and tissue factor. Demonstration of defective tissue factor binding in a variant FVII molecule (FVII-R79Q). Biochemistry 1994;33:14162-9.
25. Krishnaswamy S. The interaction of human factor VIIa with tissue factor. J Biol Chem 1992;267:23696-706.
26. Shobe J, Dickinson CD, Edgington TS, Ruf W. Macromolecular Substrate Affinity for the Tissue Factor-Factor VIIa Complex Is Independent of Scissile Bond Docking. J Biol Chem 1999;274:24171-5.
27. Butenas S, Mann KG. Kinetics of human factor VII activation. Biochemistry 1996;35:1904-10.
28. Baugh RJ, Broze GJ, Jr., Krishnaswamy S. Regulation of extrinsic pathway factor Xa formation by tissue factor pathway inhibitor. J Biol Chem 1998;273:4378-86.
29. Baugh RJ, Dickinson CD, Ruf W, Krishnaswamy S. Exosite interactions determine the affinity of factor X for the extrinsic Xase complex. J Biol Chem 2000;275:28826-33.
30. Baugh RJ, Krishnaswamy S. Role of the activation peptide domain in human factor X activation by the extrinsic Xase complex. J Biol Chem 1996;271:16126-34.
31. Bergum PW, Cruikshank A, Maki SL, Kelly CR, Ruf W, Vlasuk GP. Role of zymogen and activated factor X as scaffolds for the inhibition of the blood coagulation factor VIIa-tissue factor complex by recombinant nematode anticoagulant protein c2. J Biol Chem 2001;276:10063-71.
32. de Moerloose P, Bounameaux HR, Mannucci PM. Screening test for thrombophilic patients: which tests, for which patient, by whom, when, and why? Semin Thromb Hemost 1998;24:321-7.
33. Bom VJ, van Hinsbergh VW, Reinalda-Poot HH, Mohanlal RW, Bertina RM. Extrinsic activation of human coagulation factors IX and X on the endothelial surface. Thromb Haemost 1991;66:283-91.
34. Tankersley DL, Finlayson JS. Kinetics of activation and autoactivation of human factor XII. Biochemistry 1984;23:273-9.
35. Gailani D, Broze GJ, Jr. Factor XI activation in a revised model of blood coagulation. Science 1991;253:909-12.
36. Rawala-Sheikh R, Ahmad SS, Ashby B, Walsh PN. Kinetics of coagulation factor X activation by platelet-bound factor IXa. Biochemistry 1990;29:2606-11.
37. Lollar P, Parker ET, Fay PJ. Coagulant properties of hybrid human/porcine factor VIII molecules. J Biol Chem 1992;267:23652-7.
38. Fay PJ, Smudzin TM. Characterization of the interaction between the A2 subunit and A1/A3-C1-C2 dimer in human factor VIIIa. J Biol Chem 1992;267:13246-50.
39. Fay PJ, Beattie TL, Regan LM, O'Brien LM, Kaufman RJ. Model for the factor VIIIa-dependent decay of the intrinsic factor Xase. Role of subunit dissociation and factor IXa-catalyzed proteolysis. J Biol Chem 1996;271:6027-32.
40. Lawson JH, Butenas S, Ribarik N, Mann KG. Complex-dependent inhibition of factor VIIa by antithrombin III and heparin. J Biol Chem 1993;268:767-70.
41. Rosing J, Tans G, Govers-Riemslag JW, Zwaal RF, Hemker HC. The role of phospholipids and factor Va in the prothrombinase complex. J Biol Chem 1980;255:274-83.
42. Higgins DL, Lewis SD, Shafer JA. Steady state kinetic parameters for the thrombin-catalyzed conversion of human fibrinogen to fibrin. J Biol Chem 1983;258:9276-82.
43. Monkovic DD, Tracy PB. Activation of human factor V by factor Xa and thrombin. Biochemistry 1990;29:1118-28.
44. Hill-Eubanks DC, Lollar P. von Willebrand factor is a cofactor for thrombin-catalyzed cleavage of the factor VIII light chain. J Biol Chem 1990;265:17854-8.

45. Jesty J, Wun TC, Lorenz A. Kinetics of the inhibition of factor Xa and the tissue factor-factor VIIa complex by the tissue factor pathway inhibitor in the presence and absence of heparin. Biochemistry 1994;33:12686-94.
46. Chuang YJ, Swanson R, Raja SM, Olson ST. Heparin enhances the specificity of antithrombin for thrombin and factor Xa independent of the reactive center loop sequence. Evidence for an exosite determinant of factor Xa specificity in heparin-activated antithrombin. J Biol Chem 2001;276:14961-71.
47. Jordan RE, Oosta GM, Gardner WT, Rosenberg RD. The kinetics of hemostatic enzyme-antithrombin interactions in the presence of low molecular weight heparin. J Biol Chem 1980;255:10081-90.
48. Schoen P, Lindhout T. The in situ inhibition of prothrombinase-formed human alpha-thrombin and meizothrombin(des F1) by antithrombin III and heparin. J Biol Chem 1987;262:11268-74.
49. Pixley RA, Schapira M, Colman RW. The regulation of human factor XIIa by plasma proteinase inhibitors. J Biol Chem 1985;260:1723-9.
50. Olson ST, Sheffer R, Francis AM. High molecular weight kininogen potentiates the heparin-accelerated inhibition of plasma kallikrein by antithrombin: role for antithrombin in the regulation of kallikrein. Biochemistry 1993;32:12136-47.
51. Olson S, Srinivasan K, Bjork I, Shore J. Binding of high affinity heparin to antithrombin III. Stopped flow kinetic studies of the binding interaction. J Biol Chem 1981;256:11073-9.
52. Cesarman-Maus G, Hajjar KA. Molecular mechanisms of fibrinolysis. Br J Haematol 2005;129:307-21.
53. Collen D, Lijnen HR. Basic and clinical aspects of fibrinolysis and thrombolysis. Blood 1991;78:3114-24.
54. Bajzar L. Thrombin Activatable Fibrinolysis Inhibitor and an Antifibrinolytic Pathway. Arterioscler Thromb Vasc Biol 2000;20:2511-8.
55. Guimaraes AH, Rijken DC. Thrombin activatable fibrinolysis inhibitor (TAFI) affects fibrinolysis in a plasminogen activator concentration-dependent manner. Study of seven plasminogen activators in an internal clot lysis model. Thromb Haemost 2004;91:473-9.
56. Walker JB, Bajzar L. The Intrinsic Threshold of the Fibrinolytic System Is Modulated by Basic Carboxypeptidases, but the Magnitude of the Antifibrinolytic Effect of Activated Thrombin-activable Fibrinolysis Inhibitor Is Masked by Its Instability. J Biol Chem 2004;279:27896-904.

Appendix 1:

Entity	Description
XI	Factor XI Activates XII and IX
XIa	Activated factor XI
XII	Factor XII (Hagemon factor). Activates XI.
XIIa	Activated factor XII
XIII	Factor XIII. Crosslinks fibrin polymers to form mature clot.
XIIIa	Activated factor XIII
IX	Factor IX (Christmas factor) Activates X. Forms tenase complex
Ixa	Activated factor IX
VIII	Factor VIII. Co-factor of IX – Forms tenase complex
VIIIa	Activated factor VIII
VIIIa1	Factor VIIIa spontaneously dissociates into inactive VIIIa1 + VIIIa2
VIIIa2	Factor VIIIa spontaneously dissociates into inactive VIIIa1 + VIIIa2
IXa-VIIIa	tenase complex - activates X
IXa-VIIIa-X	IXa-VIIIa-X complex
VII	Factor VII. Activates IX and X.
VIIa	Activated factor VII
II	Factor II (prothrombin). Activates F, V, VII, XIII
Iia	Activated factor II
X	Factor X. Activates II. Co-factor of V – forms prothrombinase complex
Xa	Activated factor X
V	Factor V. Co-factor of X – forms prothrombinase complex
Va	Activated V
Va-Xa	prothrombinase complex – activates II
TF	Tissue Factor. Activates X in combination with VIIa
TF-VIIa	TF-VIIa complex
F	Fibrinogen – (Factor I) forms clot after conversion to fibrin and polymerization
Fm	Fibrin monomer – forms clot after spontaneous polymerization
HMWK	high molecular weight kininogen – co-factor for activation of XI, XII, and PK
XI	Factor XI
XIa	Activated Factor XI
XII	Factor XII
XIIa	Activated Factor XII
PK	Prekallikrein
K	Kallikrein
AT	Antithrombin III – inhibits TF-VIIa, IIa, IXa, XIa, XIIa and Xa
AT-Xa	AT-Xa complex
AT-IXa	AT-IXa complex
AT-IIa	AT-IIa complex
AT-TF-VIIa	AT-TF-VIIa complex
AT-XIa	AT-XIa complex
AT-XIIa	AT-XIIa complex
AT-K	AT-K complex
H	Heparin - co-factor of AT
AT-H	Antithrombin III - Heparin Complex
PC	Protein C
aPC	Activated PC. Inhibits VIIa
Ka	Kaolin - activates the contact portion of the intrinsic system
TFPI	Tissue Factor Pathway Inhibitor - inhibits VIIa-TF, Xa
TFPI-Xa	TFPI-Xa complex

TF-VIIa-Xa-TFPI	TF-VIIa-Xa-TFPI complex
PG	Plasminogen
tPA	Tissue Plasminogen Activator. Converts PG to P.
PAI	Plasminogen Activator Inhibitor. Inhibits tPA.
tPA-PAI	tPA-PAI complex
P	Plasmin. Degrades fibrin.
AP	Anti-Plasmin. Inhibits P.
P-AP	Plasmin - Anti-Plasmin complex
TAFI	Thrombin Activatable Fibrinolysis Inhibitor- Prevents the P mediated increased rate of PG activation.
aTAFI	Activated TAFI

Appendix 2:

#	Reaction	Pathway
1	VII + TF → VII-TF[4, 24, 25]	Extrinsic
2	VII + TF ← VII-TF[4, 24, 25]	Extrinsic
3	VIIa + TF → VIIa-TF[4, 24, 26]	Extrinsic
4	VIIa + TF← VIIa-TF[4, 24, 26]	Extrinsic
5	VIIa-TF + VII → VIIa-TF + VIIa[3, 4, 27]	Extrinsic
6	Xa + VII → Xa + VIIa[3, 4, 27]	Extrinsic
7	IIa + VII → IIa + VIIa[3, 4, 27]	Extrinsic
8	VIIa-TF + X → VIIa-TF-X[4, 26, 28]	Extrinsic
9	VIIa-TF + X ← VIIa-TF-X[4, 26, 28]	Extrinsic
10	VIIa-TF-X → VIIa-TF + Xa[4, 29, 30]	Extrinsic
11	VIIa-TF + Xa → VIIa-TF-Xa[4, 30, 31]	Extrinsic
12	VIIa-TF + Xa ← VIIa-TF-Xa[4]	Extrinsic
13	VIIa-TF + IX → VIIa-TF-IX[4, 32, 33]	Extrinsic
14	VIIa-TF + IX ← VIIa-TF-IX[4, 32, 33]	Extrinsic
15	VIIa-TF-IX → VIIa-TF + IXa[4, 32, 33]	Extrinsic
16	XII + Surface + HMWK → XIIa + Surface + HMWK	Intrinsic
17	XII + XIIa → XIIa + XIIa[3, 34]	Intrinsic
18	PK+ XIIa + HMWK → K + XIIa + HMWK[3, 34]	Intrinsic
19	XII + K + HMWK → XIIa + K+ HMWK[3, 34]	Intrinsic
20	XI + XIIa + HMWK→ XIa + XIIa +HMWK[3, 35]	Intrinsic
21	XII + XIa → XIIa + XIa[3]	Intrinsic
22	IX + XIa → IXa + XIa[3]	Intrinsic
23	X + IXa → Xa + IXa[3]	Intrinsic
24	XI + IIa → XIa + IIa[3]	Intrinsic
25	VIIIa + IXa → VIIIa-IXa[4, 32]	Intrinsic
26	VIIIa + IXa ← VIIIa-IXa[4, 32]	Intrinsic
27	VIIIa-IXa + X → VIIIa-IXa-X[4, 32, 36]	Intrinsic
28	VIIIa-IXa + X ← VIIIa-IXa-X[4, 32, 36]	Intrinsic
29	VIIIa-IXa-X → VIIIa-IXa-Xa[4, 32, 36]	Intrinsic
30	VIIIa → VIIIa1 + VIIIa2[4, 37]	Intrinsic
31	VIIIa ← VIIIa1 + VIIIa2[4, 37, 38]	Intrinsic
32	VIIIa-IXa → VIIIa1 + VIIIa2 + IXa[4, 39]	Intrinsic
33	Xa + II → Xa + IIa[3, 4, 40, 41]	Common
34	IIa + VIII → IIa + VIIIa[3, 4, 28]	Common
35	F + IIa → Fm + IIa[3, 42]	Common
36	IIa + V → IIa + Va[3, 4, 32, 43, 44]	Common
37	Xa + Va → Xa-Va[4, 32]	Common
38	Xa + Va ← Xa-Va[4, 32]	Common
39	Xa-Va + II → Xa-Va-II[4, 32]	Common
40	Xa-Va + II ← Xa-Va-II[4, 32]	Common

41	Xa-Va-II → Xa-Va + IIa[4, 32]	Common
42	XIII + IIa → XIIIa + IIa[3]	Common
43	Xa + TFPI → Xa-TFPI[4, 28, 45]	TFPI
44	Xa + TFPI← Xa-TFPI[4, 28, 45]	TFPI
45	TF-VIIa-Xa + TFPI → TF-VIIa-Xa-TFPI[4, 28]	TFPI
46	TF-VIIa-Xa + TFPI ← TF-VIIa-Xa-TFPI[4, 28]	TFPI
47	TF-VIIa + Xa-TFPI → TF-VIIa-Xa-TFPI[4, 28]	TFPI
48	AT + Xa → AT-Xa[3, 4, 46]	AT-H
49	AT + TF-VIIa → AT-TF-VIIa [3, 4, 40]	AT-H
50	AT + IXa → AT-IXa [3, 4, 46, 47]	AT-H
51	AT + IIa → AT-IIa [3, 4, 48]	AT-H
52	AT + XIa → AT-XIa[3]	AT-H
53	AT + XIIa → AT-XIIa[3, 49]	AT-H
54	AT + K → AT-K[3, 50]	AT-H
55	AT + H → AT-H[51]	AT-H
56	AT + H ← AT-H[51]	AT-H
57	AT-H + Xa → AT-Xa + H[46]	AT-H
58	AT-H + TF-VIIa → AT-TF-VIIa + H[40]	AT-H
59	AT-H + IXa → AT-IXa + H[46, 47]	AT-H
60	AT-H + IIa → AT-IIa + H[48]	AT-H
61	AT-H + XI → AT-XI + H	AT-H
62	AT-H + XII → AT-XII + H[49]	AT-H
63	AT-H + K → AT-K + H[50]	AT-H
64	PC + IIa → aPC + IIa[14]	APC
65	IIa + TM → IIa-TM[14]	APC
66	IIa + TM← IIa-TM	APC
67	PC + IIa-TM → aPC + IIa-TM[14]	APC
68	aPC +Va → aPC + V_i[14]	APC
69	PG + tPA → P + tPA[1, 17, 52, 53]	Fibrinolysis
70	mPG + tPA → tPA[1, 17, 52, 53]	Fibrinolysis
71	tPA + F_m → tPA-F_m[1, 17, 52, 53]	Fibrinolysis
72	tPA + F_m ← tPA-F_m[1, 17, 52, 53]	Fibrinolysis
73	tPA-F_m + PG → tPA-F_m-PG[1, 17, 52, 53]	Fibrinolysis
74	tPA-F_m + PG ← tPA-F_m-PG[1, 17, 52, 53]	Fibrinolysis
75	tPA-F_m-PG → tPA-F_m + P[1, 17, 52, 53]	Fibrinolysis
76	P + F_m → P[1, 17, 52, 53]	Fibrinolysis
77	tPA + PAI → tPA-PAI[17]	PAI
78	tPA + PAI← tPA-PAI[17]	PAI
79	P + AP → AP-P'[16]	AP
80	P + AP ← AP-P'[16]	AP
81	AP-P' → AP-P[16]	AP
82	AP-P' ← AP-P[16]	AP
83	aTAFI + F_m → aTAFI-F_m[1, 15, 54-56]	TAFI
84	aTAFI → $TAFI_i$[1, 15, 54-56]	TAFI

85	IIa+ TAFI → IIa-TAFI[1, 15, 54-56]	TAFI
86	IIa+ TAFI← IIa-TAFI[1, 15, 54-56]	TAFI
87	IIa-TM + TAFI → IIa-TM-TAFI[1, 15, 54-56]	TAFI
88	Ia-TM + TAFI ← IIa-TM-TAFI[1, 15, 54-56]	TAFI
89	IIa-TM-TAFI → II-TM + aTAFI[1, 15, 54-56]	TAFI
90	IIa-TAFI → IIa + aTAFI[1, 15, 54-56]	TAFI
91	IIa-TAFI + TM → IIa-TAFI-TM[1, 15, 54-56]	TAFI
92	IIa-TAFI-TM → IIa-TM + TAFI[1, 15, 54-56]	TAFI
93	IIa-TAFI-TM → IIa-TAFI + TM[1, 15, 54-56]	TAFI
94	aTAFI + F_m → aTAFI-F_m[1, 15, 54-56]	TAFI
95	aTAFI-F_m → aTAFI-F_m + Lysine[1, 15, 54-56]	TAFI
96	aTAFI → $TAFI_i$[1, 15, 54-56]	TAFI
97	IIa+ TAFI → IIa-TAFI[1, 15, 54-56]	TAFI
98	IIa+ TAFI← IIa-TAFI[1, 15, 54-56]	TAFI
99	IIa-TM + TAFI → IIa-TM-TAFI[1, 15, 54-56]	TAFI
100	Ia-TM + TAFI ← IIa-TM-TAFI[1, 15, 54-56]	TAFI
101	IIa-TM-TAFI → II-TM + aTAFI[1, 15, 54-56]	TAFI
102	IIa-TAFI → IIa + aTAFI[1, 15, 54-56]	TAFI
103	IIa-TAFI + TM → IIa-TAFI-TM[1, 15, 54-56]	TAFI
104	IIa-TAFI-TM → IIa-TM + TAFI[1, 15, 54-56]	TAFI
105	IIa-TAFI-TM → IIa-TAFI + TM[1, 15, 54-56]	TAFI
106	IIa-TAFI-TM → IIa-TM + aTAFI[1, 15, 54-56]	TAFI

Appendix 3:

Agent	Initial Concentration (microM)	# of Agents
I	8.83	883,000
II	1.4	140,000
V	0.02	2,000
VII	0.01	1,000
VIIa	0.0001	10
VIII	0.0003	30
IX	0.09	9,000
X	0.17	17,000
XI	0.025	2,500
XII	0.3	30,000
HMWK	0.9	90,000
PK	0.58	58,000
AT	3.4	340,000
TFPI	0.0025	250
Protein C	0.065	6,500

A Computational Analysis of the Synergistic Effect of Coagulation Inhibitors on the Generation of Thrombin

Nathan Menke MD[1, 2], Kevin Ward MD[1, 2], Lemont Kier PhD[3], Cha-Kun Cheng PhD[3], & Umesh Desai PhD[4]

[1]Virginia Commonwealth University Reanimation Engineering Shock Center
[2]Virginia Commonwealth University, Department of Emergency Medicine
[3]Virginia Commonwealth University, Center for the Study of Biologic Complexity
[4] Virginia Commonwealth University, Department of Medicinal Chemistry

VCU/MCV Department of Emergency Medicine
PO BOX 980401
Richmond, Virginia 23298-0401
nmenke@vcu.edu

Abstract

The coagulation system (CS) is a complex, inter-connected biological system with major physiological and pathological roles. The CS may be viewed as a complex adaptive system, in which individual components are linked through multiple feedback and feedforward loops. The non-linear relationships between the numerous coagulation factors and the interplay among the elements of the CS render the study of this biology at a molecular and cellular level nearly impossible. We present an Agent Based Modeling and Simulation (ABMS) approach for simulating these complex interactions. Our ABMS approach utilizes a subset of 52 rules to define the interactions among 33 enzymes and factors of the CS. These rules simulate the interaction of each "agent", such as substrates, enzymes, and cofactors, on a two-dimensional grid of ~12,000 cells and ~300,000 agents. Our ABMS method successfully reproduces the initiation, propagation, and termination of thrombin formation due to the activation of the extrinsic pathway. Furthermore, the ABMS is able to demonstrate the emergence of a threshold effect for thrombin generation as a result of the synergistic effect of combining anticoagulant systems.

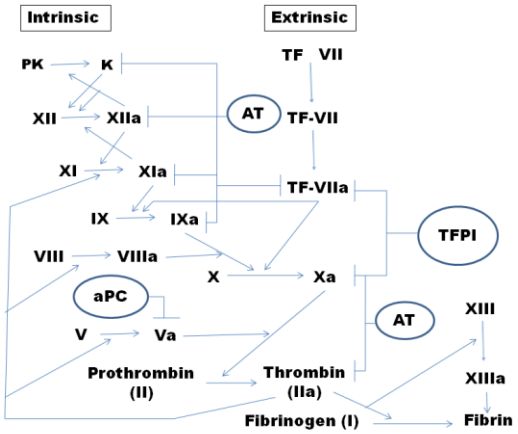

Figure 1: Coagulation Cascade

Coagulation System In the event of an injury to the endothelium, the coagulation system balances the need for localized clot formation against prevention of systemic activation. This finely tuned system is composed of an assortment of molecular and cellular "agents" (e.g. substrates, enzymes, cofactors, inhibitors, platelets, and endothelial cells) all interacting to generate a stable clot in order to rapidly obtain hemostasis[1]. The new cellular model of hemostasis proposes that the classical pathways of coagulation, i.e., the intrinsic and extrinsic pathways, mediate on specific cell surfaces in a tightly regulated manner[2-4]. In this model, activation of factor VII (extrinsic, Fig. 1) and factor XII (intrinsic, Fig. 1) results in the formation of the multi-molecular tenase and prothrombinase complexes, which eventually generate thrombin. Thrombin then cleaves fibrinogen to form fibrin monomers, which polymerize to form a three-dimensional clot.

Clot formation is regulated *in vivo* through the antithrombin III-heparin complex (AT-H), activated protein C (aPC), and tissue factor pathway inhibitor (TFPI) (Fig. 1). These regulating systems limit excessive formation of cross-linked fibrin under hemostatic conditions. The anticoagulation systems are regulated independently, but combine to synergistically control thrombin generation.

The CS may be viewed as a complex adaptive system, in which individual components are linked through multiple feedback and feedforward loops. These loops introduce non-linear relationships among the components. A static diagram such as the classically portrayed coagulation pathway (Figure 1) cannot adequately describe this dynamic evolutionary network. More importantly, the effects of several disease states on the imbalances in the CS are difficult to understand. Thus, the influence of diseases that favor coagulation (*e.g.* myocardial infarction, disseminated intravascular coagulation, cerebrovascular accidents, and venous thrombosis), or those that impair coagulation (*e.g*. hemophilias, thrombocytopenias, and von Willebrand disease) remain poorly characterized.

Computational Modeling

Computational systems biology is an emerging field that provides tools to analyze and understand complex adaptive systems such as the CS[5,6]. A major advantage of this approach is its rapid, real time analysis of multiple biological systems; each may function as a highly coordinated independent network interacting with other networks in the group at one or more branch points. These independent networks can be thought of as small molecular machines, which work co-operatively to form a large, multi-component molecular machine producing one or more physiological responses. Understanding the mechanism and co-operativity of these networks as well as predicting the physiological response to

appropriate pharmaceutical agents is an extremely difficult and intricate task. Yet, advanced systems biology techniques, e.g., computational technology, may achieve this goal with consequent major applications in understanding patho-physiological conditions and their treatment.

Table I: Entity Table

Entity	**Description**
IX	Factor IX (Christmas factor) Activates X. Forms tenase complex
VIII	Factor VIII. Co-factor of IX – Forms tenase complex
VIIIa	Activated factor VIII
VIIIa1	Factor VIIIa spontaneously dissociates into inactive VIIIa1 + VIIIa2
VIIIa2	Factor VIIIa spontaneously dissociates into inactive VIIIa1 + VIIIa2
IXa-VIIIa	tenase complex - activates X
IXa-VIIIa-X	IXa-VIIIa-X complex
VII	Factor VII. Activates IX and X.
VIIa	Activated factor VII
II	Factor II (prothrombin). Activates F, V, VII, XIII
IIa	Activated factor II (thrombin)
X	Factor X. Activates II. Co-factor of V – forms prothrombinase complex
V	Factor V. Co-factor of X – forms prothrombinase complex
V_i	Inactivated V
Va-Xa	Prothrombinase complex – activates II
TF	Tissue Factor. Activates X in combination with VIIa
TF-VIIa	TF-VIIa complex
AT	Antithrombin III – inhibits TF-VIIa, IIa, IXa, XIa, XIIa and Xa
AT-Xa	AT-Xa complex
AT-IXa	AT-IXa complex
AT-IIa	AT-IIa complex
AT-TF-VIIa	AT-TF-VIIa complex

TFPI	Tissue Factor Pathway Inhibitor - inhibits VIIa-TF, Xa
TFPI-Xa	TFPI-Xa complex
TF-VIIa-Xa-TFPI	TF-VIIa-Xa-TFPI complex
PC	Protein C – inactivates Va
aPC	Activated Protein C – activated Protein C
aPC-Va	aPC-Va complex
TM	Thrombomodulin – In combination with IIa, activates PC
IIa-TM	IIa-TM complex

To date, most computational models of the coagulation system have focused on using ordinary or partial differential equations (ODEs and PDEs)[7-9]. Differential equations describe the change in the states of the variables of the system over time and are derived from known or hypothesized kinetics. ODE models can readily simulate coagulation *in vitro* as it is a relatively homogenous system[10]; however, such models face significant limitations when modeling *in vivo* hemostasis due to complicating factors such as non-stationarity, spatial heterogeneity and the effects of blood flow. Therefore, derivation of differential equations suitable for *in vivo* modeling becomes problematic.

In order to address the shortcomings associated with ODE models, we present the application of a computational systems biology approach using agent-based modeling and simulation (ABMS) to understand the CS and determine the role of coagulation inhibitors in preventing complete activation of thrombin. ABMS provides a powerful alternative to differential equations[11-13]. ABMS is a relatively new modeling paradigm derived from cellular automata (CA)[14,15]. ABMS has mobile autonomous entities (agents) that can move through space. Each agent is allowed to assume a finite number of states, determined by a pre-defined set of rules. Every agent is individually updated at the end of each operating

period according to the pre-set rules. The rules are a function of the current state of the agent and the state of its neighbors.

Coagulation Model

Table II: Rule Table

#	Reaction	Pathway
1	VII + TF → VII-TF[7,19-21]	Extrinsic
2	VII + TF ← VII-TF[7,19-21]	Extrinsic
3	VIIa + TF → VIIa-TF[7,19-21]	Extrinsic
4	VIIa + TF← VIIa-TF[7,19-21]	Extrinsic
5	VIIa-TF + VII → VIIa-TF + VIIa[7,8,22]	Extrinsic
6	Xa + VII → Xa + VIIa[7,8,22]	Extrinsic
7	IIa + VII → IIa + VIIa[7,8,22]	Extrinsic
8	VIIa-TF + X → VIIa-TF-X[7,21,23]	Extrinsic
9	VIIa-TF + X ← VIIa-TF-X[7,21,23]	Extrinsic
10	VIIa-TF-X → VIIa-TF + Xa[7,24,25]	Extrinsic
11	VIIa-TF + Xa → VIIa-TF-Xa[7,25,26]	Extrinsic
12	VIIa-TF + Xa ← VIIa-TF-Xa[7]	Extrinsic
13	VIIa-TF + IX → VIIa-TF-IX[7,27,28]	Extrinsic
14	VIIa-TF + IX ← VIIa-TF-IX[7,27,28]	Extrinsic
15	VIIa-TF-IX → VIIa-TF + IXa[7,27,28]	Extrinsic
23	VIIIa + IXa → VIIIa-IXa[7,28]	Intrinsic
25	VIIIa + IXa ← VIIIa-IXa[7,28]	Intrinsic
26	VIIIa-IXa + X → VIIIa-IXa-X[7,28,29]	Intrinsic
27	VIIIa-IXa + X ← VIIIa-IXa-X[7,28,29]	Intrinsic
28	VIIIa-IXa-X → VIIIa-IXa-Xa[7,28,29]	Intrinsic
29	VIIIa → VIIIa1 + VIIIa2[7,30]	Intrinsic
30	VIIIa ← VIIIa1 + VIIIa2[7,30,31]	Intrinsic
31	VIIIa-IXa → VIIIa1 + VIIIa2 + IXa[7,32]	Intrinsic
32	Xa + II → Xa + IIa[7,8,33,34]	Common
33	IIa + VIII → IIa + VIIIa[7,8,23]	Common
34	IIa + V → IIa + Va[7,8,28,35,36]	Common
35	Xa + Va → Xa-Va[7,28]	Common
36	Xa + Va ← Xa-Va[7,28]	Common
37	Xa-Va + II → Xa-Va-II[7,28]	Common
38	Xa-Va + II ← Xa-Va-II[7,28]	Common
39	Xa-Va-II → Xa-Va + IIa[7,28]	Common
40	Xa + TFPI → Xa-TFPI[7,23,28]	TFPI
41	Xa + TFPI← Xa-TFPI[7,23,28]	TFPI
42	TF-VIIa-Xa + TFPI → TF-VIIa-Xa-TFPI[7,23,37]	TFPI

43	TF-VIIa-Xa + TFPI ← TF-VIIa-Xa-TFPI[7,23,37]	TFPI
44	TF-VIIa + Xa-TFPI → TF-VIIa-Xa-TFPI[7,23,37]	TFPI
45	AT + Xa → AT-Xa[7,8,38]	AT
46	AT + TF-VIIa → AT-TF-VIIa[7,8,33]	AT
47	AT + IXa → AT-IXa[7,8,38,39]	AT
48	AT + IIa → AT-IIa[7,8,40]	AT
49	PC + IIa → aPC + IIa[17]	aPC
50	IIa + TM → IIa-TM[17]	aPC
51	PC + IIa-TM → aPC + IIa-TM[17]	aPC
52	aPC +Va → aPC + V_i [17]	aPC

The model described in this paper is designed to simulate thrombin formation in the *in vitro* environment. Therefore, a limited subset of substrates, reactions, and products from the intrinsic, extrinsic, common, AT-H, TFPI, and aPC pathways have been included (Table I & II). In order to create realistic simulations, physiologic concentrations of factors were used in the *in silico* experiments (Table III). The rates associated with the reactions were taken from the literature and were assumed to be performed in saturating phospholipid and calcium conditions. The simulations were designed to test experimental conditions that create thrombin profiles reflective of the threshold phenomena associated with physiologic concentrations of coagulation inhibitors.

Table III: Baseline plasma concentration of coagulation factors.

Agent	**Initial Concentration (µM)**	**# of Agents**
TF-VIIa	Varies	Varies
II	1.4	280,000
V	0.02	4,000
VII	0.01	2,000
VIIa	0.0001	20
VIII	0.0003	60
IX	0.09	18,000
X	0.17	34,000
AT	3.4	68,000
TFPI	0.0025	500

PC	0.065	13,000
TM	Varies	Varies

Materials and Methods

Coagulation Model

The ABMS in this paper uses a two dimensional particle system whereby particles move freely and interact on a discrete spatial grid. In this specific model, we define the particles of the system as the reactants, enzymes, and products in the entity table (Table I). The spatial grid is set as a two dimensional grid where the agent's location is identified by its x and y coordinates. Each coordinate pair (x, y) delineates a unique location. The number of grid locations used in these simulations is 12,321. The number of agents in the simulations is on the order of 300,000. Each time step of the simulation represents 0.01 seconds.

Grid locations in this model are designated as either empty or occupied by one or more substrates, enzymes, or reaction products. The agents are allowed to move freely about the grid. The movement, joining, and breaking are governed by probability rules. The movement parameter determines the extent of each agent's motion (0 implies every cell is stationary). The joining parameter determines the extent of interaction between adjacent agents. The breaking parameter defines the extent of disruption of agents that have joined. This model sets the probability of joining and breaking based on experimentally determined kinetic constants. The movement parameter is set at 1. The agents are allowed to interact with all their neighbors, but meaningful interactions are limited to those in the rule table (Table II). The neighborhood of each agent in this model is defined as all agents located in the same grid location. After each time step, the agents move in a random manner to an adjacent grid location.

ABMS modeling requires the assignment of the probability of conversion associated with each chemical reaction as defined in the rule table (Table II). Reductionist *in vitro* experimental techniques have

allowed a detailed understanding of the individual chemical reactions involved in the process of coagulation. The information obtained by studying the individual reactions is used as the basis for the rules governing the updating of the ABMS at each time step. We assigned a probability of conversion value related to the kinetics of the reactions. The initial configuration is random; each substrate and enzyme is assigned a predefined number of agents based on their desired initial concentration (Table III).

In vivo, prothrombinase and tenase complexes are formed through a combination of three factors. The prothrombinase complex is formed by a combination of prothrombin, factor Xa and factor Va; the intrinsic tenase complex is formed when factors VIIIa and IXa combine with factor X. These three-body complexes are not directly simulated in ABMS, as *in vivo*, they must arise through sequential combination of two molecules. Thus, we utilized a sequential two-body collision approach to generate each complex.

The ABMS is designed to represent the *in vitro* environment. In this case, the spatial grid is in the shape of a rectangle allowing the particles to interact and bounce off the edge of the grid. There are no platelets, RBC, or WBC in the system as *in vitro* coagulation tests are run on acellular plasma.

Computation

Netlogo v4.04, a software package designed to run ABMS, was utilized to perform the simulations[16]. The user determines the subset of reactants, the subset of reactions, the subset of coagulation factors, rate constants, initial factor concentrations, and termination conditions for each simulation. The concentration of every coagulation factor was output every 100 time steps (1 virtual second). The

output of each simulation was stored in a comma separated file. All simulations were carried out on an Intel based desktop personal computer running Microsoft Windows XP. Up to six simulations were run in parallel. Each simulation ran up to 72 hours depending on the initial and stop conditions. Simulations were terminated after 90,000 iterations if the terminating conditions were not met.

Simulations

Unless otherwise stated, modeling of the system was performed under conditions that simulated literature derived mean physiologic concentrations of each soluble factor in normal humans (Table 3). The simulations were designed to determine the effects of coagulation inhibitors on thrombin (IIa) generation profiles. Comparisons between the ABMS output and experimental data determined the validity of the system.

Results

The threshold dependent formation of IIa in the presence of inhibitors such as AT, PC, and TFPI is an important feature of the coagulation system. Figure 2, demonstrates this characteristic profile that results as a function of the combination of AT and TFPI. At low concentrations of TF-VIIa (5pM), the threshold value required for production of IIa is not reached; whereas both 30pM and 130pM concentration were able to generate a short burst of thrombin. These results demonstrate the synergistic effect of inhibitors (AT and TFPI) on the extrinsic system. The combination of AT and TFPI results in the creation of a threshold concentration of TF-VIIa (between 5pM and 30pM). Below this threshold value significant amounts of thrombin are not generated.

The combination of PC and TFPI results in the threshold demonstrated in Figure 3. The experiments were initiated by TF-VIIa at 5pM. With no TM, all of the prothrombin (II) is converted to thrombin; whereas at concentrations of 0.1nM TM and 10nM TM, generation of thrombin is quenched. In this

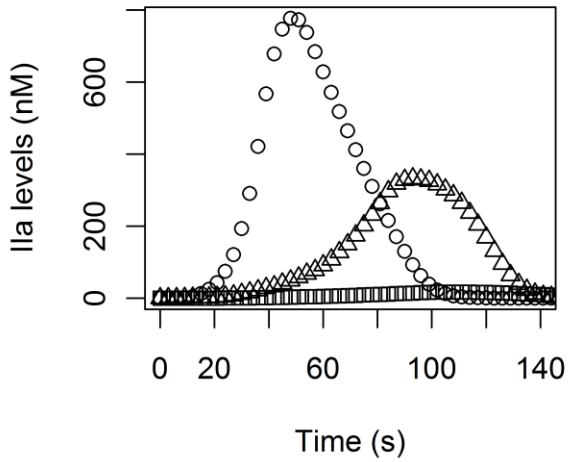

Figure 2: Thrombin generation as a function of TF-VIIa concentration in the presence of TFPI and AT. The experiments were conducted with 2.5 nM TFPI and 3.4uM AT. The initiating concentrations of TF-VIIa are 130pm (circles), 30pM (triangles), and 5pM (squares). N=5.

case, the threshold is a function of TM concentration. Thus, a bifurcation point exists between 0nM and 0.1nM of TM whereby PC in combination with TFPI prevents the burst of thrombin generation.

Figure 4 demonstrates the effects of combining AT and PC. At concentrations of 5pM of TF-VIIa no thrombin was generated (data not shown). At initial concentrations of 30pM TF-VIIa, the characteristic bell shaped curve is observed with no TM and 0.1nM TM. At 10nM concentrations of TM, the burst of thrombin is suppressed.

In figure 5, all three inhibitors are utilized. No thrombin is generated when initialized with 5pM or 30pM of TF-VIIa (data not shown). At 130pM of TF-VIIa, a burst of thrombin is observed with low

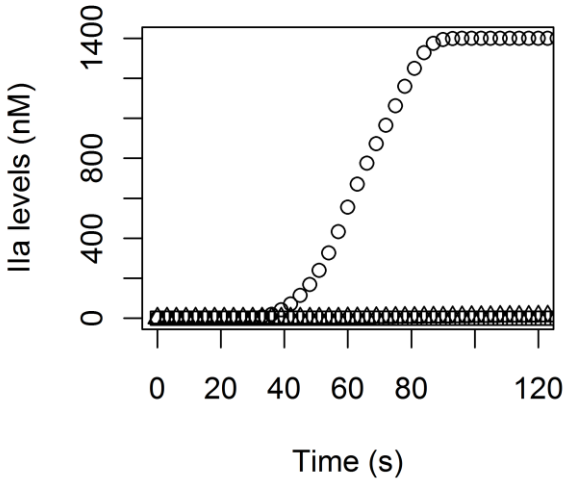

Figure 3: Thrombin generation as a function of TM concentration in the presence of TFPI and Protein C. The experiments were conducted with 2.5 nM TFPI and 65 nM Protein C. The initiating concentration of TF-VIIa is 5nM. The TM concentrations 0 (circles), 0.1 nM (triangles), and 10nM (squares). N=5.

TM concentrations (no TM and 0.1nM TM), but is suppressed at 10nM TM.

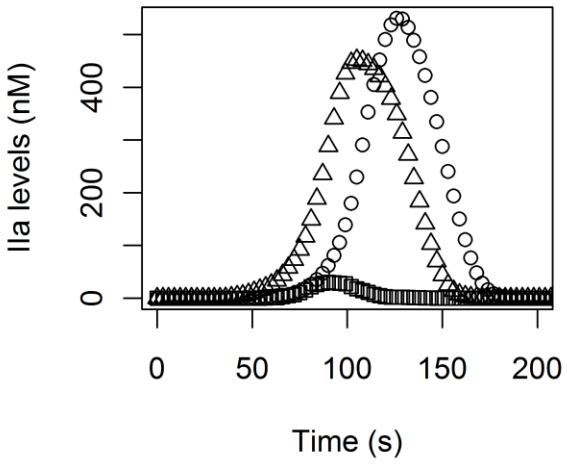

Figure 4: Thrombin generation as a function of TM concentration in the presence of AT and Protein C. The experiments were conducted with 3.4 µM AT and 65 nM Protein C. The initiating concentration of TF-VIIa is 30nM. The TM concentrations are 0 (circles), 0.1nM (triangles), and 10nM (squares). **N=5.**

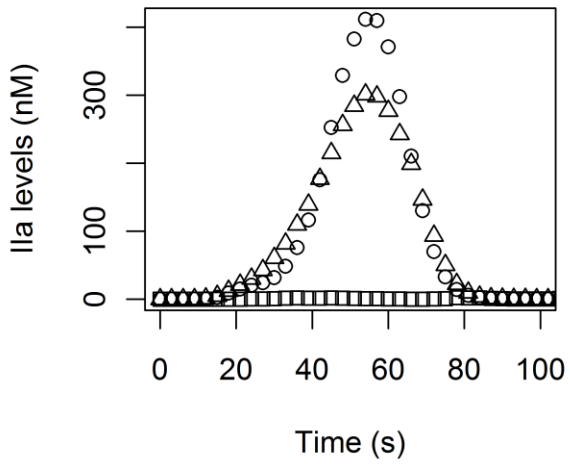

Figure 5: Thrombin generation as a function of TM concentration in the presence of TFPI, AT, and Protein C. The experiments were conducted with 2.5 nM TFPI , 3.4 µM AT, and 65 nM Protein C. The initiating concentration of TF-VIIa is 130nM. The TM are 0 (circles), 0.1 nM (triangles), and 10nM (squares). **N=5.**

Discussion

The components of the CS interact strongly at the molecular and cellular level; they thereby operate as a coherently linked system that generates both pathological and physiological responses. The highly complex CS presents a challenging problem of identifying the root cause of many known coagulation defects. To date the contribution of each system as a part of the network has not been attempted. We have developed an ABMS of the CS cascade that allows systematic evaluation of each of its components – individually and as a complex entity. The model allows a comprehensive analysis of the CS cascade that provides insight into understanding and predicting the pathophysiologic responses arising from variations in its molecular and cellular components.

Only by creating models, which account for these seemingly diverse but clearly connected processes can one hope to improve our overall understanding of the coagulation process and to create more powerful diagnostic and therapeutic options. We have employed an ABMS in our current approach due to the potential ability to quantitatively analyze individual components of each system at every point of

simulation. ABMS is a dynamic modeling and simulation tool that allows the study of dynamic non-linear networked systems. ABMS represents a non-reductionist approach of studying the biologic process as a whole, while retaining the information at an individual level. The complexity of the system has stymied experimental efforts to gain a system level understanding of the coagulation cascade and its subnetwork components. ABMS may readily provide elucidation of the pathophysiology of diseases related to the coagulation system. The model may prove informative regarding individual disease processes such as genetic and acquired disorders of coagulation.

The initial results of this paper indicate that the *in vitro* coagulation system can be readily simulated using ABMS. Our ABMS approach successfully reproduces the initiation, propagation, and termination of thrombin formation *in vitro*. Furthermore, the ABMS was able to simulate the threshold effect of thrombin formation resultant from the synergistic relationship between physiologic concentrations of coagulation inhibitors. This suppression of thrombin is the likely mechanism behind localization of the hemostasis response. The mechanism demonstrated herein provides the rationale for localized formation of a blood clot at the site of endothelial injury as opposed to a systemic vascular thrombotic response. Presumably, the thrombin concentrations upstream and downstream of the endothelial injury fail to reach self sustaining levels due to the synergistic effects of AT, TFPI, and aPC. A possible therapeutic strategy of manipulating coagulation inhibitors for the treatment of diseases involving the systemic activation of the CS, such as trauma induced coagulopathy (TIC), disseminated intravascular coagulopathy (DIC), coagulopathy associated with cardiac arrest, etc…, is suggested by the findings in this paper.

The next step in the progression of our coagulation model is to simulate the *in vivo* environment.

Expansion of the model will require the addition of blood flow, endothelial cells, white blood cells, platelets, and the full complement of coagulation proteins. Such a model will provide insight into complex disease processes that are impossible to obtain using laboratory techniques. Computational systems biology allows the design and implementation of experiments that would be unethical and dangerous in the clinical setting; instead, creation of previously unavailable diagnostic and therapeutic strategies becomes possible.

ABMS allows a real time analysis of the coagulation system that cannot be obtained through *in vivo* experiments. Additionally, ABMS provides an opportunity to understand the complex interplay among the various subsystems. The advantages of ABMS include the ability to simulate the non-linear aspects of the coagulation system. Moreover, the model is flexible and able to account for changes such as lack of inhibitors, absence of factors, or therapeutic interventions associated with disease processes. As new mediators are discovered they are easily added to the model.

Another major advantage of ABMS is the ability to monitor each coagulation factor as 'clotting' proceeds. This implies that the effect of a large number of factors that influence coagulation (*e.g*. natural and pharmaceutical anticoagulants, natural and pharmaceutical fibrinolytic agents, and intrinsic and external inflammation mediators) can be simulated readily. These ABMS are expected to provide information regarding the overall progress of clotting as well as individual coagulation factors as a function of time. Thus, ABMS of the coagulation cascade affords the ability to simulate the effect of heparins / low molecular weight heparins, coumadins, and factor Xa / thrombin inhibitors at a systemic level for the first time.

The last and most important advantage of the model is it is capable of exhibiting *emergent behaviors* in which its outputs produce unanticipated results, which can then be biologically confirmed. Such properties are particularly useful in the discovery of diagnostic and therapeutic interventions. Comprehensive modeling of the traditional coagulation cascade allows unlimited virtual experimentation on the effects of local and systemic injury on coagulation.

The time required to update the model is one disadvantage of ABMS as it is computationally expensive for large systems with many elements. Conversion of the model into other platforms may provide significantly decrease the time required to run simulations. For example, the model can be moved to an alternate ABMS platform (*I.E.* Repast) with an expected halving of the execution time. Ultimately, conversion of the model into a format that can be run on graphical processing units (GPU) may allow significant decreases in execution time (on the order of 100x) that could allow simulations to be run at a patient's bedside in real-time.

Computational modeling allows the creation of rapid and inexpensive virtual laboratories to generate and test hypotheses. More importantly, simulations provide clinical tools to design and test novel therapeutic strategies, while affording opportunities to predict adverse events during drug development. Additionally, bedside simulations will allow personalized medicine to calculate replacement factor concentrations for individual hemophiliac patients, heparin doses can be titrated, etc… Future applications of the model include discovery of new mediators, understanding of proximal and distal effects of interactions between systems, discovery of new diagnostic and therapeutic options, and development of new software and algorithms for simulation.

References

1 Messmore, HL. Hemostasis and Thrombosis: Basic Principles and Clinical Practice. *JAMA* **296**, 338-, (2006).

2 Furie, B & Furie, BC. Mechanisms of Thrombus Formation. *N. Engl. J. Med.* **359**, 938-949, (2008).

3 Monroe, DM & Hoffman, M. What Does It Take to Make the Perfect Clot? *Arterioscler. Thromb. Vasc. Biol.* **26**, 41-48, (2006).

4 Wagner, DD & Frenette, PS. The vessel wall and its interactions. *Blood* **111**, 5271-5281, (2008).

5 An, G. Mathematical modeling in medicine: a means, not an end. *Crit Care Med* **33**, 253-254, (2005).

6 Buchman, TG. Nonlinear dynamics, complex systems, and the pathobiology of critical illness. *Curr Opin Crit Care* **10**, 378-382, (2004).

7 Hockin, MF *et al.* A Model for the Stoichiometric Regulation of Blood Coagulation. *J. Biol. Chem.* **277**, 18322-18333, (2002).

8 Zhu, D. Mathematical modeling of blood coagulation cascade: kinetics of intrinsic and extrinsic pathways in normal and deficient conditions. *Blood Coagul Fibrinolysis* **18**, 637-646, (2007).

9 Panteleev, MA *et al.* Mathematical models of blood coagulation and platelet adhesion: clinical applications. *Curr Pharm Des* **13**, 1457-1467, (2007).

10 Jones, KC & Mann, KG. A model for the tissue factor pathway to thrombin. II. A mathematical simulation. *J Biol Chem* **269**, 23367-23373, (1994).

11 An, G. Agent-based computer simulation and sirs: building a bridge between basic science and clinical trials. *Shock* **16**, 266-273, (2001).

12 Bankes, SC. Agent-based modeling: A revolution? *PNAS* **99**, 7199-7200, (2002).

13 Bonabeau, E. Agent-based modeling: Methods and techniques for simulating human systems. *PNAS* **99**, 7280-7287, (2002).

14 Rider, RE. Aspects of Ulam: From Cardinals to Chaos. *Science* **246**, 134-, (1989).

15 Wolfram, S. *Cellular Automata and Complexity: Collected Papers*. (Westview Press, 1994).

16 Wilensky, U. (Center for Connected Learning and Computer-Based Modeling, Northwestern University, Evanston, IL, 1999).

17 van `t Veer, C *et al.* Inhibitory Mechanism of the Protein C Pathway on Tissue Factor-induced Thrombin Generation. Synergistic Effect in Combination with Tissue Factor Pathway Inhibitor. *J. Biol. Chem.* **272**, 7983-7994, (1997).

18 van `t Veer, C & Mann, KG. Regulation of Tissue Factor Initiated Thrombin Generation by the Stoichiometric Inhibitors Tissue Factor Pathway Inhibitor, Antithrombin-III, and Heparin Cofactor-II. *J. Biol. Chem.* **272**, 4367-4377, (1997).

19 Krishnaswamy, S. The interaction of human factor VIIa with tissue factor. *J. Biol. Chem.* **267**, 23696-23706, (1992).

20 O'Brien, DP *et al.* Surface plasmon resonance studies of the interaction between factor VII and tissue factor. Demonstration of defective tissue factor binding in a variant FVII molecule (FVII-R79Q). *Biochemistry* **33**, 14162-14169, (1994).

21 Shobe, J *et al.* Macromolecular Substrate Affinity for the Tissue Factor-Factor VIIa Complex Is Independent of Scissile Bond Docking. *J. Biol. Chem.* **274**, 24171-24175, (1999).

22 Butenas, S & Mann, KG. Kinetics of human factor VII activation. *Biochemistry* **35**, 1904-1910, (1996).

23 Baugh, RJ, Broze, GJ, Jr. & Krishnaswamy, S. Regulation of extrinsic pathway factor Xa formation by tissue factor pathway inhibitor. *J Biol Chem* **273**, 4378-4386, (1998).

24 Baugh, RJ *et al.* Exosite interactions determine the affinity of factor X for the extrinsic Xase complex. *J Biol Chem* **275**, 28826-28833, (2000).

25 Baugh, RJ & Krishnaswamy, S. Role of the activation peptide domain in human factor X activation by the extrinsic Xase complex. *J Biol Chem* **271**, 16126-16134, (1996).

26 Bergum, PW *et al.* Role of zymogen and activated factor X as scaffolds for the inhibition of the blood coagulation factor VIIa-tissue factor complex by recombinant nematode anticoagulant protein c2. *J Biol Chem* **276**, 10063-10071, (2001).

27 Bom, VJ *et al.* Extrinsic activation of human coagulation factors IX and X on the endothelial surface. *Thromb Haemost* **66**, 283-291, (1991).

28 de Moerloose, P, Bounameaux, HR & Mannucci, PM. Screening test for thrombophilic patients: which tests, for which patient, by whom, when, and why? *Semin Thromb Hemost* **24**, 321-327, (1998).

29 Rawala-Sheikh, R *et al.* Kinetics of coagulation factor X activation by platelet-bound factor IXa. *Biochemistry* **29**, 2606-2611, (1990).

30 Lollar, P, Parker, ET & Fay, PJ. Coagulant properties of hybrid human/porcine factor VIII molecules. *J Biol Chem* **267**, 23652-23657, (1992).

31 Fay, PJ & Smudzin, TM. Characterization of the interaction between the A2 subunit and A1/A3-C1-C2 dimer in human factor VIIIa. *J Biol Chem* **267**, 13246-13250, (1992).

32 Fay, PJ *et al.* Model for the factor VIIIa-dependent decay of the intrinsic factor Xase. Role of subunit dissociation and factor IXa-catalyzed proteolysis. *J Biol Chem* **271**, 6027-6032, (1996).

33 Lawson, JH *et al.* Complex-dependent inhibition of factor VIIa by antithrombin III and heparin. *J Biol Chem* **268**, 767-770, (1993).

34 Rosing, J *et al.* The role of phospholipids and factor Va in the prothrombinase complex. *J Biol Chem* **255**, 274-283, (1980).

35 Hill-Eubanks, DC & Lollar, P. von Willebrand factor is a cofactor for thrombin-catalyzed cleavage of the factor VIII light chain. *J Biol Chem* **265**, 17854-17858, (1990).

36 Monkovic, DD & Tracy, PB. Activation of human factor V by factor Xa and thrombin. *Biochemistry* **29**, 1118-1128, (1990).

37 Jesty, J, Wun, TC & Lorenz, A. Kinetics of the inhibition of factor Xa and the tissue factor-factor VIIa complex by the tissue factor pathway inhibitor in the presence and absence of heparin. *Biochemistry* **33**, 12686-12694, (1994).

38 Chuang, YJ *et al.* Heparin enhances the specificity of antithrombin for thrombin and factor Xa independent of the reactive center loop sequence. Evidence for an exosite determinant of factor Xa specificity in heparin-activated antithrombin. *J Biol Chem* **276**, 14961-14971, (2001).

39 Jordan, RE *et al.* The kinetics of hemostatic enzyme-antithrombin interactions in the presence of low molecular weight heparin. *J Biol Chem* **255**, 10081-10090, (1980).

40 Schoen, P & Lindhout, T. The in situ inhibition of prothrombinase-formed human alpha-thrombin and meizothrombin(des F1) by antithrombin III and heparin. *J Biol Chem* **262**, 11268-11274, (1987).

Future Directions

The next step in the progression of our coagulation model is to simulate the *in vivo* environment. Expansion of the model will require the addition of blood flow, endothelial cells, white blood cells, platelets, and the full complement of coagulation proteins. Such a model will provide insight into complex disease processes that are impossible to obtain using laboratory techniques. Computational systems biology allows the design and implementation of experiments that would be unethical and dangerous in the clinical setting; instead, creation of previously unavailable diagnostic and therapeutic strategies becomes possible.

The time required to update the model is one disadvantage of ABMS as it is computationally expensive for large systems with many elements. Not only does this necessitate long development times, but limits the use of the model to offline situations. Conversion of the model into other platforms may provide significantly decrease the time required to run simulations and increase its utility as a clinical tool. For example, the model can be moved to an alternate ABMS platform (*I.E.* Repast) with an expected halving of the execution time. Ultimately, conversion of the model into a format that can be run on graphical processing units (GPU) may allow significant decreases in execution time (on the order of 100x) that could allow simulations to be run at a patient's bedside in real-time.

TIC: A Computational Model of In Vivo Trauma Induced Coagulopathy*

Objective: The PULSE initiative identified prevention of diffuse coagulopathies to be a priority in resuscitation science. Trauma Induced Coagulation (TIC) is a significant complication of

* Presented at the 2008 American Heart Association Annual Meeting, and was awarded the young investigator award.

trauma involving the complex nonlinear interplay of the coagulation and inflammation system (CIS). Its complexity poses significant challenges for systematic clinical study. Modeling via computational approaches may prove to be a valuable adjunct. We developed a model of TIC using a 2-D Agent Based Model (ABM).

Methods: A 2-D particle system was developed in which particles move and interact on a discrete spatial grid composed of 'cells'. The particles of the system are cells (endothelial, WBC, platelets), reactants, enzymes, and reaction products. The number of 'cells' used in the simulations is 1,000,000 with a coagulation factor density of 16%. The particles' actions are determined by a set of rules derived from coagulation kinetics and cell behaviors. The system is designed to model a blood vessel in vivo including blood flow. The model is perturbed by alterations in systemic variables (temperature, pH, coagulation factor concentration, oxygenation).

Results: The effects of temperature, pH, and coagulation factor dilution were synergistic on the model resulting in increased INR values ranging from 1.5 to 7.76. A state of anti-coagulation and hyperfibrinolysis existed independent of temperature and pH. Endothelial cell activation from hypovolemia resulted in the increased expression of TM, TFPI, and tPA with a concomitant decrease in PAI. This resulted in a state of anticoagulation from the diversion of thrombin to the activation of PC (by binding to thrombin) combined with increased TFPI. Increased levels of tPA combined with decreases in PAI result in a state of hyperfibrinolysis that dissolves any clot formed in the anti-coagulation environment.

Conclusion: The simulation indicates that the effects of trauma on the CIS can be readily simulated. The ABM successfully modeled TIC seen in vivo due to endothelial cell activation from hypoperfusion as supported by the literature. The ABM will be used to target mediator levels for clinical verification as well as to develop preclinical and clinical testing of therapies that may modulate the CIS to enhance outcomes.

DIC: A Computational Analysis of the Coagulopathy Associated with Disseminated Intravascular Coagulopathy*

Objective: The PULSE initiative identified prevention of diffuse coagulopathies to be a priority in resuscitation science. Disseminated Intravascular Coagulopathy (DIC) is a significant complication of diseases such as sepsis and cancer. DIC involves the complex nonlinear interplay of the coagulation, fibrinolytic, and inflammatory systems (CIF). Its complexity poses a significant challenge for systematic clinical study; thus, modeling via computational approaches may prove to be a valuable adjunct. We developed a model of DIC using a 2-D Agent Based Model (ABM) implemented in the Netlogo modeling platform.

Methods: A 2-D particle system was developed in which particles move and interact on a discrete spatial grid composed of 'cells'. The particles of the system are cells (endothelial, WBC, platelets), cytokines, reactants, enzymes, and reaction products. The number of 'cells' used in the simulations is 5041 with approximately 500,000 agents. The agents' actions are determined by a set of rules derived from coagulation kinetics and cell behaviors. The system is designed to model a blood vessel *in vivo* including blood flow. The grid is in the shape of a rectangle. The

* Presented at the 2009 Annual SwarmFest.

sides of the rectangle represent endothelial cells and allow agents to interact with the endothelial cells or bounce off the walls. The ends are empty and allow the loss and introduction of agents. Blood flow is simulated by pulsatile movement of the particles through the system. The model is perturbed by the introduction of elevated levels of TNF-α in order to simulate the systemic inflammatory response from an insult such as sepsis.

Results: The simulation represents the formation of DIC due to elevated levels of TNF-α and subsequent activation of the inflammatory system. The activation of the coagulation system leads to the formation of microvasculature clot formation and a consumptive coagulopathy that results in the impairment of hemostasis. Table 1 demonstrates the alteration in the plasma levels of Antithrombin III (AT), Fibrinogen (F), platelet (plt), and Fibrin Split Products (FSP). As can be expected, the levels of AT, F and plts decrease as they are consumed by the systemic activation of the coagulation system, and the levels of FSP continue to increase as the clot is continually dissolved by the fibrinolytic system.

Conclusion: The simulation indicates that the effects of systemic inflammation on the CIF can be readily simulated using ABM. The ABM effectively modeled DIC as the end product of elevated cytokine levels as may be seen in sepsis. The demonstrated parameters and resultant coagulopathy are consistent with clinical DIC found in the literature. The goal in creating an ABM of DIC is to develop preclinical and clinical testing of therapies that may modulate the CIF to enhance patient outcomes.

Time (h)	AT (μM)	Fibrinogen (μM)	Platelet (x 10^9)	FSP(μg/mL)

0	4.50	88.20	300	0.0
1	4.37	83.74	291	0.3
4	3.65	74.91	271	2.7
8	2.74	64.29	227	6.0
12	1.80	29.63	39	33.5
16	1.07	22.06	11	37.5

Table 1: Plasma levels of AT, F, Plt, and FSP in DIC

Cardiac Arrest: A Computational Model of the Effect of Cardiac Arrest on the Coagulation System*

Objective: The PULSE initiative identified prevention of diffuse coagulopathies to be a priority in resuscitation science. Coagulopathy is a potential significant complication of cardiac arrest that involves the complex nonlinear interplay of the coagulation and inflammation system (CIS). This complexity has made it difficult to study it in an integrative fashion at the microvessel level in cardiac arrest. We developed a 2-D Agent Based Model (ABM) to begin to better understand the CIS in cardiac arrest.

Methods: The ABM utilizes a 2-D particle system. Particles move and interact on a discrete spatial grid. The particles of the system are the cells, reactants, enzymes, and reaction products. The system is designed to model a blood vessel in vivo. The grid is in the shape of a rectangle. The sides of the rectangle represent endothelial cells; particles are capable of interacting with the endothelial cells. In a steady state, blood flow was suddenly discontinued for 20 minutes followed by return of spontaneous circulation (ROSC) for another 20 minutes. The levels of circulating coagulation factors and their products and function were continually monitored.

* Presented at the 2008 American Heart Association Annual Meeting.

Results: After 20 minutes of no flow, we observed a state of hypercoagulability, impaired fibrinolysis, and systemic microthrombi formation consistent with post-arrest clinical studies in the literature. Endothelial cell response to hypoxia results in elevated levels of TAT and fibrin monomers consistent with activation of the coagulation system. Concomitant lack of D-dimer and FSPs demonstrated the decreased expression of TM, TFPI, and tPA. Following ROSC, the activation of the anticoagulation system and pro-inflammatory mediators resulted in a disruption of the equilibrium between the coagulation, anti-coagulation, fibrinolytic and inflammatory systems consistent with a clinical state of low grade DIC. This was also consistent with the literature.

Conclusions: The ABM model simulates the effects of cardiac arrest on the CIS and may be useful for studying arrest induced CIS changes as well as what affects various interventions such as hypothermia may have. Data obtained will be used to target mediator levels for verification as well as to design studies that may modulate the CIS to improve outcomes.

GPU based: Utilizing GPU Computing to Analyze Complex Biological Systems*

The coagulation system (CS) is a complex, inter-connected biological system with major physiological and pathological roles. The CS may be viewed as a complex adaptive system, through which multiple feedback and feed-forward loops link its individual components. Non-linear relationships between the numerous coagulation factors render the study of this biology at a molecular and cellular level nearly impossible. We have employed an Agent Based Modeling Simulation (ABMS) in our current approach to the analysis of the CS. One of the most

* Submitted to the 2010 ACM International Conference on Bioinformatics and Computational Biology

significant drawbacks to using ABMS is the computational expense associated with large systems.

To date, our efforts to successfully model the CS have been stymied by the time required to run simulations. The large number of elements (on the order of 10^6) requires days to weeks to run basic simulations. We hypothesized that conversion of the model into other platforms may significantly decrease this time. We present a comparison of the run-times of 4 ABMS models: 1 & 2) common platforms Netlogo and Repast; 3) C program designed to run on a single processor and 4) C program designed to utilize the parallel architecture of the Graphics Processing Unit (GPU). As expected, it is observed that GPU-based execution affords significant improvement (on the order 10^3) over the conventional ABMS platforms on the runtimes of our complex CS model.

GPU computing provides the opportunity to obtain near supercomputer performance on a desktop computer. The use of this virtual supercomputer can fuel complex systems analysis without the need for costly high performance computing resources. Our results indicate that complex models of the human CS can be implemented using GPU based computing with significant gains in performance. The use of such models will allow the creation of rapid and inexpensive virtual laboratories that can be used to generate and test hypotheses and provide clinical tools to design and test novel therapeutic strategies.

Summary

By definition, a complex system exhibits emergent and self organized behaviors. They typically involve many heterogeneous components that interact in a nonlinear manner usually involving feedforward and feedback loops which are used to amplify or dampen signals. Complex systems are bound by their components. Through production and utilization of information from their internal and external environments, these components collectively give rise to complex, changing patterns and behaviors. As a result, unique properties emerge. These properties lead to a common definition of complex systems: a large number of simple components with simple behavior that gives rise to complex collective behavior despite the lack of an overlying controller and sophisticated information processing and adaptation.

The complex behavior that arises from such systems is called emergent behaviors. If the organized behavior occurs despite the lack of a controller, the system is labeled "self-organizing" Complex systems are ubiquitous through the natural world. Analysis of complex systems requires interdisciplinary measures to describe these sophisticated systems. Computational modeling offers an attractive *in silico* approach to such analysis.

Computational systems biology is a rapidly growing field that provides tools to analyze and understand dynamic evolutionary networks. A major advantage of this approach is its rapid, real time analysis of overlapping biological systems, each of which can be a highly coordinated independent network interacting with other networks in the group at one or more branch points. These independent networks can be thought of as small molecular machines, which work co-operatively to form a large, multi-component molecular machine producing one or more

physiological responses. Understanding the mechanism and co-operativity of these networks as well as predicting the physiological response to appropriate pharmaceutical agents is an extremely difficult and intricate task. Advanced systems biology techniques, *e.g.* computational technology, hold major promise in achieving this goal and consequently may be extremely useful in understanding patho-physiological conditions and their treatment.

In order to develop useful integrative systems biology approaches, computational tools integrate complexity theory to predict responses of relevant processes to interventions. Mathematical models represent one such method. The failure of animal models to accurately predict the usefulness of therapies and the difficulty of enrolling large numbers of human subjects in studies has been a major roadblock in the study of complex diseases. Mathematical models offer a non-invasive intermediary step that allows hypothesis and therapies to be tested prior to clinical studies. Thus, an *in silico* model would potentially increase the success rate of clinical trials or aid in designing more appropriate animal studies. Manipulation of the model would then provide direction to the subsequent methodologies necessary to take the next steps in discovery. These animal or clinical studies would then in turn, validate the model.

Ideally, a well-constructed computational model will offer a rapid and inexpensive virtual laboratory to simulate the effects of biological hypotheses prior to testing these theories *in vitro* or *in vivo[77]o*. Accurate predictions by any model, from cell cultures to *in vivo* animal models to mathematical models, are dependent on the accuracy of the relation between the model and the corresponding real-world process. They are highly dependent on certain data imputations that are derived from animal data, clinical results, or assumptions based on observations or general

agreements within the community studying the disease. Such models require extensive validation; however, it will eventually provide insight into processes that are initially difficult to observe in an intact system. Thus, a successful computational model will not only fill the gaps in our knowledge, it will also identify previously unrecognized gaps as well.

In addition to the benefits associated with theoretical advances, simulations provide clinical tools to design and test novel therapeutic strategies, while affording opportunities to predict adverse events during drug development. Bedside simulations will allow personalized medicine in that replacement factor concentrations can be calculated for individual hemophiliac patients, heparin doses can be titrated, etc… Other applications of the model include discovery of new mediators, understanding of proximal and distal effects of interactions between systems, discovery of new diagnostic and therapeutic options, and development of new software and algorithms for simulation.

Normal wound healing is a carefully choreographed process that results in a mature scar, which restores the anatomic and functional integrity of the dermis[25]. The process is divided into an orderly progression of individual phases. The hemostatic phase is controlled by platelets, which ensure wound stabilization and recruits inflammatory cells into the wounded tissue. The inflammatory phase, which is initially dominated by neutrophils and subsequently by macrophages, prepares the wound bed by killing bacteria and removing devitalized tissue as well as recruiting fibroblasts. The proliferative phase is characterized by fibroblasts laying down a provisional ECM matrix. The remodeling phase is a balance of collagen synthesis and degradation that results in a mature scar that maximizes wound tensile strength. The complexity

of acute wounds have stymied clinical investigators. Computational biology shows promise in providing an alternative avenue of study for wound healing.

We have modified an ODE model of the acute systemic response to inflammation a soft tissue injury. Our model includes factors such as bacterial contamination and wound oxygenation. Assuming normal conditions, our model predicts the typical progression of healing behavior for a wound. The ODE model was also able to successfully simulate the impairment in wound healing found in a hypoxic wound environment and a contaminated wound. For example, under hypoxic conditions, we observe a non-healing wound where the damage persists despite the absence of pathogens. With extremely low levels of oxygen our model predicts a chronic infection where the wound does not heal and pathogens persist in the wound. Both of these states are well documented clinically.

We also examined the situation of elevated and depressed fibroblasts mortality rates. Clinically, instances of elevated fibroblast mortality are seen in diabetic and elderly patients. We observed non-healing wounds in the context of high rates of fibroblast mortality. Additionally, a scenario of moderately low fibroblast mortality and high initial pathogen levels predicts the state of chronic infection. Finally, we examined the case where fibroblast production is either impaired or enhanced. Impaired fibroblast production results in a non-healing state; however with an increase in production, wounds heal at notably faster rates. This provides a framework from which to test a new hypothesis in a living model, *i.e.* improve fibroblast production in an effort to increase wound healing rates.

Our model successfully simulated results typical of hypoxic wound environments with significant bacterial contamination. Though most of our results are not overly surprising, we are satisfied and encouraged that our model is qualitatively accurate in its predictions of real systems. This provides some level of model calibration. Translation of our model to the level of clinical relevance will require an enormous number of important variables both at the local and systemic levels. We are now in the process of examining systemic mediators and their effects on healing at the local environment. This includes hormonal differences thus taking into account gender differences and the effects of systemic inflammation.

Another difficult clinical problem is that of diseases associated with coagulation and fibrinolysis. Coagulation is a complex process by which blood forms solid clots. It is an important part of hemostasis defined as the cessation of blood loss from a damaged vessel. A damaged blood vessel wall is covered by a platelet- and fibrin-containing clot to stop bleeding. Coagulation is initiated almost instantly after an injury to the blood vessel damages the endothelium (lining of the vessel). Fibrinolysis is a complex process by which pre-formed clot is proteolitically degraded once the underlying endothelial injury has been repaired. The CF systems interact strongly at the molecular and cellular level; they thereby operating as a coherently linked system, to generate several pathological and physiological responses. The highly complex CF system presents a challenging problem of identifying the root cause of many known coagulation defects. To date the contribution of each system as a part of the network has not been attempted. Furthermore, the difficulties in studying a system that has the following properties: nonstationarity, spatial heterogeneity, and blood flow. The CF system also can be defined as a complex system: 1) large number of heterogenous components (zymogens, enzymes, cofactors,

inhibitors, membranes, and cells), 2) no overlying controller (the CF reactions are all local and based on molecular interactions), 3) non-linear (the biochemical reactions among the components are all non-linear), and 4) emergence (threshold effects for thrombin generation, localized clot formation, and delayed clot lysis). Given the difficulties associated with the study of the CF system, the study of such a complex system may benefit from computational analysis.

We have developed an ABMS of the CF cascade that allows systematic evaluation of each of its components – individually and as a complex entity. The model allows a comprehensive analysis of the CF cascade that provides insight into understanding and predicting the pathophysiologic responses arising from variations in molecular and cellular components. ABMS allows a real time analysis of the CF systems that is difficult if not impossible to obtain through in *vivo* experiments. Additionally, ABMS provides an opportunity to understand the complex interplay among the various subsystems at any point in time. Reductionist *in vitro* experimental techniques have allowed a detailed understanding of the individual chemical reactions involved in the process of coagulation. ABMS represents a non-reductionist approach of studying the biologic process as a whole, while retaining the information at an individual level. The information obtained by studying the individual reactions is used as the basis for the rules governing the updating of the ABMS. The advantages of ABMS include the ability to simulate the non-linear aspects of the coagulation system. As the agents are able to change state based on their environment, the model adapts and accounts for changes such as dearth/excess of coagulation inhibitors, absence of factors, or therapeutic interventions. The time required to update the model is one disadvantage of ABMS as it is computationally expensive for large systems with many elements; however a specific advantage of this model is its ability to allow

for the addition of newly discovered mediators, which can impact upon both coagulation and inflammation. More importantly, the model has a high probability of exhibiting *emergence* in which its outputs produce unanticipated results, which can then be biologically confirmed. Such properties are particularly useful in the discovery of diagnostic and therapeutic interventions. Comprehensive modeling of the traditional coagulation cascade allows virtual experimentation of the effects of local and systemic injury on coagulation.

The *in vitro* CF system can be readily simulated using ABMS. Our ABMS approach successfully reproduces the initiation, propagation, and termination of thrombin formation *in vitro*. Furthermore, the ABMS was able to simulate the threshold effect of thrombin formation resultant from the synergistic relationship between physiologic concentrations of coagulation inhibitors. This suppression of thrombin is the likely mechanism behind localization of the hemostasis response. The mechanism demonstrated herein provides the rationale for localized formation of a blood clot at the site of endothelial injury as opposed to a systemic vascular thrombotic response. Presumably, the thrombin concentrations upstream and downstream of the endothelial injury fail to reach self sustaining levels due to the synergistic effects of AT, TFPI, and aPC. A possible therapeutic strategy of manipulating coagulation inhibitors for the treatment of diseases involving the systemic activation of the CS, such as TIC, DIC, coagulopathy associated with cardiac arrest, etc…, is suggested by the findings in this paper. The model also successfully simulated aPTT and PT times at normal physiologic conditions, abnormal physiologic conditions (hemophilia B and AT-H binding defect), and after pharmaceutical interventions (warfarin and heparin). The non-linearities of the CF system were captured using this ABMS. The ability to generate results similar to those obtained experimentally has been

demonstrated. The error bars associated with the data are unique to ABMS and provide the ability to simulate experiments and clinical trials.

The next step in the progression of our coagulation model is to simulate the *in vivo* environment. Expansion of the model will require the addition of blood flow, endothelial cells, white blood cells, platelets, and the full complement of coagulation proteins. Such a model will provide insight into complex disease processes that are impossible to obtain using laboratory techniques. Computational systems biology allows the design and implementation of experiments that would be unethical and dangerous in the clinical setting; instead, creation of previously unavailable diagnostic and therapeutic strategies becomes possible.

The time required to update the model is one disadvantage of ABMS as it is computationally expensive for large systems with many elements. Conversion of the model into other platforms may provide significantly decrease the time required to run simulations. For example, the model can be moved to an alternate ABMS platform (*i.e.* Repast) with an expected halving of the execution time. Ultimately, conversion of the model into a format that can be run on graphical processing units (GPU) may allow significant decreases in execution time (on the order of 100x) that could allow simulations to be run at a patient's bedside in real-time.

References

1. Strange K (2005) The end of "naive reductionism": rise of systems biology or renaissance of physiology? Am J Physiol Cell Physiol 288: C968-974.
2. Neugebauer EA, Willy C, Sauerland S (2001) Complexity and non-linearity in shock research: reductionism or synthesis? Shock 16: 252-258.
3. Miller JH, Page SE (2007) Complex adaptive systems : an introduction to computational models of social life / John H. Miller and Scott E. Page. Princeton, New Jersey: Princeton University Press. xix, 263 p. p.
4. Marshall JC (2000) Complexity, chaos, and incomprehensibility: parsing the biology of critical illness. Crit Care Med 28: 2646-2648.
5. Wolkenhauer O, Mesarovic M (2005) Feedback dynamics and cell function: Why systems biology is called Systems Biology. Mol Biosyst 1: 14-16.
6. Lewin R (1992) Complexity : life at the edge of chaos. New York
7. Witten TM (1980) A note on the structure of system state spaces and its implications on the existence of non--repeatable experiments. Bull Math Biol 42: 267-272.
8. Gurel OaR, O.E. (eds.) (1979) Bifurcation Theory and It's applications in Scientific Disciplines. New York, NY: New York Academy of Sciences Press.
9. Wiggins S (1980) Global Bifurcations and Chaos: Analytical Methods. New York, NY: Springer-Verlag Press.
10. Cherbit G, editor (1991) Fractals: Non-integral Dimensions and Applications. Chichester, England: John Wiley & Sons.
11. Moon FC (1992) Chaotic and Fractal Dynamics: An Introduction for Applied Scientists and Engineers. New York, NY: John Wiley & Sons.
12. Ebeling W, Peschel, M. and Weidlich, W. (1992) Models of Selforganization in Complex Systems. Berlin, Germany: Akademie Verlag GMBH.
13. Oltvai ZN, Barabasi AL (2002) Systems biology. Life's complexity pyramid. Science 298: 763-764.
14. Buchman TG (2004) Nonlinear dynamics, complex systems, and the pathobiology of critical illness. Curr Opin Crit Care 10: 378-382.
15. Seely AJ, Christou NV (2000) Multiple organ dysfunction syndrome: exploring the paradigm of complex nonlinear systems. Crit Care Med 28: 2193-2200.
16. Grimm V, Revilla E, Berger U, Jeltsch F, Mooij WM, et al. (2005) Pattern-Oriented Modeling of Agent-Based Complex Systems: Lessons from Ecology. Science 310: 987-991.
17. Velupillai KV (2005) The unreasonable ineffectiveness of mathematics in economics. Camb J Econ 29: 849-872.
18. Guimera R, Mossa S, Turtschi A, Amaral LAN (2005) From the Cover: The worldwide air transportation network: Anomalous centrality, community structure, and cities' global roles. PNAS 102: 7794-7799.
19. Berry BJL, Kiel LD, Elliott E (2002) Adaptive agents, intelligence, and emergent human organization: Capturing complexity through agent-based modeling. PNAS 99: 7187-7188.
20. Buchman TG, Cobb JP, Lapedes AS, Kepler TB (2001) Complex systems analysis: a tool for shock research. Shock 16: 248-251.

21. Seely AJ, Macklem PT (2004) Complex systems and the technology of variability analysis. Crit Care 8: R367-384.
22. Goldstein B, Faeder JR, Hlavacek WS (2004) Mathematical and computational models of immune-receptor signalling. Nat Rev Immunol 4: 445-456.
23. WEISS JN, QU Z, GARFINKEL A (2003) Understanding biological complexity: lessons from the past. FASEB J 17: 1-6.
24. Lazarus GS, Cooper DM, Knighton DR, Margolis DJ, Pecoraro RE, et al. (1994) Definitions and guidelines for assessment of wounds and evaluation of healing. Arch Dermatol 130: 489-493.
25. Menke N, Diegelmann R (2006) Biochemical Pathways of Wound Healing: Implication for Development of Disease-Specific Diagnostics. In: Makowski G, editor. Advances in Clinical Chemistry: Elsevier. pp. 167-187.
26. Menke M, Menke N, Boardman C, Diegelmann R (2008) Biologic therapeutics and molecular profiling to optimize wound healing. Gynecol Oncol 111: S87-91.
27. Clark RA (2001) Fibrin and wound healing. Ann N Y Acad Sci 936: 355-367.
28. Weiss SJ (1989) Tissue destruction by neutrophils. N Engl J Med 320: 365-376.
29. Nwomeh BC, Liang HX, Diegelmann RF, Cohen IK, Yager DR (1998) Dynamics of the matrix metalloproteinases MMP-1 and MMP-8 in acute open human dermal wounds. Wound Repair Regen 6: 127-134.
30. Nwomeh BC, Liang HX, Cohen IK, Yager DR (1999) MMP-8 is the predominant collagenase in healing wounds and nonhealing ulcers. J Surg Res 81: 189-195.
31. Diegelmann RF, Cohen IK, Kaplan AM (1981) The role of macrophages in wound repair: a review. Plast Reconstr Surg 68: 107-113.
32. Witte MB, Barbul A (1997) General principles of wound healing. Surg Clin North Am 77: 509-528.
33. Lawrence WT (1998) Physiology of the acute wound. Clin Plast Surg 25: 321-340.
34. Laurent TC, Laurent UB, Fraser JR (1996) The structure and function of hyaluronan: An overview. Immunol Cell Biol 74: A1-7.
35. Terranova VP, Aumailley M, Sultan LH, Martin GR, Kleinman HK (1986) Regulation of cell attachment and cell number by fibronectin and laminin. J Cell Physiol 127: 473-479.
36. Kirsner RS, Eaglstein WH (1993) The wound healing process. Dermatol Clin 11: 629-640.
37. O'Toole EA (2001) Extracellular matrix and keratinocyte migration. Clin Exp Dermatol 26: 525-530.
38. Clark RA (1993) Biology of dermal wound repair. Dermatol Clin 11: 647-666.
39. Lobmann R, Ambrosch A, Schultz G, Waldmann K, Schiweck S, et al. (2002) Expression of matrix-metalloproteinases and their inhibitors in the wounds of diabetic and non-diabetic patients. Diabetologia 45: 1011-1016.
40. Wysocki AB, Staiano-Coico L, Grinnell F (1993) Wound fluid from chronic leg ulcers contains elevated levels of metalloproteinases MMP-2 and MMP-9. J Invest Dermatol 101: 64-68.
41. Yager DR, Zhang LY, Liang HX, Diegelmann RF, Cohen IK (1996) Wound fluids from human pressure ulcers contain elevated matrix metalloproteinase levels and activity compared to surgical wound fluids. J Invest Dermatol 107: 743-748.
42. Menke N, Ward K, Witten T, Bonchev D, Diegelmann R (2007) Impaired wound healing. Clin Dermatol 25: 19-25.

43. Maintzer M (1996) Thinking in Complexity: The Complex Dynamics of Matter, Mind and Mankind. Berlin, Germany: Springer-Verlag Berlin.
44. Bar-Yam Ye (2000) Unifying Themes in Complex Systems. Cambridge, MA: Perseus Books.
45. Witten TM (1998) Mathematical and Computational Tools for Gerontologic Research; Yu BP, editor. Boca Raton, FL CRC Press.
46. Jensen HJ (1998) Self-organized Criticality: Emergent Complex Behavior in Physical and Biological Systems. Cambridge, England: Cambridge University Press.
47. Bonchev D.G. and Rouvray DHe (2005) Complexity in Chemistry, Biology, and Ecology. New York, NY: Springer.
48. Witten TM (1985) A return to time, cells, systems and aging: III. Critical elements, hierarchies, and Gompertzian dynamics. Mech Ageing and Dev 32: 141--177.
49. Lichtman MA, Williams WJ (2006) Williams hematology. New York: McGraw-Hill, Medical Pub. Division. xxvii, 2189, 2108 p. p.
50. Butenas S, Mann KG (2002) Blood coagulation. Biochemistry (Mosc) 67: 3-12.
51. Monroe DM, Hoffman M (2006) What Does It Take to Make the Perfect Clot? Arterioscler Thromb Vasc Biol 26: 41-48.
52. Bergum PW, Cruikshank A, Maki SL, Kelly CR, Ruf W, et al. (2001) Role of zymogen and activated factor X as scaffolds for the inhibition of the blood coagulation factor VIIa-tissue factor complex by recombinant nematode anticoagulant protein c2. J Biol Chem 276: 10063-10071.
53. Esmon CT (2003) The Protein C Pathway. Chest 124: 26S-32.
54. Tsiang M, Jain AK, Gibbs CS (1997) Functional Requirements for Inhibition of Thrombin by Antithrombin III in the Presence and Absence of Heparin. J Biol Chem 272: 12024-12029.
55. van `t Veer C, Mann KG (1997) Regulation of Tissue Factor Initiated Thrombin Generation by the Stoichiometric Inhibitors Tissue Factor Pathway Inhibitor, Antithrombin-III, and Heparin Cofactor-II. J Biol Chem 272: 4367-4377.
56. Walker JB, Bajzar L (2004) The Intrinsic Threshold of the Fibrinolytic System Is Modulated by Basic Carboxypeptidases, but the Magnitude of the Antifibrinolytic Effect of Activated Thrombin-activable Fibrinolysis Inhibitor Is Masked by Its Instability. J Biol Chem 279: 27896-27904.
57. Jesty J, Beltrami E (2005) Positive Feedbacks of Coagulation: Their Role in Threshold Regulation. Arterioscler Thromb Vasc Biol 25: 2463-2469.
58. Colman RW, Clowes A, George J, Goldhaber S, Marder V (2006) Chapter 1. In: Colman RW, Clowes A, George J, Goldhaber S, Marder V, editors. Hemostasis and Thrombosis. 6th Edition ed. Philadelphia: Lippincott Williams & Wilkins.
59. Cesarman-Maus G, Hajjar KA (2005) Molecular mechanisms of fibrinolysis. Br J Haematol 129: 307-321.
60. Collen D, Lijnen HR (1991) Basic and clinical aspects of fibrinolysis and thrombolysis. Blood 78: 3114-3124.
61. Broze GJ (1996) Thrombin-dependent inhibition of fibrinolysis. Curr Opin Hematol 3: 390-394.
62. Chmielewska J, Ranby M, Wiman B (1988) Kinetics of the inhibition of plasminogen activators by the plasminogen-activator inhibitor. Evidence for 'second-site' interactions. Biochem J 251: 327-332.

63. Christensen U, Bangert K, Thorsen S (1996) Reaction of human alpha2-antiplasmin and plasmin stopped-flow fluorescence kinetics. FEBS Lett 387: 58-62.
64. Collen D, Wiman B (1978) Fast-acting plasmin inhibitor in human plasma. Blood 51: 563-569.
65. Gorlatova NV, Cale JM, Elokdah H, Li D, Fan K, et al. (2007) Mechanism of Inactivation of Plasminogen Activator Inhibitor-1 by a Small Molecule Inhibitor. J Biol Chem 282: 9288-9296.
66. Guimaraes AH, Rijken DC (2004) Thrombin activatable fibrinolysis inhibitor (TAFI) affects fibrinolysis in a plasminogen activator concentration-dependent manner. Study of seven plasminogen activators in an internal clot lysis model. Thromb Haemost 91: 473-479.
67. Érdi P (2008) Complexity explained. Springer complexity. Berlin: Springer. pp. xv, 397 p.
68. Cowley AW, Jr., Liang M (2006) Physiology and genomics: toward systems biology. Sheng Li Xue Bao 58: 1-4.
69. Kitano H (2002) Systems biology: a brief overview. Science 295: 1662-1664.
70. Kitano H (2002) Computational systems biology. Nature 420: 206-210.
71. Kahlem P, Birney E (2006) Dry work in a wet world: computation in systems biology. Mol Syst Biol 2: 40.
72. Buchman TG (2004) In vivo, in vitro, in silico. Crit Care Med 32: 2159-2160.
73. Clermont G, Bartels J, Kumar R, Constantine G, Vodovotz Y, et al. (2004) In silico design of clinical trials: a method coming of age. Crit Care Med 32: 2061-2070.
74. Geris L, Vander Sloten J, Van Oosterwyck H (2009) In silico biology of bone modelling and remodelling: regeneration. Phil Trans R Soc A 367: 2031-2053.
75. Thomas CE, Ganji G (2006) Integration of genomic and metabonomic data in systems biology--are we 'there' yet? Curr Opin Drug Discov Devel 9: 92-100.
76. Waters KM, Pounds JG, Thrall BD (2006) Data merging for integrated microarray and proteomic analysis. Brief Funct Genomic Proteomic.
77. An G (2004) In silico experiments of existing and hypothetical cytokine-directed clinical trials using agent-based modeling. Crit Care Med 32: 2050-2060.
78. An G (2005) Mathematical modeling in medicine: a means, not an end. Crit Care Med 33: 253-254.
79. An G (2001) Agent-based computer simulation and sirs: building a bridge between basic science and clinical trials. Shock 16: 266-273.
80. Borrelli RL, Coleman CS (2004) Differential equations : a modeling perspective. New York: Wiley. xii, 718 p. p.
81. Vodovotz Y, Clermont G, Chow C, An G (2004) Mathematical models of the acute inflammatory response. Curr Opin Crit Care 10: 383-390.
82. Hockin MF, Jones KC, Everse SJ, Mann KG (2002) A Model for the Stoichiometric Regulation of Blood Coagulation. J Biol Chem 277: 18322-18333.
83. Bankes SC (2002) Agent-based modeling: A revolution? PNAS 99: 7199-7200.
84. Bonabeau E (2002) Agent-based modeling: Methods and techniques for simulating human systems. PNAS 99: 7280-7287.
85. Rider RE (1989) Aspects of Ulam: From Cardinals to Chaos. Science 246: 134-.
86. Wolfram S (1994) Cellular Automata and Complexity: Collected Papers: Westview Press.
87. Wolfram S (2002) A New Kind of Science: Wolfram Media.
88. Gilbert GN (2008) Agent-based models. Los Angeles: Sage Publications. xiii, 98 p. p.

89. Jennings NR (2000) On agent-based software engineering. Artificial Intelligence 117: 277-296.
90. Jennings NR (2001) Building Complex Software Systems: The Case for an Agent-Based Approach. Communications of the ACM 44: 35-41.

VITA

Nathan Benjamin Menke was born on May 11, 1975, in Buffalo, New York. He graduated from Westerville North High School, Ohio in 1993. He graduated Magna Cum Laude with a Bachelor of Science in Biochemistry and Computer and Information Science from The Ohio State University in 1997. In his junior undergraduate year he was inducted into the Phi Beta Kappa society, Phi Kappa Phi society, and Golden Key National Honor Society. He graduated Summa Cum Laude with a Doctor of Medicine from The Ohio State University in 2002; in his junior year of medical school he was inducted into the Alpha Omega Alpha honor society. Upon completion of his clinical residency in Emergency Medicine, he enrolled in the Virginia Commonwealth University Ph.D. program in the fall of 2005. He attended the Complex System Summer School, Santa Fe Institute (2007). He has held academic appointments at the Virginia Commonwealth University Medical Center (Clinical Instructor 2005-2006; Assistant Professor 2006-2009) and Lincoln Medical and Mental Health Center, New York (Attending Physician/Core Faculty 2010-current).

While in the doctorate program, Dr. Menke received the Young Investigator Award at the American Heart Association Annual Scientific Sessions (2008), 6th International Conference on Complexity in Acute Illness (2007), and 1st International Conference on Wound Healing and Technology (2006). He received a travel award to the American Academy of Artificial Intelligence Fall Symposium (2009). He was awarded the Phi Kappa Phi Graduate Student Award (2009). He is the recipient of NIH Loan Repayment Program (2007), Jeffress Memorial Trust Award (2007), and NIH T32 Post-Doctoral Fellowship (2005).